Modelling and Data Processing in Pulmonary Function

Modellering en dataverwerking
in de longfunctie

CIP-DATA KONINKLIJKE BIBLIOTHEEK, DEN HAAG

Verbraak, Antonius Franciscus Marie

Thesis Erasmus Universiteit Rotterdam, Faculteit Geneeskunde
- With ref. - With summary in Dutch
ISBN 90-9011250-2
Subject headings: lung / modelling / mathematical / mechanical / simulator

Cover design: P.A.M. Verbraak, Tilburg
Printing: Ridderprint, Ridderkerk

Copyright © A.F.M. Verbraak 1998
All rights reserved. Save exceptions by the law, no part of this publication may be reproduced, stored in a retrieval system of any nature, or transmitted in any form or by means, electronic, mechanical, photocopying, recording or otherwise, including a complete or partial transcription, without the prior written permission of the author, or where appropriate, of the publishers of the articles.

Modelling and Data Processing in Pulmonary Function

Modellering en dataverwerking
in de longfunctie

Proefschrift

ter verkrijging van de graad van doctor
aan de Erasmus Universiteit Rotterdam op gezag van de
Rector Magnificus Prof. Dr. P.W.C. Akkermans M.A.
en volgens het besluit van het College voor Promoties.

De openbare verdediging zal plaatsvinden op
7 januari 1998 om 15:45 uur

door

Antonius Franciscus Marie Verbraak
geboren te Tilburg

Promotiecommissie:

Promotores: Prof. dr. ir. J.E.W Beneken, Technische Universiteit Eindhoven, NL
Prof. dr. J.M. Bogaard
Prof. dr. A. Versprille

Overige leden: Prof. dr. ir. J.H. v. Bemmel
Prof. dr. ir. N. Bom
Prof. dr. ir. P.F.F. Wijn, Technische Universiteit Eindhoven, NL

This study was supported by a grant from:
The Dutch Asthma Foundation, Leusden, NL

Additional financial support by:
Jaeger Benelux, Breda, NL
Medeco Health and Industrial Care Products, Oud Beijerland, NL
Siemens Nederland, The Hague, NL

CONTENTS

	List of abbreviations and symbols	5
Chapter 1	Introduction	9
Chapter 2	A lung function information system *J. Biomed. Eng. 1991;13:27-34.*	15
	Appendix	31
Chapter 3	Serial lung model for simulation and parameter estimation in body plethysmography *Med. & Biol. Eng. & Comput. 1991;29:309-317.*	37
Chapter 4	A computer controlled mechanical lung model *Med. & Biol. Eng. & Comput. 1995;33:776-783.*	57
Chapter 5	A computer controlled flow resistance	73
Chapter 6	A new approach to mechanical simulation of the lung	87
Chapter 7	Final Considerations	103
	Conclusions	107
	Summary	109
	References	113
	Samenvatting	123
	Dankwoord	131
	Curriculum Vitae	135

Abbreviations

A/D	analog to digital conversion
AZR	academic hospital Rotterdam
CC	compressible component
CCL-1	computer-controlled lung simulator, first generation
CCL-2	computer-controlled lung simulator, second generation
CCL_A	active simulation, normal breathing
$CCL_{A,P}$	active inspiration and passive expiration
CCL_P	passive simulation, artificial ventilation
CID	Central Instrumentation Department
COPD	chronic obstructive pulmonary disease
class *N*	normal lung
class *E*	emfysematic lung
class *F*	fibrotic lung
class *A*	asthmatic lung
class *U*	upper airway disease
EE	square error
EPP	equal pressure point
EUR	Erasmus University Rotterdam
FEV_1	forced expiratory volume in 1 second
FRC	functional residual capacity
FS1,FS2,FS3	file server at the lung function department
HIS	hospital information system
HIS-LAN	local area network of the hospital.
LFC	water-filled compartment
LFC-CC	connection between the *LFC* and the compressible component
LFIS	lung function information system
P_{A1},P_{A2}	pressure inside the bellows 1 and 2, respectively
PC-LAN	personal computer - local area network
PID	patient identification number
P_{liq}	connection point to fill the *LFC* with water and to measure the pressure
R_{aw1},R_{aw2}	airway component for lung 1 and 2, respectively
Re	Reynolds number
RV	residual volume
S_1,S_2	two extreme positions of the piston
T_1,T_2	position of bellows 1 and 2, respectively
T_3	position of the piston
TGV	thoracic gas volume
TLC_{ref}	reference for total lung capacity
P_{A1},P_{A2}	pressure inside the bellows 1 and 2
V_1,V_2	volume of bellows 1 and 2, respectively
VC	vital capacity

Symbols

η_{air}	dynamic viscosity of air, 18.3 10^{-6}	(Pa.s)
ρ_{air}	specific mass of air at room temperature, 1.205	($kg.m^{-3}$)
ρ_{liq}	specific mass of air liquid room temperature, 998	($kg.m^{-3}$)
A	area of flow	(m^2)
A_{bls}	effective surface of the bottom plate of each bellows	(m^2)
A_{sli}	area of the slit	(m^2)
C_{eff}	compliance as calculated with *Reff*	($L.kPa^{-1}$)
C_L	lung compliance	($L.kPa^{-1}$)
C_{rs}	total respiratory compliance	($L.kPa^{-1}$)
C_{th}	thorax compliance	($L.kPa^{-1}$)
D_{cyl}	external diameter of the cylinder	(m)
D_{hydr}	hydraulic diameter	(m)
D_{sle}	internal diameter of the sleeve	(m)
E_{bls}	elastic constant of bellows at position h_{bls}	($N.m^{-1}$)
E_L	elastance of the lungs	($kPa.L^{-1}$)
E_{mxb}	elastance of the Maxwell body	($kPa.L^{-1}$)
f_R	resistance factor for control of the *CCR*	($m.s^{-2}$)
$f_{V'}$	flow factor for control of the *CCR*	($m.s^{-2}$)
g	constant of gravitation	($m.s^{-2}$)
h_{bls}	position of bottom plate of a bellows	(m)
h_{sli}	height of the slit	(m)
k	index of curvature	(kPa^{-1})
K_1	linear resistance of the upper airways	($kPa.s.L^{-1}$)
K_2	turbulent resistance of the upper airways	($kPa.s^2.L^{-2}$)
K_3	linear resistance parameter model-2	($kPa.s.L^{-1}$)
K_4, K_5	linear resistance parameters model-3 for inspiration and expiration, respectively	($kPa.s.L^{-1}$)
K_6, K_7	linear resistance parameters model-4 for inspiration and expiration, respectively	(kPa.s.L-1)
K_8, K_9	turbulent resistance parameters model-4, for inspiration and expiration, respectively	($kPa.s^2.L^{-2}$)
I_{cal}	calculated position for *CCR* control	(m)
I_{sli}	length of the slit	(m)
N_{curve}	curvature of the pressure pattern	(-)
P_0	intercept on the pressure axis at $V_L = 0$	(kPa)
P_A	alveolar pressure	(kPa)
$P_{A,c}$	alveolar pressure in the mechanical model	(kPa)
P_{bar}	barometric pressure	(kPa)
P_{box}	pressure over the body plethysmograph	(kPa)
P_{br}	pressure in the airways	(kPa)
P_c	pressure over the compressible airways	(kPa)
P_{es}	pressure in the oesophagus	(kPa)
$P_{es,off}$	pressure offset in the oesophagus	(kPa)
P_L	lung recoil pressure	(kPa)
$P_{L,stat}$	static lung recoil pressure	(kPa)
$P_{L,FRC}$	lung recoil pressure at FRC	(kPa)
$P_{liq}(h)$	pressure in the liquid at level h	(kPa)
$P_{liq}(h_{bls})$	pressure in the liquid at level h_{bls}	(kPa)
$P_{liq,off}$	pressure at $h_{bls}=0$ when $P_A=0$ and $P_{grav}=0$	(kPa)
P_m	mouth pressure	(kPa)

P_{meas}	measured pressure	(kPa)
P_{mus}	pressure exerted by the muscles	(kPa)
P_{pl}	pleural pressure	(kPa)
P_s	pressure over the small airways	(kPa)
$P_T(0)$	tracheal pressure at the beginning of expiration (t = 0)	(kPa)
$P_T(t)$	tracheal pressure at time t	(kPa)
$P_{T,calc}(t)$	calculated tracheal pressure at time t in the expiration	(kPa)
$P_{T,end}$	tracheal pressure at end of expiration	(kPa)
P_{th}	thoracic pressure	(kPa)
P_{tr}	tracheal pressure	(kPa)
$P_{tr,c}$	tracheal pressure in the mechanical model	(kPa)
P_{tms}	point of curvature for the compressible element	(kPa)
P_u	pressure over the upper airways	(kPa)
R	flow resistance	(kPa.s.L^{-1})
R_c	compressible airways resistance	(kPa.s.L^{-1})
R_{c0}	weighting constant for the compressible airways	(kPa.s.L^{-1})
Re	Reynolds number	(-)
R_{eff}	effective flow resistance	(kPa.s.L^{-1})
Re_{sli}	Reynolds number in the slit	(-)
R_{mxb}	viscosity of the Maxwell body	(kPa.s.L^{-1})
R_p	resistance line through extreme pressure points	(kPa.s.L^{-1})
R_s	resistance of the small airways	(kPa.s.L^{-1})
R_{sim}	resistance to be simulated	(kPa.s.L^{-1})
R_{sli}	resistance of the slit	(kPa.s.L^{-1})
$R_{sli\text{-}lam}$	laminar flow resistance in the slit	(kPa.s.L^{-1})
$R_{sli\text{-}tur}$	turbulent flow resistance in the slit	(kPa.s.L^{-1})
R_t	resistance of the combined airways	(kPa.s.L^{-1})
$R_{t,c}$	resistance of the combined airways in the mechanical model	(kPa.s.L^{-1})
R_u	upper airways resistance	(kPa.s^2.L^{-2})
t_{exp}	total expiration time	(s)
U_c	steering signal	(Volt)
V'	flow	(L.s^{-1})
V'_A	flow into the alveolar space	(L.s^{-1})
V'_L	airflow into the lung	(L.s^{-1})
$V'_{L,c}$	airflow into the mechanical model	(L.s^{-1})
V_1	volume of concertina bellows (lung 1)	(L)
V_2	volume of concertina bellows (lung 2)	(L)
V_A	alveolar volume	(L)
V_c	volume of the compressible element	(L)
V_{c0}	weighting constant (see text)	(-)
V_{cN}	maximum volume of the compressible element for normals	(L)
V_L	lung volume (alveolar + airways)	(L)
$V_{L,c}$	lung volume (alveolar component + airways components)	(L)
V'_m	flow at the mouth	(L.s^{-1})
V_{max}	maximum volume (asymptote of the exponential equation)	(L)

CHAPTER 1

INTRODUCTION AND OUTLINE OF THE THESIS

INTRODUCTION

Computing technology has developed rapidly over the last three decades. The performance of computers has grown in all classes, from the smallest microcomputers through the largest supercomputers [1, 2]. The ongoing increase in the number of transistors per chip for microcomputers and memory has resulted in faster and cheaper computers [3]. This increase in performance of the microcomputer explains the use of this type of computer in almost every field of society nowadays. Computers have become indispensable in many fields of the hospital, e.g. for storage and retrieval of patient information, data analysis, financial administration and word-processing.

In this thesis, three types of technological development in the pulmonary function laboratory and intensive care department of the University Hospital Dijkzigt Rotterdam are described in which computers were an essential condition: 1) data processing in the lung function department, 2) mathematical modelling and parameter estimation, and 3) the development of a mechanical model to be used for simulating normal breathing and artificial ventilation.

Data processing in clinical routine

Twenty years ago the first automatic data processing was introduced at the lung function laboratory. In the early stages of automatic data processing at the

laboratory, a program was developed that processed the data measured by the lung function technician from recordings of breathing manoeuvres performed by patients. The data had to be corrected for the type of spirometer, temperature and barometric pressure and scaled to lung function values. Because at that time no computer was available at the University Hospital Dijkzigt or the medical faculty of the Erasmus University Rotterdam, a computer was used from the IBM computer centre at Zoetermeer. At the end of each day the numbers were coded on a punched card by means of a machine at the medical faculty. During the night these data were read by a card reader and sent over to the IBM computer. The next morning, if no wrong data input was noticed or a computer fault had appeared, the printout of lung function variables was available at the medical faculty. This was the first computer printed report at our department.

In 1977 a mini-computer became available at the Central Instrumentation Department (*CID*) in the medical faculty. A modem connection enabled the input of data at the lung function laboratory. A questionnaire guided the technician during the input of data via a keyboard printer. Mistakes in the input of data diminished and the lung function report was available within a few minutes. This processing of the lung function data could be done twice a day.

The availability of microcomputers (*PDP-11/03, Digital Equipment Corporation*) in 1978, enabled a next step in the development of data processing at the laboratory. The lower price of this type of computer made a local application for signal processing at a laboratory financially possible. A computer (fl. 120,000 for a computer with 32k words and 5MB disk), a graphic video terminal (fl. 30,000), and an electrostatic graphic printer (fl. 60,000) were purchased and installed at the lung function laboratory. The input of data could be performed at every moment of the day. For many years, two other hospitals used this microcomputer by means of a modem connection, similar to the way our laboratory used the computer at the *CID*. With this microcomputer a set of programs was developed to demonstrate the feasibility for development of a system to process the data from flow-volume and spirographic measurements on-line. The program allowed the technician to give full attention to the patient and to process the data of the patients on-line, even in case of difficulties in relation to pathology.

At the same time a system was developed at the Max Planck Institute in Göttingen in which microcomputers without local facilities for storage of data were connected to one central microcomputer. This development facilitated the third phase in the development of the data processing at the pulmonary function laboratory in Rotterdam. A network of computers processed the data on-line real-time including a central storage of data. During the measurement the technician received information about the measured lung function variables together with their reference values. Data, measured in different measurement rooms, were

integrated into one lung function report. A connection with the hospital information system guaranteed consistent patient data. The results were stored in the hospital information system and administrative procedures were also executed on-line.

The introduction of personal computers had a large impact. Mainly through the introduction of the 8086 processor and its successors (*INTEL Corporation, USA*) and the operating system *MS-DOS* (*Microsoft Corporation, USA*) the computer became a standard device in the work environment. Nowadays, the prices of computer hardware is much lower, being about fl 4000 for a fast complete system and about fl 500 for a graphic printer with more possibilities than the electrostatic printer/plotter. At the laboratory the network based on PDP-11 computers was transformed to personal computer (*PC*) based systems.

Modelling

A model is a representation of a (e.g biological) system in another (e.g. electrical / mathematical) system independent of the first system in order to get (new) information of that system. An effective model is restricted to the specific objectives to be studied [4]. To study the physiological nature of an organ or system of organs with use of another system (model), the essential characteristics of the physiological relationships between variables are defined in analogous relationships between variables in the model [5]. Such a model can be represented by either a physical system or mathematical equations.

Models can be used for many purposes [5]:

1. to elucidate biomedical mechanisms by implementation of known physiological relations into mathematical equations and mechanical structures,
2. to extract specific information from measured signals,
3. to study the effects of changes in the structure and properties on the behaviour of a system as a computer-assisted learning tool or training device, and
4. to reduce animal experiments for education and by performing preceding simulations of phenomena before an animal experiment is done.

In the research described in this thesis two types of modelling have been applied: mathematical and mechanical (physical) modelling. In a mechanical model the simulation of physical variables is an essential part of the simulation, input and output will be given e.g. as gasflow and pressure.

A *mathematical model* is a representation of a (physiological) process by means of equations, the input and the output will be given in numerical terms. These type of models enable to study a process in an analytical or numerical way. The

increasing power of computers and the development of powerful numerical methods have enabled the implementation of complex models against low costs. The mathematical relations in the model and the values of specific parameters will define its behaviour. Uhl and Lewis [6] were probably the first to use computer techniques to model the effects of the input-output relation for lung function studies. They described a model in which the compliance of the lung and the resistance of the airways were defined in order to describe the relation between the pleural pressure in the lung and the flow measured at the mouth.

Parameter estimation techniques enable the estimation of the underlying structure or behaviour of the model from measured signals. A sensitivity analysis of the parameters in a model will not only give a better understanding of the behaviour of the model, but will also indicate the reliability of the parameters when they are derived from measured data.

In a *mechanical model* the physiological process is simulated with physical components. Mechanical modelling can be regarded as a bridge between mathematical models and measurements performed on healthy volunteers and patients. With a mechanical model the interaction between program and lung function equipment will approach the physical reality as far as possible. They are used to test lung function equipment [7-10], and to coach technicians and physicists in a simulated patient environment [11, 12].

Meyer designed a microcomputer-controlled respiratory servo system [9] and a hydraulically operated cylinder-piston and a solenoid valve assembly. The flexibility of selection between different breathing patterns enabled the implementation of complex sequences of breathing manoeuvres in accordance with the breathing pattern of healthy volunteers and patients. Up to that time only sinusoidal breathing patterns were simulated by means of a piston assembly eccentric connected to a rotating wheel. Myojo [13] described a breathing simulator with a split/cam valve without a piston or bellows. The opening of the split/cam valve was controlled by a stepper motor under microcomputer-control. With this system, inspiratory flow patterns could be simulated as seen during spontaneous breathing. Jansen et al. [14] used a bolt and spindle combination to construct a ventilator which imposed different types of patterns on experimental animals. These patterns could be changed from one breath to another. We adapted this technique to develop a mechanical lung model, which was intended to function as a mechanical model for testing programs in pulmonary routine and for instruction. The limited possibilities to simulate proper compliance and compressible airways were eliminated by the development of a new modelling technique. This second generation of the mechanical lung model offered so much potential for new applications that it became a main topic of this thesis.

OUTLINE OF THE THESIS

The application of computers for the Lung Function Information System (*LFIS*) is described in Chapter 2. This *LFIS* performs data analysis of pulmonary function tests at different locations. It is connected to the Hospital Information System (*HIS*) for the retrieval of patient data and the storage of lung function variables of the patients to generate follow-up reports and to support financial and administrative management.

Next we present a non-linear mathematical model of pulmonary airways dynamics (Chapter 3) describing the relationship between the pressure in the alveoli and the flow at the mouth. In this model the indentificability and sensitivity of the estimated parameters were studied.

A mechanical model, described in Chapter 4, consists of a computer controlled piston driving two lung compartments by means of a liquid-filled intermediate compartment. A compressible segment of the airways was simulated with use of a penrose tube in the liquid-filled chamber.

A further development of the mechanical model is presented in Chapters 5 and 6. The techniques described in these two chapters, enable new possibilities to simulate different aspects of mechanical lung behaviour. Not only simulation of normal breathing as done with the model described in Chapter 4, but also artificial ventilation could be simulated. This development decreased the limitations of the model described in Chapter 4.

In the closing Chapter 7, a summary is given of the present situation with a perspective to future applications and developments.

CHAPTER 2

A LUNG FUNCTION INFORMATION SYSTEM; LFIS

AFM Verbraak, E Hoorn, JJ de Vries, JMB Bogaard, A Versprille

INTRODUCTION

In 1964 Schonfeld et al. [15] described the use of computer techniques for the analysis of the pulmonary function measurements; since then many such programs have been developed. Progress in the application of automatic data processing has run in parallel with the development of the technical facilities and in many of the first systems remote computers were used for the analysis of the data [16-18]. In the first development the signals, the patient number and the spirometer calibration factor were stored on a magnetic tape and processed afterwards [15, 16, 19]. Next, on-line processing was established through connections between equipment and remote computers [20-22]. Programs for the calculation of the lung function values of hand-measured data and the generation of a lung function report have been published by several authors [21, 23-29]. Stand-alone real-time systems were described for either clinical routine or research objectives. Examples of these are the flow-volume curve and spirography [30-32], the body plethysmography [33-35], measurements of lung compliance [36], and exercise testing [37-40]. In many respects the automation improved the data processing [41] substantially and several authors have investigated potential benefits [23, 25, 32, 42].

To our knowledge no integration of the various types of measurements at different locations in the lung function laboratory have been published, let alone for

a system connected to a Hospital Information System (*HIS*). We aimed to develop a lung function information system (*LFIS*), including its connection to the *HIS*, to serve the data processing of a wide variety of lung function routines and research measurements, and in addition to serve administrative procedures. The development implied two stages:

1. the off-line automatic processing of data obtained by hand from the signals of lung function tests, and
2. the on-line real-time data processing of the signals.

In this paper we described the concepts of the system, its hardware and software. Furthermore, we evaluate the profit in time and the improvement in quality compared with the conventional by-hand situation.

METHODS

In industry and other research centres no proper software package has been available to fulfil the requirements of *LFIS*. Available software developed by the industry, was only suitable for their particular lung function equipment and the sources of their programs were not available. Therefore, we could not adapt their software to our specifications and we had to develop our own integrated system. Firstly, we defined the general requirements for the automatic data processing.

General requirements

The input of patient data had to be done at the administration desk as well as in the different laboratory rooms. During the measurements the lung function technician had to control the measurement procedures and check on-line the results of the manoeuvres. Therefore, a real-time calculation and a graphic presentation of the most important signals on the graphical terminals (Figure 2.1) were conditional for the lung function technician to be able to judge whether maximal values of several variables were obtained.

Maximum flexibility in the software program was necessary to define an individual program of measurements adapted to the specific conditions of a patient. This flexibility had to include the ability of the technician to change the selection afterwards and appended values from other measurements.

The results of the measurements performed in the different rooms had to be presented alpha-numerically as well as graphically in a final report. The connection to the *HIS* delivered the general data concerning the patient.

Realization of the system

At time of writing the system was composed of one central computer and seven satellite computers, each attached to the lung function equipment. The benefits of a centralized system were combined with those of several stand-alone systems [43].

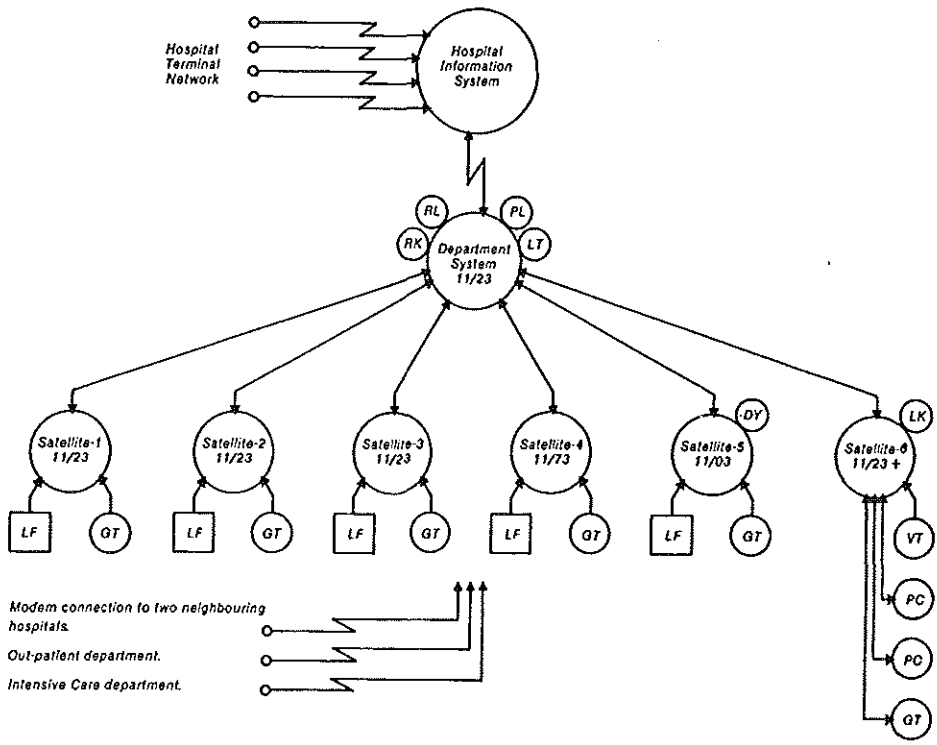

Figure 2.1:
Distributed Computer System of the Pulmonary Function Laboratory.
DY: Floppy disk (.5MB); GT: Graphic terminal; LK: Hard disks (40 MB);
LP: Laser printer; LT: Matrix printer; PC: Personal Computer;
RK: Hard disks (7.5 MB); RL: Hard disks (25 MB); VT: Video Terminal;
LF: LFunct. Equipment; 11/23;11/23+;11/73: PDP-11 computers.

The main advantages of this approach are:

1. centralisation of expensive devices, databases, and software;
2. gradual development of the system corresponding to the automation of new pulmonary function tests;
3. expansion of the system dependent upon an increasing load on the pulmonary function laboratory as well as on the development of new measurements;

4. parallel data processing of measurements in the satellites which guarantees a fast system response;
5. a relatively modest central system;
6. a relatively small vulnerability of the total system which guarantees a continuous service of the pulmonary function laboratory. During disorders and maintenance of the central system a satellite can be used as such, and during the breakdown of a satellite only one unit of lung function measurements is out of function without affecting the overall service of the laboratory.

Commercially available hardware and system software were selected as far as possible.

Application software

The programs were written in *Fortran* and for some special functions (e.g. Analog to Digital (A/D)-conversion) an assembler language was used. The software was structured in such a way that it could be adapted to the changes in hardware and to the requirements of the software.

Table 2.1: System File (see text).

Item	Options and settings
General	Version of system set-up, current data, last time the system was used, barometric pressure, minimal and maximal allowed laboratory numbers, current laboratory number
Allowed Programs	Names of the programs
HIS communication	User name of the system, password of the system, location code, session type (test/production), login-flags, time-out flags
Follow-up	Last date when the major change in follow-up report was made

The information concerning the system configuration is defined at two levels. Firstly, the system file (Table 2.1) contains all the variables and settings that are common for all satellites, e.g. the barometric pressure and the settings for the communication with the *HIS*. Secondly, the satellite file (Table *2.2*) contains the specific information for each workstation, such as the type of computer hardware in the satellite and the identification of the lung function equipment connected to the satellite and the laboratory number of the patient to be tested. The start-up procedure and the execution of the application programs are adapted to the settings stored in the system file and the satellite file. Through information stored in these files, a mixture of different types of hardware is supported by the

software, which avoids the development of specific programs that are only valid for a specific hardware configuration.

Table 2.2: Satellite File (see text).

Item	Options and settings
Equipment set	Several lung function devices per satellite
Terminal type	Graphic terminal (Tektronix 4025, VT240), alpha-numeric (VT 100)
Room number	Room number where the satellite is located
Default printer	Laser (LN-03), Matrix (MT 85)
Data switches	Normal, inverted
A/D convertor	A/D or A/D and D/A programable gain, fixed gain
Real-time clock	Programable, fixed frequency
Processor	11/03, 11/23, 11/73, (No) floating point hardware

Additionally, a chaining facility is supplied by the system software to enable a program to call another program directly without input from the laboratory technician. To avoid the need for input of already known data by the technician, a common area in the memory is used for exchange of variables between programs. The chaining facility is implemented at five levels. The first program in the chain has the highest level. When a program in the chain is started it, checks whether it has been activated by another program in the chain or by a technician. When it is activated from another program it checks whether it is called from a higher or a lower level. Then the program reads the data from the common area in the memory and controls whether it is started at its beginning or at some other point. This latter option enables to use whole programs as subroutines in other programs.

A maximal flexibility in the patient-computer-technician interaction was a main problem in the on-line automatic data processing. Function keys and a menu structure were used for the communication between computer and technician. Parameters already known can be passed as much as possible from one program to another. Switches of the lung function equipment and a special switch panel are read by the program to activate options in the program. These switches control the routine measurements. Moreover, special options can be activated for research and debugging facilities. Such a set-up requires minimum attention from the technician to the computer system during the measurements.

It is essential that all data stored in the *HIS* are correct. Therefore, the technician has many possibilities to correct earlier decisions and cancel or change variables. These alterations are a prerequisite for an automated system to have a correct database.

System hardware

The hardware of the system was based on *LSI*-11 processors (*Digital Equipment Corp. MA, USA*). Standardization in the hospital was based on this type of computer which facilitated the start of the automatic data processing (e.g. the transfer of off-line programs from a remote computer to the new system of the department). The development was initiated with one stand-alone system incorporating a mass storage device, a real-time clock, an *A/D* converter, a digital input and output module, a printer and a graphical terminal. This system was used to demonstrate the feasibility of the data processing according to the requirements as mentioned previously. Using the same structure for the central computer and the satellites we could , the components necessary for the real-time data acquisition from the stand-alone system to the satellite, the stand-alone computer was upgraded to the central system.

In the total network as presented in Figure 2.1, three function levels can be distinguished:

1. The *HIS* consists of a twin system (*VAX 11/785, Digital Equipment Corp. MA, USA*) with more than 800 terminals. It provides the general patient data to the *LFIS* for integration with the measured lung function data. Moreover, the *HIS* is used for long-time storage of lung function data which must be available on-line.
2. The central department computer functions mainly as a management computer for all satellites. It contains those devices that can be shared by the satellites. The system consists of a processor (*PDP 11/23*), memory (*32kW*), background memory (*25 Mb*), console terminal (*LA36*), laser printer (*LN03-plus*), needle printer (*MT 85*) and communication lines to the *HIS* and to the satellites.
3. The satellites handle the on-line and off-line program execution under direct control of the lung function technician. The satellites contain the facilities for the *A/D* conversion, the read-out of equipment switch settings, and a high resolution graphic display (640*480 pixels).

In principle these satellites contain no facilities for the storage of programs and data. In the satellites the processors, the memory, the *A/D* convertor, the real-time clock and the attached terminal are from different types. Although the satellites have prescribed tasks, their possibilities can be extended with special functions such as a *D/A* convertor and a floppy-disk drive. One of the satellites,

number 6, is used for off-line activities (e.g. for the administration desk and for program development). It also functions as a back-up system for the central computer. This satellite is equipped with a local Winchester disk (*CDC-Lark, 20Mbyte*) and a magnetic tape (*Cipher 891-2*). Additionally, a personal computer (*PC*) is connected to it. Mainly this *PC* is in use for exchange of files, text processing and statistical analysis.

System software.
The system-software is based on commercially available packages. Basically it is a single-user, real-time operating system with a foreground-to-background monitor (*RT-11, Digital Equipment Corp., MA, USA*). On top of this the *STAR-11* (*Hammond Software, Göttingen, Germany*) package is run. In the host, *STAR-11* handles in the foreground the communication with the satellites, while the background can be used for application programs or software cache. A maximum of 16 satellite systems can be served by this operating system. At the time of writing we had connected seven systems. In each satellite at least one *RT-11* work-place is created. By means of the system software *SHARE-11* (*Hammond Software*) a multi-user environment was created in satellite number 6. As pointed out earlier, this satellite is used for none-time critical functions. Finally, satellite 7 can be used as a stand-alone system or as a satellite.

Organization of Data Acquisition
The patient routine measurements, administration and patient-linked research at the pulmonary function laboratory, are reviewed in Figure 2.2. On arrival the patient is registered in the laboratory system and a laboratory number is given as a reference for all measurements to be performed. Then, the patient data are read from the *HIS* and stored as a patient file in the laboratory system. When no patient data are available from the *HIS* a local input is made. Information that is important for the lung function tests and the final report, such as the anthropometric data of the patient, the preliminary diagnosis and the name of the physician who requested the tests, are added to the *HIS* data. When the patient has been tested previously, the essential information for the performance of the next testing is automatically transferred from the *HIS* to the laboratory system. Such information indicates the presence of spirometry-induced asthma, the necessity of using the arm span as a measure for length for patients with scoliosis, the level of cooperation of the patient, and any language problems. The information that is important for the next test is indicated and stored in the *HIS*.
Furthermore, during the measurements the patient file in the laboratory computer is updated with the information for financial administration and workload registration.

A broad spectrum of programs is implemented in the laboratory system. These are used for either clinical routine or research, e.g. spirometry, flow-volume, body plethysmography, capnography, compliance, exercise testing, ventilatory CO_2-sensitivity, hyperventilation provocation testing, single breath diffusing capacity for *CO* (*DLCO*) and rebreathing *DLCO*. The on-line and off-line programs can be performed in different rooms and different sequences. The sampled signals and the calculated data, relevant for the technician to guide the patient through the measurements, are displayed on the graphical terminal.

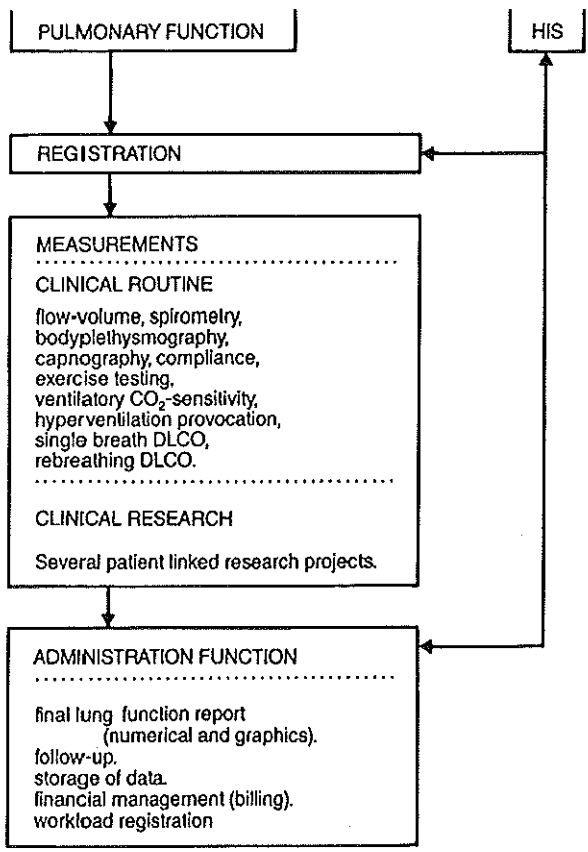

Figure 2.2:
Organization of data acquisition and financial and administrative procedures at the Pulmonary Function Laboratory.

During the measurements the values obtained are compared with their reference values. Each computer program creates at least two files. One binary file is used to store all sampled data together with a logging of activities undertaken by the technician for the technical control of the measurement process. Storage of the signals and the logging enable an off-line recalculation. In addition, the stored signals can be used for specific research projects. In the second binary file, the result file, the calculated data, which will be integrated in the final report, are stored. Moreover, additional files can be created either for additional calculations and research purposes or for integration of graphics information in the final lung function report.

Maximal accuracy and reliability guarantee long-term use of the database and, therefore, corrections of the measured data have to be done before the final lung function report is printed. All programs for on-line data acquisition in routine lung function have an additional off-line program for processing hand-measured functions either to change or to delete values obtained on-line. Selection and rejection of manoeuvres and calculated data can be done during and at the end of the series of measurements. The various decisions made by the technician are supported by the program. The technician can always overrule the computer.

In the final lung function report, the results of the lung function tests are compared with their reference values. The interpretation of the data can be typed by the secretary through a standard text processor and can be included in the final report. When necessary the values of the previous tests are read from the *HIS*, linked up with the new data and generated into a follow-up, graphically presented over a time span of 1, 5 or 10 years. Some variables are presented as a percentage of their reference values (Figure 2.3a), other data are plotted in absolute values (Figure 2.3b). The effects of a bronchodilator are also indicated.

Finally, the measured values are authorized and stored in the *HIS*. In addition, the workload registration and the financial administration is transferred via the *HIS*.

Each morning a backup of the result files of the preceding day is made on another disk. The other files are also copied to another disk and removed from the routine disk. These files are only stored for one day. A different procedure can be followed for special research measurements; these files could be copied to a special disk or a magnetic tape for further analysis at a later date.

2.3a

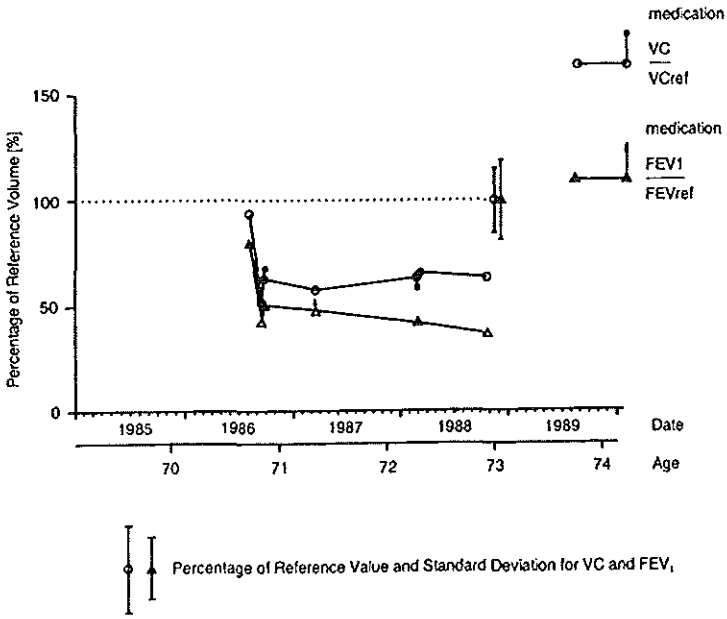

2.3b

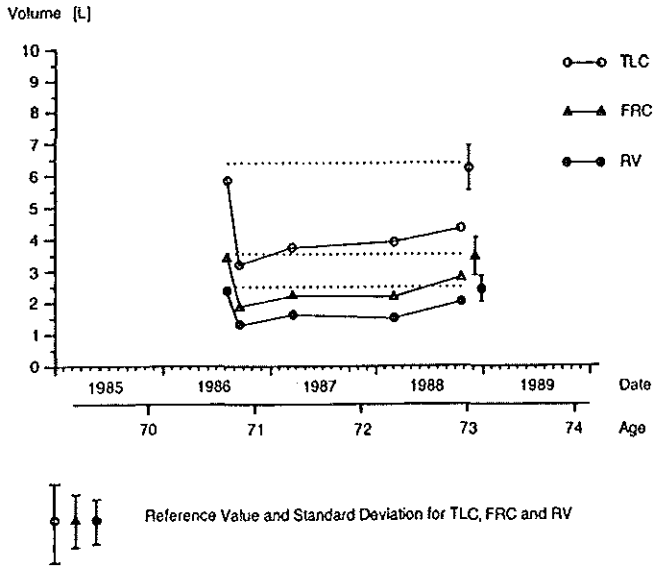

Figure 2.3:
Follow-up reports.

a. *This follow-up report represents the change of the Forced Expiratory Volume in one second (FEV_1) and Vital Capacity (VC) and the changes after medication with a bronchodilator. Data are given in percentage of the reference values.*
b. *This follow-up report represents the absolute values of Total Lung Capacity (TLC), Functional Residual Capacity (FRC) and Residual Capacity (RV) together with the reference values and the standard deviation for the last measurement.*
The x-axis can be plotted over a time period of 1, 5 or 10 years.

RESULTS

The automatic data processing in the lung function laboratory resulted in an increase in quantity and an improvement in quality of the lung function tests.

Increase in quantity

To estimate the gain of time by the automatic data processing with respect to the conventional situations, we have calculated the time necessary for the performance of measurements and data analysis for three situations:

1. in the conventional situation where the technician had to do all data processing by hand, including the writing of the final results in a final pre-printed report.
2. at the first stage of automatic data processing in which the raw data of the measurements were calculated off-line and automatically printed in a final report, including comparison with reference values.
3. utilizing full on-line data processing from measurements to the final report.

Table 2.3 shows the increase in capacity, as related to the automatic data processing, for the set of four measurements that are performed most frequently. The number of tests performed on patients is normalized with respect to the number of spirometric measurements executed annually. The weight factor is the number found by dividing the total number of measurements of each type by the number of spirometry measurements, which was 3500 in 1987. Thus, the number of CO-diffusion determinations was 0.17 * 3500 = 600. The measurements and the calculation time were connected to the weight factors to get a weighted gain of time for the four types of lung function tests. Thus the real measurement time for a CO-diffusion measurement was 5.1/0.17 min = 30 min. In 1974 the total number of lung function tests was 12,543 performed with five technicians. In 1987 the number was 19,540 performed with 5.8 technicians.

The time for measurements is equal for the three situations, and is largely influenced by the degree of illness, intelligence and cooperation of the patient and by any language problems that may arise.

The time values in Table 2.3 were obtained from the information given by five technicians, and the analysis of the production per technician over a few months in all situations. Our estimation of a gain of about 35% (86.3/64.1) by off-line data processing with respect to the conventional situation is in agreement with that of Protti et al. [11]. The numbers indicate a further gain to more than 66% (86.3/51.8) when using on-line data processing. The total number of tests performed at the laboratory is another indication for the gain of quantity. Since 1974 the profit in the number of tests is 34% when normalized per technician.

This number is the overall result of the laboratory, which is smaller than the profit of about 60% in the spirometry of Table 2.3. These differences are due to:

1. correction in the gain by on-line data processing of activities other than lung function testing per se, whereas no such correction is present in the increase of the number of tests.
2. introduction of other tests since 1974, such as body plethysmography, exercise testing, CO2-response measurements.
3. use of another type of bronchodilator, which resulted in an increase in measurement time of 10-15 minutes because of the greater time delay between administration to a patient and the measurement of the reaction.
4. execution of measurements for special research projects, which were not performed before that time. In tests with time-consuming data analysis, such as compliance and body plethysmography, the profit in time is much larger when using on-line data processing.

Table 2.3: Gain of time due to automatic data processing (*ADP*).

			Weighted time for calculation and reports		
Type of Measurement	Weight factor for measurements	Weighted time for measurements	Conventional (technician) (min/patient)	Off-line (*ADP*) (min/patient)	On-line (*ADP*) (min/patient)
Spirometry	1.00	15.	20.	10.	5.
Spirometry after medication	57.00	8.6	11.4	5.7	2.9
Residual volume	57.00	11.4	11.4	5.7	2.9
CO-diffusion	17.00	5.1	3.4	2.6	0.9
		40.1	46.2	24.	11.7
Total time including measurement time			86.3	64.1	51.8
Decrease in workload from		conventional to off-line *ADP*:		0.74	
		off-line *ADP* to on-line *ADP*:		0.81	
		conventional to on-line *ADP*:		0.60	

Improvement in quality

The off-line automatic data processing eliminated incidental miscalculations by hand. The on-line data processing also diminished the inaccuracies in the sampling of the analogue signal, which was performed by measuring the deflections on the recording paper of the spirometer and other devices by hand. In addition, there is a standardization in the analysis of, for example, the starting point of the

Forced Expiratory Volume in 1 second (FEV_1) manoeuvre and the calculation of O_2 uptake by regression analysis on successive end-expiratory levels from the spirogram. On-line data processing implied correction of signals for different types of drift in different types of tests, e.g. slow-pressure drift and temperature drift. The integration of information from different measurements, and the presentation of data together with the reference values (Figure 2.4) enable a better interpretation of the results. By hand this would cause a significant increase in time, (not included in Table *2.3).* The same holds for the generation of the follow-up report (Figure 2.3a and b).

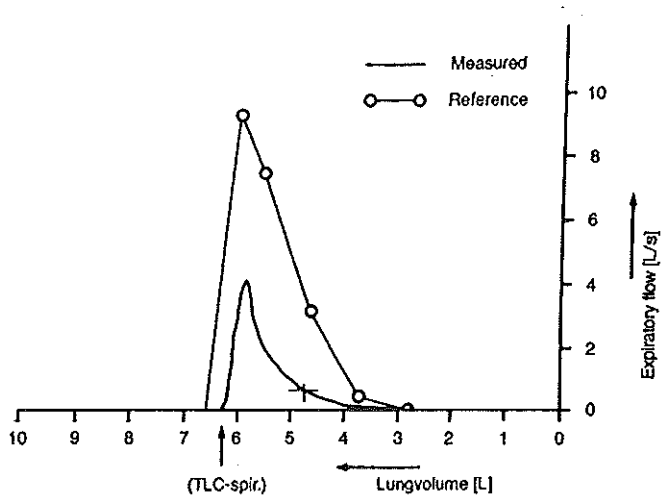

Figure 2.4:
A forced expiratory flow-volume curve of a patient is presented in combination with its reference curve. The curves are plotted 'Volume-based' starting at measured TLC (by spirometry) and reference TLC, respectively. + indicates the FEV_1 .

An additional result of the automatic data processing is the introduction of new measurement techniques that otherwise could not be applied routinely and which improve the diagnosis. Examples are the on-line calculation of the effective airway resistance in body plethysmography [44, 45], the use of parameter estimation techniques based on model simulations [46], and the analysis of the capnography signal, not only against time but also against volume [47].
Finally, most values of the different manoeuvres are given on-line to the technician. Formerly, the technician had to calculate the values by hand between the different manoeuvres to decide whether to stop the measurements or continue to

obtain maximal values. The automatic data processing allows the technician to pay more attention to the patient.

DISCUSSION AND CONCLUSIONS

The benefits obtained from the computerized system are: an improved accuracy and precision of observations and results, the standardization of terminology and format, increased accessibility and availability of patient data, a reduction in observer variation, the provision of individual patient records with multiple observations in a manageable form and an improved legibility of the patients data report. Moreover, the data stored in the *HIS* could be used for a wide range of administrative needs, e.g. billing, status reporting and the provision of basic data for the follow-up. The lung function laboratory is responsible for the consistency of the data stored in the *HIS*. The *HIS* guarantees a reliable storage of data. Moreover, a back-up is made of the data on a separate disk at the laboratory.

The introduction of off-line automatic data processing has as its main effect an increase in capacity against minimal costs. The additional implementation of on-line real-time automatic data processing resulted in a further improvement in capacity, but mainly it improved the quality of measurements and enabled the introduction of new measurement techniques, which could not be performed otherwise. The presentation of measured values and the reference values in one figure improved the interpretation of the lung function tests.

The vulnerability of the *LFIS* appeared to be minimal due to the decentralized system approach. The central department computer, which is used by all satellites, was kept as simple as possible. Therefore, the risk of breakdown was reduced. If the central system could not be used because of technical or maintenance problems, one of the satellites took over its function and at least three laboratory rooms could remain in routine use. The interchangeability of the system components influenced the reliability of the system as a whole in a positive sense. Down-time due to problems in one of the satellites or cable problems will only affect the satellite involved. In case of severe problems in the host system, it takes 10 min to restart the network with satellite no. 6 as the new host system. Through the decentralized system approach, instead of one central computer, it was possible to enlarge the automatic data processing more easily and to follow the newest technology for the additional satellites. In our set-up we made use of the micro-processor (*PDP 11/23, Digital Equipment Corporation, MA, USA*). Programs are available on certain conditions and after mutual consultation. At the moment the new developments are based on personal computers and programmed in Pascal. In the near future the whole system set-up will be

converted to *PC*-based systems and Ethernet cabling.

In 1988 approximately 20,000 lung function measurements were performed on about 4000 patients. Lung function equipment of different manufacturers was used because of the changing demand with respect to specifications and because of the time differences in the purchase of the equipments.

In contrast to other reports [15, 18], in our opinion the technician must be specially trained if automatic data processing is introduced, as they have a higher level of responsibility. Because the results of the measurements become available on-line, the technician has to decide during the tests whether to go on with the measurement, to go to the next measurement or to stop. In addition, the technicians have to understand at least the principles of automatic data processing to be able to judge the results given by the computer systems and to be able to see whether the hardware or software functions satisfactorily.

The multiprocessor network, integrated at the department level and hospital level, resulted in a flexible and reliable system. The success of the developed system was partly due to the attention given to the pitfalls in developing a system, as summarized by Friedman et al.[48]. There has been a strong interaction between the physicians, the lung function technicians and computer experts. A division of the projects to clearly separated parts has given well-defined results for the department. By the purchase of commercial parts as far as possible, we could limit ourselves to those problems specific to the processing of lung function data. In addition the hospital management has supported the project to a large extent and continues to do so. To guarantee optimal use of automatic data processing, it must always be possible to change the programs to test and introduce new techniques, that follow new medical insights, and take up new demands from the department. This is essential especially in an academic environment.

APPENDIX

The data processing described in this chapter reflects the situation in 1990. This appendix serves to present an update of the *ADP* at the lung function laboratory. Since 1990 the mutual communication between computers has been improved by availability of new hardware and software for network communication. Furthermore, with the introduction of personal computers fast data processing became available against low costs. This induced many new technical developments such as program development tools and new display techniques. Moreover, many commercially available programs, such as for text processing and statistics, became available to the personal desk.

DATA COMMUNICATION: HIS

The development of new hardware and communication software enabled the transmission of data over large distances at higher speed, and connections via the network between many computers. Such achievements did not only affect the data communication at the lung function laboratory, but also influenced the data communication in the university hospital in general.
A simplified scheme of this network is given in Figure 2.A1. The serial lines are the oldest communication lines for selected and authorized access of local users to the hospital information system (*HIS*). Nowadays, their simple alpha/numerical

terminals are connected to the central *HIS* computers via terminal server connections and a local area network of the hospital (*HIS-LAN*). Other local users have a personal computer which is directly connected to the local area network (*PC-LAN*). These users can also have selected and authorized access to the *HIS*. About 1700 terminals in the hospital are directly connected to the *HIS-LAN* by means of the conventional serial communication. About 1200 *PC*-based workstations are connected via the *PC-LAN*. Now, there is a continuous replacement of terminals by *PC*-based systems.

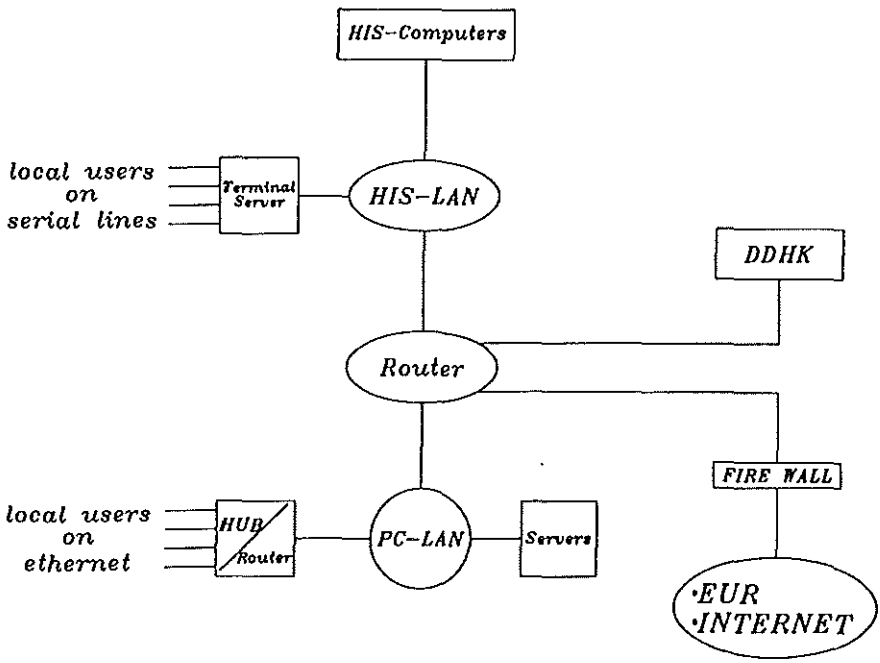

Figure 2.A1:
A schematic view showing the network facilities at the University Hospital. Local users on serial lines have connection to the HIS computers only, while local users on PC-LAN can have access to the HIS computers as well as to dedicated computers (servers) and facilities outside the hospital. Local users are connected via multiple terminal server or one or more electronic devices such as, HUB, bridge or router connected to the systems. Connections between the HIS-LAN, PC-LAN, oncology hospital (DDHK), and via a fire wall to external systems such as, the Erasmus University (EUR) and other systems via Internet.

Both the *HIS-LAN* and *PC-LAN* have connections to different locations in the Dijkzigt Hospital, Sophia Children's Hospital and Daniel den Hoed Cancer Centre. Connections between the *HIS-LAN* and *PC-LAN* enable the interchange of information between both systems. Most essential connections are made twofold via

different paths, which guarantee a connection between different locations, when one of the connections is broken. Via a *fire wall* a connection is provided with the Wide Area Network outside the hospital, e.g. to the medical faculty, library and Internet. The *fire wall* watches over the communication into and out of the hospital.

DATA COMMUNICATION LUNG FUNCTION

In 1990 each satellite computer at the pulmonary function laboratory was connected to the central computer of the laboratory. These satellite computers processed the measurement data at the laboratory and stored the results in the central computer. Via a serial connection (1200 baud) information was exchanged with the Hospital Information System (*HIS*). After a transition period, since 1994 only *PC* based systems are used as local workstations. With respect to the earlier monochrome terminals the new computers have better and faster display techniques, which improve the interaction between user and computer. The introduction of fast communication lines facilitated faster and more redundant communication between computers at different locations in the University Hospital Rotterdam, consisting of the Sophia Children's Hospital, Dijkzigt Hospital and Daniel den Hoed Cancer Centre. Maximal 50 users at the same time can have access to each of the fileservers of the lung function laboratory (Figure 2.A2). One fileserver system (*FS1*) handles not only the measurement data of the lung function workstations in the Dijkzigt Hospital, but also those of the Sophia Children's Hospital. This data acquisition will be extended to the lung function laboratory in the Daniel den Hoed Cancer Centre. The *FS1* provides a central storage of data and programs. It consists of a twin computer system which guarantees a continuous service when one of these systems is broken.
Recently the electronic storage of selected bronchoscopic images, a subsequent editing process, and a voice-over commentary is implemented for the department of pulmonary diseases. This application is multi-media oriented and based on the software for the audio-pictorial endoscopy reporting system[49] and adapted for bronchoscopic measurements by the electronic data processing department. The second fileserver (*FS2*) handles the storage of these images and the disposal to local users in the hospital. A third fileserver (*FS3*) is in use for all data processing which is not directly concerning patient care. This system is used for program development, administration, research projects, text processing and many other software programs.
Mainly custom-made lung function equipment is connected to the network, but with the increasing availability of commercial lung function equipment with incor-

porated automatic data processing, the lung function network will change to a conglomerate of equipment in which the data are combined to one patient record.

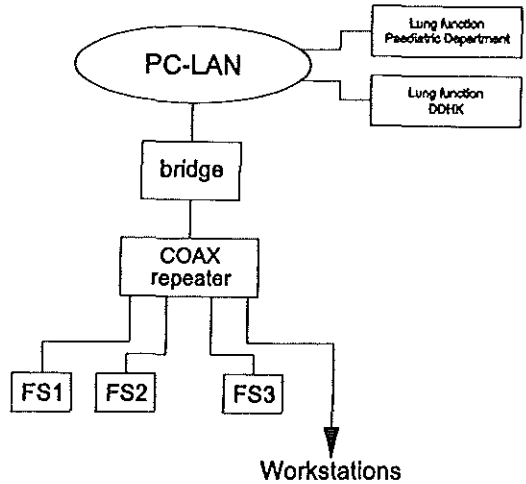

Figure 2.A2:
A schematic view showing the network facilities at the department of pulmonary diseases. The FS1 and FS2 systems are used for patient care at the lung function departments (FS1) in the three locations: Sophia Children's Hospital, Dijkzigt Hospital and Daniel den Hoed Cancer Centre and for storage of images (FS2) measured with the bronchoscope at Dijkzigt. FS3 is used for other types of data processing, such as for research, administration and program development. These systems and local users on the lung function department are mutually connected via a coax repeater and bridge connected to the rest of the PC-LAN. For further explanation, see text.

PATIENT RECORD

Each patient receives a unique patient identification (*PID*) number. In a computer-based patient record, identified by this *PID* number, information on medical investigations are stored. In the central computer of the *HIS* the majority of patient information (medical and administrative) is stored together with links to other computers, where additional information on the patient can be found. So, when a physician in the hospital is connected to the *HIS* via a login procedure, she/he can receive information about all kinds of data of a specific patient. For instance, the retrieval of lung function data via the *HIS* will need a connection to the local fileserver at the lung function laboratory where these specific data of the patient are stored. This facility is only available to local users who are attached to the *PC-LAN*. Up to now, the simple terminals are mostly distributed widely and not

every department has access to the *PC-LAN*, but more and more access to the *PC-LAN* will be available at every site in the hospital.
Because of the many advantages of a computer-based record over a paper-based record[50] a proper storage and handling of all patient data generated throughout the hospital and even outside will be of growing importance.

CHAPTER 3
THE SERIAL LUNG MODEL FOR SIMULATION AND PARAMETER ESTIMATION IN BODY PLETHYSMOGRAPHY

AFM Verbraak, JMB Bogaard, JEW Beneken, E Hoorn, A Versprille

INTRODUCTION

A direct calculation of airway resistance from driving pressure and airflow was enabled by body plethysmography. Because the difference between the volume displacement at the mouth and the simultaneous change in chest volume is caused by compression or expansion of intra thoracic gas, the plethysmograph can be used for measurements of thoracic gas volume and the alveolar pressure (P_A) inside the thorax. In 1956, et al.[51], re-established the method for clinical routine.

By plotting P_A against simultaneously measured flow at the mouth (V'_m), a pressure-flow loop was obtained. Only when P_A and V'_m yield a linear relationship the airway resistance (R) can be derived directly according to Ohm's law $R = P_A / V'_m$, where the ambient pressure is reset to zero. However, for different types of pulmonary pathology, non-linearities were found between P_A and V'_m, not permitting such a direct derivation of R.

Matthys et al.[52] made a classification of patterns that were caused by different distributions of elastic and resistive properties of the lung, and by the pressure and flow differences in different parts of the lung.

Usually, estimates of airway resistance were obtained graphically from the body plethysmographic pressure-flow diagrams. Reinert et al.[53] restricted their analysis to the linear parts of pressure-flow curves. Ulmer et al.[54] estimated

airway resistance from a few discrete data, as e.g. total resistance (R_t), which is calculated from the line through the two extreme values of pressure in the inspiratory and expiratory part of the curve and from lines through mean pressure points at flow rates of 0.5 $L.s^{-1}$ during inspiration and expiration [55]. In 1975 Smidt et al.[56] proposed to calculate an effective flow resistance variable (R_{eff}), which was related to the dissipation of energy during the whole respiratory cycle. R_{eff} was defined as the integral of pressure times volume increments divided by the integral of flow times volume increments. This variable was comparable with the effective resistance as defined in alternating current theory. Holland et al.[45] showed that R_{eff} was almost independent of those errors in P_A, which were associated with differences in humidity and temperature between inspired and expired air.

System identification and parameter estimation on the input-output data receive increasing acceptance in physiological research [57]. Until now only a few papers in the field of body plethysmography dealt with modelling techniques to estimate the physiological variables describing lung mechanics. Banerjee et al.[58] and Cettl et al.[59] attributed the degree of looping of the P_A - V'_m patterns to parallel in homogeneity and modelled it by two *RC*-branches in parallel, as described by Otis et al.[60]. Another group of authors [61-64] modelled a serial in homogeneity, describing the lung as an alveolar compartment, lower and upper airways and a compliant element in between, allowing a simulation of airway compression during expiration. The serial model of Feinberg et al.[62] was based on a comprehensive mathematical basis, rather than on a physiologically well-defined lung model to obtain a quantitative indication of various aspects of lung mechanics. An estimation routine fitted the model to the data, obtained during panting. Golden et al.[64] used the same type of model with a restricted number of parameters. From this restricted model they derived a selected set of parameters from the measured signals, obtained during panting.

The serial models published so far are dependent on panting manoeuvres to approximate a constant lung volume during the measurements. We extended the lung model described by Golden et al.[64], with lung compliance dependent on lung volume, to adapt it to the circumstances of normal breathing. Additionally, we have improved the model by giving a better physiological basis for the compressible element based on more recent publications. Furthermore, we evaluated the sensitivity and the uniqueness of the estimated parameters and the influence of noise.

THEORY AND METHODS

The serial lung model

For the definition of the model the functional approach of Golden et al. [64] was used. The model (Figure 3.1) was restricted to serial in homogeneity with respect to both resistance and elastic properties of the airways. All alveoli were lumped to one compartment (V_A), which was connected to ambient air by a tube representing the lumped airways. This tube consisted of three parts in series: one for the small airways, a compressible element in between, and one for the upper airways.

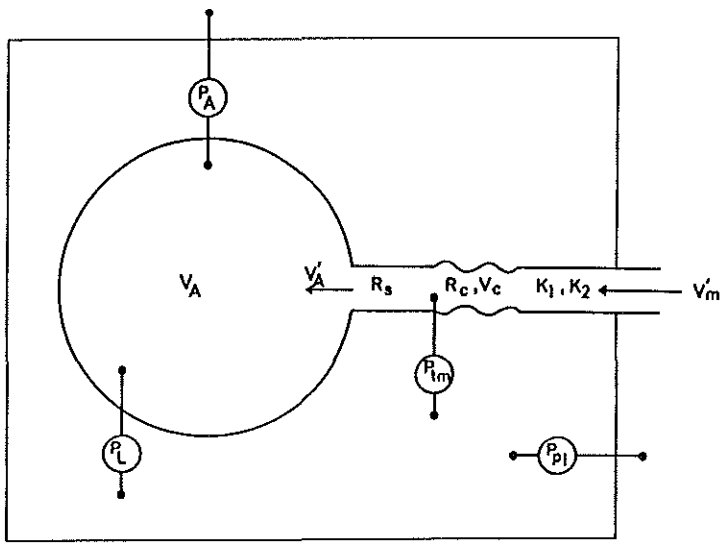

Figure 3.1:
The serial lung model.
For explanation of the different variables see list of symbols and text.

The alveolar compartment and the intrapulmonary airways were influenced by the intra thoracic pressure, which was equal to pleural pressure (P_{pl}). Golden et al. [64] assumed lung recoil pressure (P_L) to be constant because of the small lung volume changes during the panting manoeuvres. The elastic properties were modelled such that P_L increased when alveolar volume (V_A) increased.

In the range of normal breathing we assumed that the increase of P_L against the change in alveolar volume yields:

$$P_L(t) = P_{L,FRC}(0) + \frac{1}{C_L}\int V'_A(\tau)\partial\tau \qquad (3.1)$$

where:

C_L	*lung compliance, in $L.kPa^{-1}$,*
$P_{L,FRC(0)}$	*P at functional residual capacity (FRC), which is the lung volume at the end of normal expiration, and thus at the beginning of normal inspiration, in kPa*
$t = 0$	*moment at which inspiration starts, in s*
$V'_A(\sigma)$	*flow into the alveolar compartment at time $t = \sigma$, giving inspiratory volume at any value of t by integration, in $L.s^{-1}$*

In the case of normal breathing, as in our model, the magnitude of the flow is such that the pressure drop produced by convective acceleration can be neglected, and so airway pressure at different sites in the airways is assumed to be a function of frictional pressure loss only.

Airway resistances

The resistance of the upper airways (R_u) was modelled as a rigid part. R_u included a flow-dependent term, and was expressed by the "Rohrer equation" [65]:

$$P_u = R_u V'_m = K_1 V'_m + K_2 V'^2_m \qquad (3.2)$$

where:

P_u	*pressure drop in the upper airways, in kPa*
K_1	*factor related to the pressure drop due to laminar flow in the upper airways, in $kPa.s.L^{-1}$*
K_2	*factor related to the pressure drop due to turbulent flow in the upper airways, in $kPa.s^2.L^{-2}$*
V'_m	*flow at the mouth ,in $L.s^{-1}$*

The resistance of the small airways R_s was assumed to be constant and we neglected the influence of the lung volume changes during the breathing manoeuvre at volumes above *FRC*. Based on the dimensions of these airways a Poiseuille flow was assumed. So, the linear pressure drop (P_s) in these airways is given by

$$P_s = R_s V'_A \qquad (3.3)$$

where:

R_s	*resistance of the small airways, in $kPa.s.L^{-1}$*

The resistance of the compressible element represented the resistance in those airway generations, which are susceptible to the changes in transmural pressure (P_{tm}) being the difference between intra bronchial and pleural pressure. The

functional behaviour of the compressible element was modelled as a nonlinear relationship between P_{tm} and its cross-sectional area. P_{tm} of the compressible element was located between this element and the small airways and was assumed to be the same over the whole element. Furthermore, a constant length and an equal cross-sectional area over its length is assumed. Thus, the cross-sectional area can be expressed in terms of volume (V_c). Assuming a laminar flow the resistance in a tube of constant diameter (r) and length will be proportional to $1/r^4$ and thus to $1/V_c^2$. V_c was normalised to the maximum volume (V_{cN}) of the compressible element for the normal lung, having a recoil pressure of 0.5 kPa at *FRC* level.

The largest changes in volume will occur for changes in P_{tm} around zero. The site in the element where P_{tm} equals zero is called the equal pressure point (*EPP*), [66, 67]. The location of the *EPP* depends on the elasticity of the lung and the small airway resistance (R_s).
This dependence is described by equations (3.4-3.7).

$$P_{tm}(x) = P_{br}(x) - P_{pl} \tag{3.4}$$

where:

$P_{br}(x)$	*intra bronchial pressure as function of the location x in the airways, in kPa*
P_{pl}	*pleural pressure, in kPa*

If during breathing eqn. 3.3 is valid then:

$$P_{br}(x) = P_A + R_s(x)V'_A \tag{3.5}$$

where:

Rs(x)	*cumulated airway resistance from the alveolus to the location x in the airways, in kPa.L^{-1}.s*

P_{pl} is the sum of recoil pressure (P_L) and alveolar (P_A):

$$P_{pl} = P_L + P_A \tag{3.6}$$

From eqns. 3.4, 3.5 and 3.6:

$$P_{tm}(x) = P_L + R_s(x)V'_A \tag{3.7}$$

EPP will be found at the location x where $P_{tm}(x) = 0$. Then the driving pressure for the flow is given by P_L and is determined by the small airway resistance ($R_s(x)$). This means that the *EPP* is shifted upstream or downstream, dependent on recoil pressure and/or small airway resistance.
The stiffness of airways increases from the alveoli towards the mouth [68]. The model described neither the location of the *EPP* within the tapered serial system

with gradually changing R_s in detail, nor the dependence of the airway compliance on generation number. Therefore, it was necessary to find another solution for the modelling of the changing properties of the compressible element in dependence on the location (x) of the *EPP*. A low P_L means a more peripheral located and less stiff compressible element with a larger volume at maximal distension. Therefore, we modelled the elastic properties of the compressible element in dependence on the P_L values.

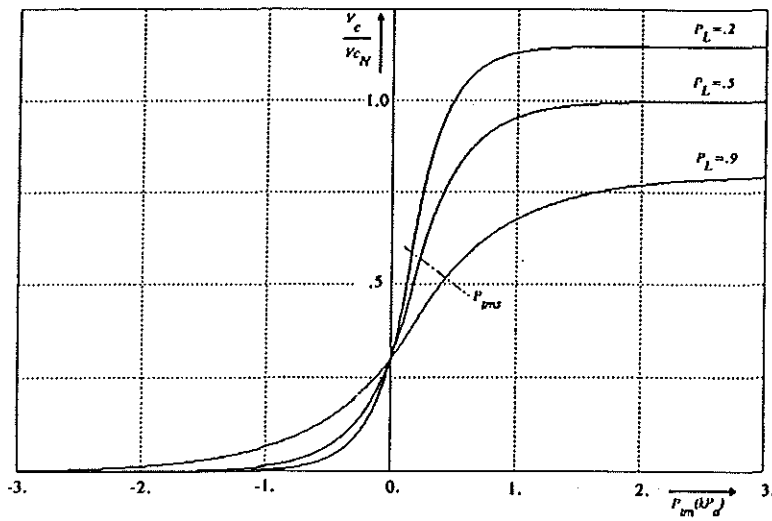

Figure 3.2:
The relation between the normalized volume of the compressible segment (V_c / V_{cN}) and the transmural pressure (P_{tm}) with the lung recoil pressure as parameter. For symbols see list of symbols and text.

The mathematical description of the volume behaviour of the compressible element in terms of P_{tm} (Figure 3.2) is as follows:

$$P_{tm} \geq P_{tms} \qquad \frac{V_c}{V_{c_N}} = S - \frac{S^2}{1.2} \times \left[\frac{0.6}{S}\right]^{\left(\frac{P_{tm}}{P_{tms}}\right)} \tag{3.8a}$$

$$P_{tm} < P_{tms} \qquad \frac{V_c}{V_{c_N}} = 0.3 \times \left[\frac{0.6}{S}\right]^{\left(-\frac{P_{tm}}{P_{tms}}\right)} \tag{3.8b}$$

$$P_{tms} = 0.15 + 0.05P_L \tag{3.9a}$$

$$S = 1.25 - \frac{P_L}{2} \tag{3.9b}$$

where:
S *an auxiliary variable to optimize calculations.*

The equations (3.8a-3.9b) describe the relationship between the transmural pressure over the compressible element and the volume of this element, with lung recoil pressure as a parameter. These relationships are adapted from literature and have been based on measurements in dogs and extrapolated to humans [69-72]. For mathematical convenience the curves were considered to be sigmoidal and split up into an upper and a lower part with an intersection at $P_{tm} = P_{tms}$, where P_{tms} is the point of curvature. P_{tms} depends on lung recoil pressure (eq. 3.9a). A continuous set of curves was used over the whole range of static lung recoil pressure values. The volume of the compressible element (V_{c0}) at maximal transmural pressure for $P_L = 0.5$ kPa was chosen as 0.125 L and the resistance of the compressible airways R_{c0} was chosen as 0.06 kPa.s.L^{-1}, as an estimate for the airway generations 2 to 10 [68]. The choice of these generations within the 23 generations of the bronchial tree is also based on the experimental evidence for the location of the *EPP*. In Figure 3.2 the normalised values of V_C are plotted against P_{tm} for three values of P_L (0.2, 0.5 and 0.9).

The flow at the mouth is dependent on the small airway resistance (R_s), the resistance of the compressible element (R_c), the upper airway resistance (R_u) and alveolar, pleural and recoil pressure (P_A, P_{pl} and P_L). For the complete mathematical description of the lung model with a compressible element, lung model 1, is represented by the following equations, which can be derived:
Model-1:

$$P_{pl} = P_A - P_L \tag{3.10}$$

$$P_L - P_{tm} + R_s V'_A = 0 \tag{3.11}$$

$$P_{tm} + P_{pl} + (R_c + K_1)V'_m + K_2(V'_m)^2 = 0 \tag{3.12}$$

$$R_c = R_{c0}\left[\frac{V_{c0}}{V_c}\right]^2 \tag{3.13}$$

where:
R_c *resistance of the compressible element, in kPa.s.L^{-1}*
V_c *volume of the compressible element, in L*

R_{c0} *defines the overall magnitude of* R_c,
V_{c0} *determines the relative volume of the compressible element at which* R_c *will be of influence.*

$$V_c(t) = V_c(0) + \int_{\tau=0}^{t} (V'_m - V'_A)\partial\tau \qquad (3.14)$$

$$P_L(t) = P_{L,FRC} + \frac{1}{C_L} \int_{\tau=0}^{t} V'_m \partial\tau \qquad (3.15)$$

$$P_{tm} = (V_c, P_L) \qquad (3.8a\text{-}3.9b)$$

where:
V'_A *flow into the alveolar compartment, in* $L.s^{-1}$,
V'_m *flow at the mouth, in* $L.s^{-1}$
R_s; P_L; K_1 *and* K_2 *are the model parameters.*

Simplified models

In cases where the influence of compressibility of the airways could be neglected, e.g. stiff lungs and normal lungs at low flow, simpler models were used with a restricted number of parameters if compared with the basic model. Models 2, 3 and 4 were defined by an absence of compressibility and different dominant properties determining the behaviour of model-1.

Model-2:
A linear resistance parameter (K_3 (kPa..s.L^{-1})) for inspiration and expiration is introduced:

$$P_A = K_3 V'_m \qquad (3.16)$$

Model-3:
Different linear resistances parameters (K_4,K_5 (kPa.s.L^{-1})) for inspiration and expiration are introduced:

$$P_{A,in} = K_4 V'_{m,in} \qquad (3.17)$$

$$P_{A,ex} = K_5 V'_{m,ex} \qquad (3.18)$$

where:
$P_{A,in}$: *alveolar pressure during inspiration, in kPa*
$P_{A,ex}$: *alveolar pressure during expiration, in kPa*

Model-4:
Different linear and turbulent resistance parameters (K_6, K_7 (kPa.s.L^{-1})) and (K_8,K_9 (kPa.s^2.L^{-2})) are used for inspiration and expiration, respectively:

$$P_{A,in} = K_6 V'_{m,in} + K_8 V'^2_{m,in} \qquad (3.20)$$

$$P_{A,ex} = K_7 V'_{m,ex} + K_9 V'^2_{m,ex} \qquad (3.19)$$

Parameter estimation
The parameter estimation technique and the simulation of the serial lung model were connected in the way indicated in Figure 3.3. With the serial lung model (simulation) an output signal (V'_m) was calculated for a given P_A. Based on the same stimulus P_A and with use of one of the described mathematical models (1, 2, 3 or 4) the computer calculated (estimation) a predicted response (V'_{pred}) for a given set of start parameters. Then, a new set of parameters was computed to reduce the difference in square error (*EE*) between V'_{pred} and the known V'_m. This was continued either for a maximal predefined number of 20 iterations or for a smaller number when the difference in *EE* between the two responses was reduced below 0.0001.
For the parameter estimation technique the Marquardt algorithm [73] was applied, which is a modified Gauss-Newton algorithm. The loss function $EE = (V'_{pred} - V'_m)^2$ was minimised. With the Marquardt algorithm the step size of each adjustment can be influenced by means of a factor μ. By changing μ after each iteration it was possible to control dynamically the convergence of the estimation ($\mu = 0$, Gauss Newton; $\mu = \infty$ steepest descent with step size zero). At the start of the estimation μ was set at 0.1. If the error was smaller in the next iteration, μ was adjusted to 0.4 μ , and if the error was larger the last iteration was repeated after μ was changed to 10 μ. The two factors 0.4 and 10 were found empirically.

Forcing the serial model with simulated signals
First the serial model was stimulated by a sinusoidally changing P_A. Because of unequal inspiratory and expiratory resistances (models 1, 3 and 4) the sinusoidal alveolar pressure curve had to be corrected to minimise the difference (Δ V) between the lung volume at the start ($\sigma = 0$) and that at the end ($\sigma = t$) of the simulated respiratory cycle below 0.01 in Litre. The change in lung volume, Δ V, between start and end of the respiratory cycle was found from the value obtained after integration of the output V'_m over the whole respiratory cycle. The

minimisation of Δ V was realised by the introduction of an offset in the zero line of the sinusoidal alveolar pressure signal.

A higher expiratory than inspiratory resistance needed a shift of the zero line into the direction of the inspiratory pressure curve, giving a larger amplitude and duration of the expiratory pressure curve. For the inspiratory part of the curve the opposite changes occurred. The offset in the zero line was calculated from the volume shift Δ V and the overall resistance R_{eff} [45], by an iterative process.

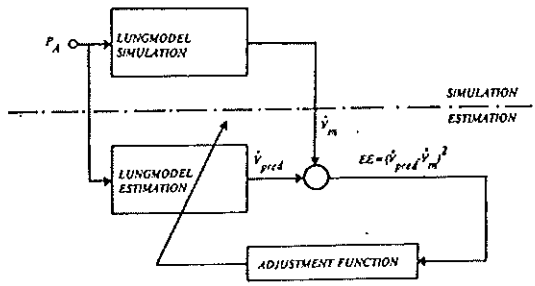

Figure 3.3:
The parameter estimation process, for explanation see text.

Choice of parameters for testing the simulation

The parameter values for model-1 were divided into five classes: the normal lung (*N*), the emphysematous lung (*E*), the fibrotic lung (*F*), the asthmatic lung (*A*) and the lung with a large increase in upper airway resistance (*U*). The characteristic values for the various parameters were chosen from reviews of pulmonary pathophysiology [60, 61, 74, 75], and those for upper airway resistance for class U were derived from a group of patients with bilateral vocal cord paralysis [76].

Table 3.1 :
Values for the parameters (K_1; K_2; R_s; P_L) and lung compliance C for the different groups *N*, *E*, *F*, *A* and *U*.

	K_1	K_2	R_s	$P_{L,FRC}$	$C_{L,FRC}$
N	0.05	0.02	0.03	0.5	2.0
E	0.05	0.02	0.3	0.1	5.0
F	0.05	0.02	0.03	0.9	1.0
A	0.1	0.06	0.3	0.5	2.0
U	0.29	4.6	0.03	0.5	2.0

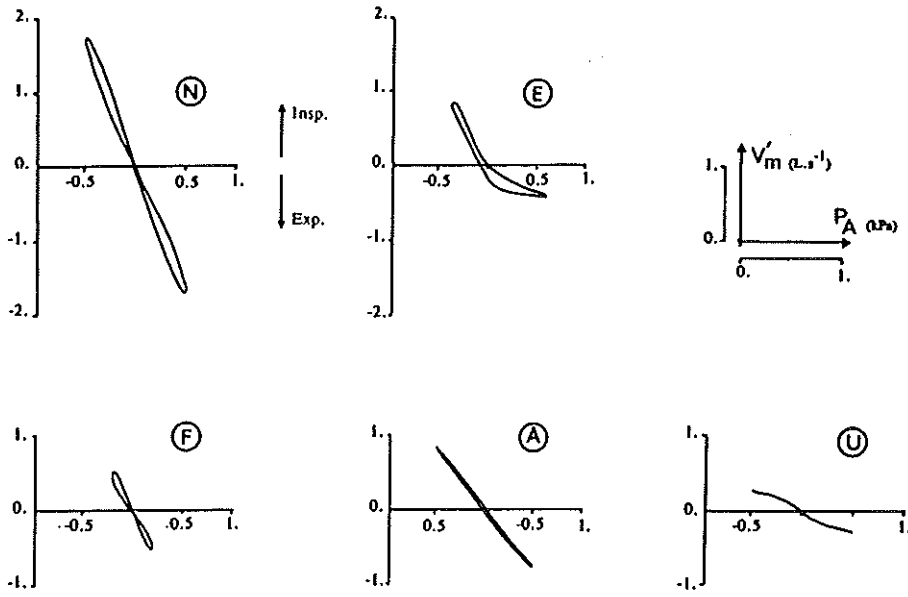

Figure 3.4:
Simulations performed with model-1 and the parameters of Table 3.1 for the different groups N, E, F, A and U. Belonging value are given in Table 3.2.

Table 3.2:
Value for the simulations with model-1 as given in Figure 3.4.
P_A is the amplitude of the simulated pressure curve, VT is tidal volume, R_{PA} is the resistance calculated by means of the peak pressure and the associated flow value. R_{eff} is calculated for the total curve as well as for the inspiratory ($R_{eff,in}$) and expiratory ($R_{eff,in}$) part separately.

	P_A	VT	R_P	R_{eff}	$R_{eff,in}$	$R_{eff,ex}$
N	0.50	1.09	0.29	0.29	0.28	0.30
E	0.50	0.42	0.82	0.71	0.44	1.21
F	0.20	0.33	0.43	0.41	0.40	0.41
A	0.50	0.53	0.62	0.61	0.58	0.64
U	0.50	0.21	1.77	1.60	1.60	1.60

Emphysema was modelled by a lower value of the recoil pressure $P_{L,FRC}$ and thus an increased lung compliance (C_L). Because of a lower $P_{L,FRC}$ the traction on the walls of the respiratory bronchioles is smaller and consequently pleural pressure will be less negative with respect to alveolar pressure (eqn. 3.6), causing a narrowing of the small airways and therefore an increase in R_s. In fibrosis the characteristic physiological disorder is the increased stiffness of the lung tissue, which was modelled by an increase of $P_{L,FRC}$ and a decrease of C_L. In asthma both upper and small airway resistances are increased, which was reflected in increased values for K_1, K_2 and R_s. To simulate patients with an upper airway obstruction only K_1 and K_2 were greatly increased, according to the results obtained from patients with bilateral vocal-cord paralysis as mentioned above.

Uniqueness

The validity of the parameters obtained by a parameter estimation technique depends on the uniqueness of the parameter values. To evaluate the uniqueness, simulations were made for the five classes N, E, F, A and U as mentioned in Table 3.1. The uniqueness of the calculated parameter set and the convergence of the iterative estimation procedure were analyzed by estimating the parameters of a class, when starting from the parameter values belonging to the other classes, e.g. simulation of N, and starting of parameters E, F, A and U, respectively.

Sensitivity

The squared error $EE = (V'_{pred} - V'_m)^2$ was determined after application of stepwise changes in the parameters in order to study the sensitivity of the parameter estimation technique. This was done in two ways:

1. by determination of the interdependence of pairs of parameters, and
2. by studying the influence of fluctuations in each of the parameters on the resulting squared error.

Noise

Random noise was applied to the input signal of alveolar pressure and to the output signal of flow of the serial lung model. The mean noise level was 0.02 (kPa) for the pressure and 0.02 in $L.s^{-1}$ for the flow. The deviation of the parameter estimates in the different classes from the selected input parameter values with which the simulation was performed, was investigated by starting with values of the class itself and values obtained from the normal situation. For the normal situation also the starting values for the emphysema class were applied. The noise was generated by a noise generator of Digital Equipment Corporation which was implemented in the *Fortran-IV* library belonging to the *RT-11* operating system.

RESULTS

The results of simulations of the different pathological classes as defined in Table 3.1 are presented in Figure 3.4. These simulations were based on a sinusoidal alveolar pressure change with an amplitude of 0.5 kPa for class N, E, A and U and 0.2 kPa for class F, all at a rate of 0.5 Hz. The lower values of alveolar pressure in class F are necessary for the calculation of the element volume with the Runge Kutta algorithm in case of an almost stiff compressible element because of high P_L values.

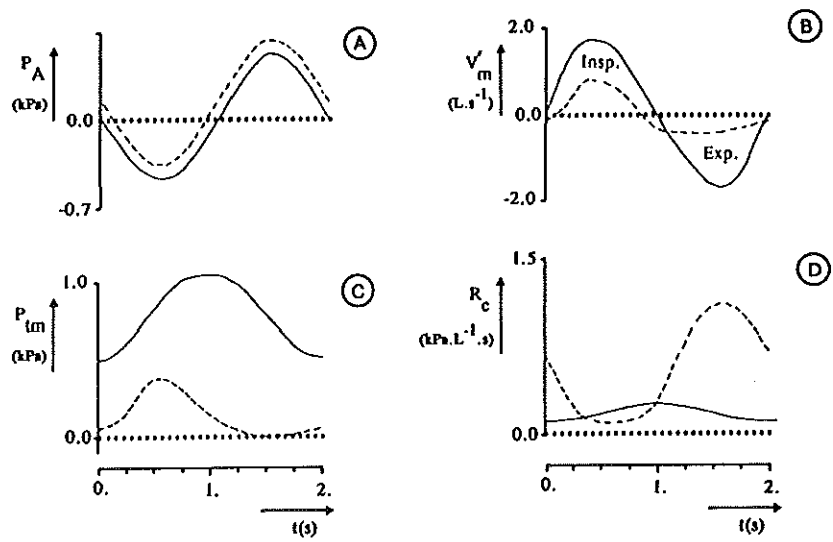

Figure 3.5:
The variation of different values with time as calculated with model-1 in Normal (——) and Emphysema (-----) during normal breathing.
For symbols see list of symbols and text.

The difference between the maximum of alveolar pressure in inspiration and that in expiration for emphysema (Figure 3.4E) was caused by a shift of the zero line in the alveolar pressure. This shift was necessary to obtain an equal inspiratory and expiratory volume, as mentioned before. The characteristics of the simulated curves were in agreement with recordings of normals and patients, as documented among others by Matthys et al. [77]. For each curve the resistance R_t and the effective flow resistances for inspiration ($R_{eff,in}$), expiration ($R_{eff,ex}$) and total ventilatory cycle (R_{eff}) were calculated (Table 3.2). To illustrate the mechanical behaviour of a lung with emphysema, the input variable P_A, the output variable V'_m and the resulting variables P_{tm} and R_c were plotted as a function of

time for both classes *E* and *N* (Figure 3.5). The offset in the zero line of alveolar pressure (Figure 3.5A) compensated for a higher overall expiratory resistance (Figure 3.5D) leading to a smaller peak flow V'_m (Figure 3.5B). In case of emphysema P_{tm} was around zero during a part of the expiratory phase (Figure 3.5C). In this part the calculated resistance (R_c) of the collapsible element was relatively large (Figure 3.5D). For the fibrotic case, not shown, the resistance R_c was almost constant during the respiratory cycle.

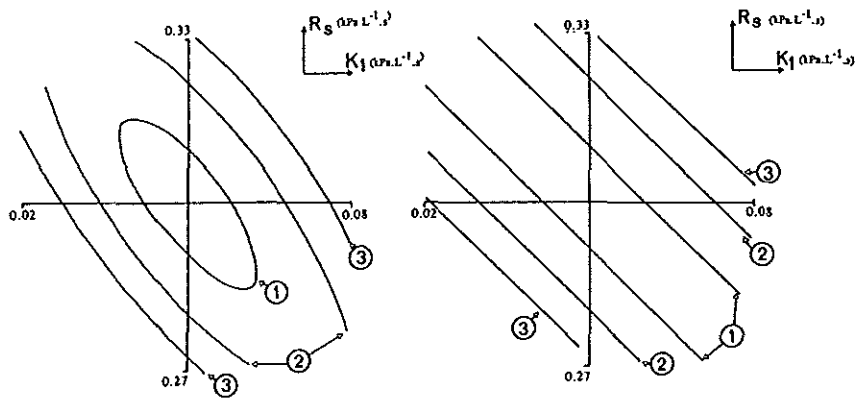

Figure 3.6:
Plots of contour lines (1: EE = 0.01; 2: EE = 0.05; 3: EE = 0;) as function of parameters K_1 and R_s for a highly collapsible (P_L=0.1) and a stiff compressible segment (P_L=0.9), respectively.
Optimal parameter values: K_1 = 0.05; K_2 = 0.02; R_s = 0.3 and P_L = 0.1 in Figure 3.6.a and P_L = 0.9 in Figure 3.6b. For these calculations the influence of volume changes on P_L was neglected (1/C = 0).
In both Figures:
X-axis 0.02 < K_1 < 0.08;(kPa.s.L^{-1})
Y-axis 0.27 < R_s < 0.33;(kPa.s.L^{-1})

In the estimation procedure the parameters used in the simulations could be determined, independent of the start parameters. For the emphysematous lung with low P_L and high R_s the parameters converged faster than those in the other classes.

For the class E and F the dependence between the parameters is shown in Figure 3.6. In this Figure the contour lines where parameter combinations have the same loss function *EE*, were plotted. In each plot the parameters K_1 and R_s fluctuated around their optimal values of 0.05 and 0.3, respectively. The parameter P_L had different values, 0.1 and 0.9, respectively. The parameter K_2 was 0.02 and was constant in both cases. In the simulation of fibrosis the

contour lines were almost straight, whereas in emphysema they were more elliptical. This implied that for fibrosis K_1 and R_s were almost completely interdependent, i.e. cannot be estimated separately.

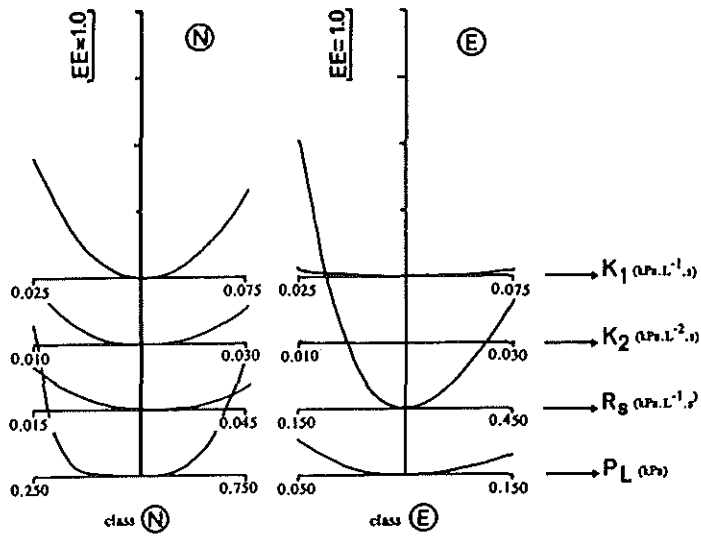

a b

Figure 3.7:
Plots of the EE as function of a perturbation plus and minus 50% of the parameter for the normal and emphysema case. Remaining parameters have the value belonging to the class value. For these calculations the influence of volume change on change in P_L was neglected (1/C = 0).
3.7a: class N; 3.7b. class E.
For symbols see list of symbols and text.

Figure 3.7 presents the *EE*-changes for the *N* and *F* class, after individually changing the four parameters between 50% and 150% of their optimal values for each class. From this Figure it can be seen that the influence of a change in the parameter values K_1, K_2 and R_s on the squared error was different for the two classes *N* and *E*. For the normal lung the parameters had more or less an equal influence on the resulting squared error, whereas for the emphysematic lung the parameters K_1 and K_2 were far less important for reducing the squared error.
Noise superimposed on the model output V'_m had no appreciable influence on the parameter estimates. This was not the case when noise was added to the input variable P_A, as is shown in Table 3.3. If the starting values were chosen from the same pathology class or from the normal class the total resistance from the bronchial tree, as given by the effective flow resistance, appeared to be not

Table 3.3:
Residual Square Error (*EE*), parameter estimates (K_1; K_2; R_s; P_L) and effective flow resistance estimate (R_{eff}) with and without addition of random noise of 0.02 (kPa) to the input signal P_A and of 0.02 ($L.s^{-1}$) to V'_m. In the Table the class of which the start parameters were taken is indicated. For each pathology class input parameters were as defined in Table 3.1 and starting values were chosen both according to the same class and to the normal class. For further explanation see text.

Simulate class	Start class	Noise level	*EE*	K_1	K_2	R_s	$P_{L,REC}$	R_{eff}
N	*N*	0	0.00	0.05	0.02	0.03	0.50	0.29
	N	0.2	0.33	0.05	0.02	0.03	0.50	0.29
	E	0.2	0.33	0.04	0.03	0.03	0.50	0.29
E	*E*	0	0.00	0.05	0.02	0.30	0.10	0.71
	E	0.2	0.27	0.05	0.03	0.30	0.10	0.72
	N	0.2	0.26	0.01	0.08	0.30	0.10	0.72
F	*F*	0	0.00	0.05	0.02	0.03	0.90	0.41
	F	0.2	0.18	0.05	0.05	0.02	0.90	0.41
	N	0.2	0.18	0.04	0.05	0.02	0.90	0.41
A	*A*	0	0.00	0.10	0.06	0.30	0.50	0.61
	A	0.2	0.20	0.13	0.09	0.26	0.40	0.61
	N	0.2	0.17	0.20	0.10	0.19	0.34	0.61
U	*U*	0	0.00	0.20	4.60	0.03	0.50	1.60
	U	0.2	0.03	0.29	4.60	0.03	0.05	1.60
	N	0.2	0.03	0.40	4.14	0.00	0.55	1.59

influenced by random noise. For the *N*, *E* and *F* classes hardly any differences were found in all parameters. The *A* and *U* classes showed somewhat larger differences for all parameters. Except for the *A* and *U* class, it was possible to obtain an accurate P_L estimate in all situations. The same was true for the *N* class if the *E* parameters were taken as starting values; although, as mentioned

above, the R_{eff} was not influenced by the separation in R_s and upper airway resistance. This last value as characterised by K_1 and K_2 was less accurate.

Table 3.4 shows the parameter estimates for the complex model-1 and those of the three simplified models. The parameters of the simplified models-2,-3 and -4 were obtained by fitting these models to the curves simulated with the complex model-1. This was done for the five separate classes (*N*, *E*, *A*, *F* and *U*). In these simulations noise was not superimposed. The estimation with model-1 agrees with the values given in Table 3.3 in the case of absence of noise. Except for the application of the model-2 (one linear resistance) in the emphysema case, in all other simplified model fits the estimate for the effective flow resistance of the total respiratory cycle was close to the effective flow resistance calculated with the complex model. Because of the asymmetry of the inspiratory and expiratory part of the curve in the emphysema class a separate resistance for each part(model-3) was necessary to obtain a reliable estimate of the effective flow resistance for the whole cycle.

Although most obvious for the *U* class, in all cases model-4 with a linear and turbulent resistance parameter for inspiration and expiration gave a good fit based on *EE*. Only for the class *U* curve and the expiratory part of class *E* curve were the parameters for the turbulent resistance part (K_7 and K_9) markedly larger than those for the linear part (K_6 and K_8). In the emphysema case the expiratory curve was largely determined by airway compression. In all other cases the turbulent resistance parameters were much smaller than the linear ones.

DISCUSSION

Estimation of pulmonary parameters, based on model fitting of body plethysmographic pressure-flow tracings, has been performed by a small number of investigators [63, 64]. These attempts provided a better understanding of body - plethysmographic alveolar pressure-flow data. In this present study an extended version of the serial lung model of Golden has been used [64]. We introduced a definition of the compressible element which is based on more recent investigations and incorporated the dependence of lung recoil pressure on a changing alveolar volume.

The aim of this present study was to evaluate (1) a physiologically well-defined serial lung model with respect to its ability for the simulation of patient curves, and (2) to study the uniqueness and sensitivity of a parameter estimation technique for the fit to the simulated curves.

The behaviour of the serial model was studied by simulating different

Table 3.4:
Results of the estimation process for the primary (-1) and the simplified (-2,-3,-4) models, performed on signals generated by means of a simulation with model-1. Indicated are for each class and each fitted model the resulting square error, the total effective flow resistance (R_{eff}), the effective flow resistance for in- and expiration separately ($R_{eff,in}$ and $R_{eff,ex}$) and the resistance line through the extreme points (R_p).

Class	Model	Parameter values				EE	R_{eff}	$R_{eff,in}$	$R_{eff,ex}$	R_p
N	1	K_1 = 0.05	K_2 = 0.02	R_s = 0.03	P_t = 0.50	0.00	0.29	0.28	0.30	0.29
	2	K_3 = 0.29				3.69	0.29	0.29	0.29	0.29
	3	K_4 = 0.29	K_5 = 0.30			3.55	0.29	0.29	0.30	0.29
	4	K_6 = 0.29	K_7 = 0.00	K_8 = 0.28	K_9 = 0.01	3.54	0.29	0.29	0.30	0.30
E	1	K_1 = 0.05	K_2 = 0.02	R_s = 0.30	P_t = 0.10	0.0	0.71	0.44	1.21	0.82
	2	K_3 = 0.98				11.2	0.98	0.97	0.97	0.98
	3	K_4 = 0.45	K_5 = 1.32			2.06	0.75	0.45	1.32	0.79
	4	K_6 = 0.45	K_7 = 0.01	K_8 = 0.01	K_9 = 3.29	1.52	0.74	0.45	1.27	0.81
F	1	K_1 = 0.05	K_2 = 0.03	R_s = 0.03	P_t = 0.90	0.00	0.41	0.40	0.41	0.43
	2	K_3 = 0.43				1.36	0.43	0.43	0.43	0.43
	3	K_4 = 0.42	K_5 = 0.43			1.36	0.43	0.42	0.43	0.43
	4	K_6 = 0.37	K_7 = 0.10	K_8 = 0.43	K_9 = 0.00	1.35	0.42	0.42	0.43	0.43
A	1	K_1 = 0.10	K_2 = 0.06	R_s = 0.30	P_t = 0.50	0.00	0.61	0.58	0.64	0.62
	2	K_3 = 0.61				0.32	0.61	0.61	0.61	0.61
	3	K_4 = 0.58	K_5 = 0.64			0.14	0.61	0.58	0.64	0.61
	4	K_6 = 0.53	K_7 = 0.07	K_8 = 0.60	K_9 = 0.06	0.12	0.61	0.58	0.64	0.61
U	1	K_1 = 0.20	K_2 = 4.60	R_s = 0.30	P_t = 0.50	0.00	1.60	1.60	1.60	1.76
	2	K_3 = 1.62				0.15	1.62	1.62	1.62	1.62
	3	K_4 = 1.62	K_5 = 1.62			0.15	1.62	1.62	1.62	1.62
	4	K_6 = 0.51	K_7 = 4.34	K_8 = 0.26	K_9 = 5.43	0.00	1.59	1.59	1.60	1.77

combinations of parameters (Table 3.1). The model produced patterns (Figure 3.4) for the different types of pathology which agreed quite well with the patterns as defined by Matthys. In the classes representing the normal condition and patients with fibrosis, asthma and an increased upper airway resistance, a non-linear behaviour of the model was virtually absent because the influence of the compressible element is negligible, since either R_s was small or P_L was relatively large. For emphysema, where both R_s was increased and the P_L was decreased the effect of the compressible element was more pronounced. Large differences in the time course of some output variables were found (Figure 3.5) between the classes for the normal condition and for emphysema, respectively:

1. the transmural pressure in class E was below zero during part of the breathing cycle, which indicates the presence of a marked compression even during the normal breathing,
2. the area of the compressible element in class E decreased greatly and, therefore, resistance R_C was much larger during expiration than it was during expiration in the normal case (Figure 3.4E).

The difference in the values of effective flow resistance, calculated for the inspiratory ($R_{eff,in}$) and expiratory ($R_{eff,ex}$) resistance, also showed this effect of expiratory airway compression. The model appeared to be sufficiently accurate for simulation of the characteristic loop patterns, related to pulmonary pathology, in spite of a (for practical purposes necessary) simplified description of the compressible element.

For simulations without additional noise the parameter estimation routine gave unique solutions for the parameter values belonging to each class. It was shown that the sensitivity of the parameter estimation technique depended on the values of the parameters of each class (Figure 3.7). In the normal condition (class *N*) the sensitivity for the different parameters was more or less the same. For emphysema (class *E*) the parameters R_s and P_L were much more important than K_1 and K_2. Thus K_1 and K_2 appeared to be of little importance in reducing the error in the parameter estimation scheme. Therefore, the accuracy of the estimation of K_1 and K_2 will be smaller than that of both other parameters (Table 3.3, Figure 3.6a and 3.6b). The application of noise confirmed the results on the sensitivity of the model fit for the various parameters in dependence on the pathology class. In the case of upper airway obstruction the factor K_2 has such a dominant influence that the other parameters have almost no influence on the resulting effective flow resistance and on the shape of the curve.

In circumstances where the influence of the compressible element was minimal, the serial long model could be simplified. In such situations, a good estimation of the different parameter values in model-1, which characterised the resistance of the serial connection of the elements, was not possible. Then a

model with only one serial resistance element with a laminar and a turbulent term could be used as was shown in Table 3.4. This did not hold for the E case where the four models yield appreciably different estimates.

We conclude that the serial lung model is able to fit curves which are influenced by a serial mechanical inhomogeneity, especially defined by the behaviour of the compressible element. Moreover, parameter estimation was able to recognise in the cases described, even in the presence of noise on the model input, the most relevant aspects of the lung mechanical behaviour.

CHAPTER 4
A COMPUTER-CONTROLLED MECHANICAL LUNG MODEL FOR APPLICATION IN PULMONARY FUNCTION STUDIES

AFM Verbraak, JM Bogaard, JEW Beneken, A Versprille

INTRODUCTION

The complexity of lung function measurements and data analysis entail a need for validation of all phases of data acquisition and analysis. Validation of software can be performed by generation of raw data with a mathematical model with known parameters. When these raw data are read into a program to be tested, the calculated results must be in agreement with the parameters used for the simulation [78]. With a mechanical lung model with known physical characteristics the reliability of the measurement equipment, as well as software, can be tested. In addition, a lung model enables accurate reproduction of pulmonary function signals when required.

Several models have been described which could simulate only one type of breath [7, 8, 10]. The model of Pedersen et al. [10] consisted of a pressure chamber full of copper chips and was activated by release of air from a container under pressure. After inflation to twice the atmospheric pressure, it delivered 8.2L of air during deflation. Bouhuys et al. [7] developed a device to simulate flow-volume curves by means of a cam mounted on a motor. By changing the cam the shape of the flow-volume curve could be altered. Maximum flow could be changed by changing the size of an orifice in the outlet line. Boutellier et al. [8] devised a piston-pump system to generate respiratory data. This model was able to generate breaths of constant volume and known gas concentrations. With

all the above-mentioned systems different types of breath could be simulated by a manual change of the mechanical hardware, whereafter the simulation had to be restarted.

The introduction of computers enabled to change quickly between different settings of the simulator. Meyer [9] designed a microcomputer controlled respiratory servo system, using a hydraulically operated cylinder-piston and solenoid valve assembly. The flexibility to select different breathing patterns enabled the implementation of complex sequences of breathing manoeuvres. Myojo [13] described a breathing simulator with a split/cam valve without a piston/cylinder or bellows. The opening of the split/cam valve was controlled by a stepper motor under microcomputer control. This system enabled to simulate inspiratory flow patterns as seen during spontaneous breathing, although it was not reported whether it was possible to change breathing patterns during simulation. Jansen et al. [79] described a computerized ventilator system for animal studies. Instead of the hydraulic system of Meyer they used an electromechanical system, which was relatively small and easy to implement in the construction of a ventilator. The system was able to perform special breathing manoeuvres inserted between breathing cycles of normal mechanical ventilation.

We adapted the idea of computer control to drive a physical lung model for use in the pulmonary function laboratory to test lung function equipment, to validate software, to simulate impaired pulmonary mechanics and to perform simulations of special breathing patterns and pulmonary pathology. Primarily we intended to use this computer controlled mechanical lung model to perform pulmonary function tests on special breathing patterns in a body plethysmograph. We describe the mechanical lung model and some examples of its applications.

THE MECHANICAL LUNG MODEL

The lung model consists of three components: the actual lung model, an electromechanical servo system and a computer system to control the model.

Mechanical construction

The construction of the mechanical lung model is shown in Figure 4.1. It consists of a round container made from glass, an aluminium upper plate and a piston at the bottom. The container is filled with water, which represents pleural space and which we call the liquid-filled compartment (*LFC*). It contains two concertina bellows (V_1 and V_2) which represent the two lungs. The *LFC* contains two connections P_{liq} and *LFC-CC*. P_{liq} is used to fill the *LFC* with water and to

measure the pressure inside the *LFC*, and *LFC-CC* to connect the water compartment around the compressible component (see below) with the *LFC*. Leakage between piston and container is prevented with another bellows. Vertical movements of the piston are established with an electrical motor which rotation is transformed to longitudinal displacement by precision satellite roller screws (*Rollvis, Switzerland*). To simulate breathing patterns the piston is driven by a steering program according to a pre-defined pattern. The position of the piston is sensed by a potentiometer (T_3), attached to the piston. Two optical switches (S_1 and S_2) at the two extreme positions of the piston are activated when the piston reaches its end limits. When one of the optical switches is activated the system is stopped. Each lung bellows has a conducting rod, T_1 and T_2, respectively, which is attached to an aluminum bottom plate. To each rod a potentiometer is attached to sense the position of each bellows separately. The bellows V_1 and V_2 have an outlet R_{Aw1} and R_{Aw2}, respectively, which give access to the "airways", and two outlets P_{A1} and P_{A2} to measure the pressure inside the bellows.

Because water is incompressible, the volume displacement of the piston is equal to the sum of the volume changes of the two bellows. Thus the position of one bellows depends on the position of the piston and that of the other bellows. As the diameter of the bellows is smaller than the diameter of the piston, the bottom plates of the bellows will move faster than the piston. This difference in motion is even larger when one of the bellows is fixed or restricted in movement. Therefore, without precautions, depending on the amount of water in the *LFC*, a collision can occur between piston and bellows, and between bellows and the upper plate.

The airways are simulated by perspex pipes, which are constructed. These pipes have been made in a modular way. Flow resistances and flow and pressure transducers can be positioned at different places. A standard Lilly pneumotachometer head (*Jaeger, Würzburg, Germany*) fits into the pipes. A compressible component, made of a stretched Penrose drain, can be inserted in series with the airway components. The Penrose drain, a thin-walled floppy tube made of rubber, is fixed in a vertical position between the two pipes (Figure 4.1) and stretched about 10%. The pipes have an external diameter of 2. 10^{-2} m. The vertical position of the penrose drain can be shifted over 4. 10^{-2} m. The maximum length of the drain is 10^{-1} m. The drain is surrounded by water, and is in direct contact with the *LFC*. The compressible component simulates the changing resistance in the airways due to the changing transmural pressures that are present in the physiological situation. At the outlet/inlet of the pipe system a shutter can be used to close the airway opening.

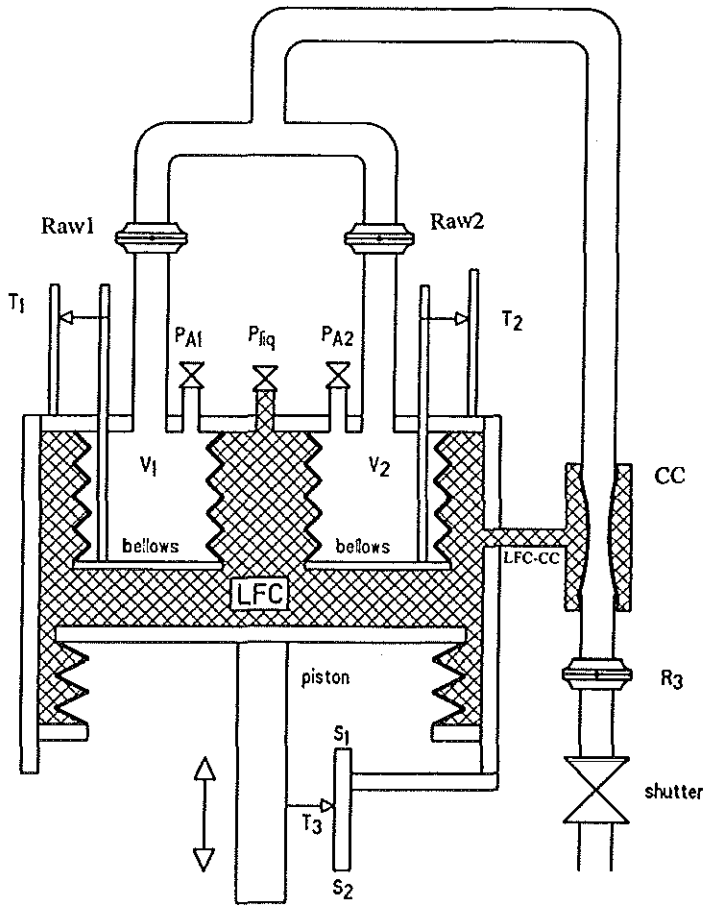

Figure 4.1
Diagram of the mechanical lung model. Two airway components R_1 and R_2 are connected to the outlets of the concertina bellows. P is the outlet to measure the pressure of the liquid-filled compartment (LFC). The liquid of the LFC could be connected to the liquid around the compressible component (CC) through the connection LFC-CC. S_1 and S_2 are the optical switches for the end-limits. T_1 and T_2 are the potentiometers for the position of the bellows and T_3 is the potentiometer for the position of the piston. P_{A1} and P_{A2} are the outlets to measure the pressure inside the bellows.

During occlusion of the pipe system, very high positive and negative pressures can develop in the LFC and bellows due to the power of the motor-driven system. Therefore, a protective device is constructed in the pipe system to avoid destruction of pressure transducers or bellows.

Bellows

The rubber bellows are stabilized by metal rings inside and outside each fold. The compliance of the bellows is determined when the bellows were outside the lung model and is circa 20 L.kPa^{-1}, respectively. The bellows in the lung model is subject to forces caused not only by the compliance of the bellows itself, but also by its weight and that of the attached materials, the pressure inside the bellows and the pressure of the water around the bellows. The influence of the pressure against the side of the bellows is neglected. The diameter of the bottom plate of the bellows is 0.15 m. The position of the bottom of a bellows can be derived from the volume of the bellows, according to

$$h_{bls,1} = \frac{V_{A,1}}{A_{bls}} * 10^{-3} \qquad (4.1)$$

where:

A_{bls}	*effective surface of the bottom plate of each bellows, in m^2*
$h_{bls,1}$	*position of the bottom plate of bellows 1 (lung 1), in m*
$V_{A,1}$	*volume of the bellows 1 without external pipes, in L.*

The level h = 0 is the level of the bottom plate when $V_{A,1}$ is zero. The pressure at level $h_{bls,1}$ in the water of the *LFC* near the bottom of a bellows is equal to the pressure at all other points (h) in the *LFC* if a correction for the hydrostatic pressure component is made. This relation is given by:

$$P_{liq}(h) = P_{liq}(h_{bls,1}) - \rho_{liq} * g_{liq} * (h - h_{bls,1}) \qquad (4.2)$$

where:

$P_{liq}(h)$	*pressure, in the water at level h, in kPa*
$P_{liq}(h_{bls,1})$	*pressure, in the water at level $h_{bls,1}$, in kPa*
ρ	*density of the water, in kg.m^{-3}*
g	*constant of gravitation, in m.s^{-2}*

For the stationary situation the pressure from the bellows on the water is equal to the pressure from the water on the bellows. This pressure is the summation of the pressure due to the elasticity of the bellows as a function of the position, the pressure inside the bellows and an offset pressure.

This can be presented as:

$$P_{liq}(h_{bls,1}) = \frac{E_{bls}}{A_{bls}} * h_{bls,1} + P_{liq_{A,1}} + P_{liq,off} \qquad (4.3)$$

where:

$P_{liq,off}$ *pressure at* $h_{bls,1}=0$ *when* $P_A=0$ *and* $P_{grav}=0$, *in kPa*
$P_{A,1}$ *pressure in the bellows 1, in kPa;*
E_{bls} *elastic constant of the bellows at position* $h_{bls,1}$, *in* $N.m^{-1}$

The offset pressure is caused by the level of measurement, an additional pressure component due to the mass of bellows and attached materials and a pressure due to the elasticity when level *h* is zero. The compliance is defined as $C_{bel} = \Delta V_A / \Delta P_{liq}(h_{bls,1})$, giving:

$$\frac{1}{C} = \frac{\Delta P_{liq}(h_{bls,1})}{\Delta V_{A,1}}$$

$$= \frac{(\frac{E_{bls}}{A_{bls}} + \rho_{liq} * g_{liq}) * \Delta h_{bls,1}}{A_{bls} * \Delta h_{bls,1}} \qquad (4.4)$$

$$= (\frac{E_{bls}}{A_{bls}^2} + \frac{\rho_{liq} * g_{liq}}{A_{bls}})$$

where :

C_{bel} *compliance for the bellows, in* $L.kPa^{-1}$

In accordance with equation (4.4), when the bellows are placed in the water, the compliance decreases to 1.6 $L.kPa^{-1}$. When both bellows are functioning a coupling exists via the water.

The minimal volume of the bellows and pipe system is 0.45 L. The height of the *LFC* is such that when both lungs are used in parallel and filled with the proper amount of water, they can not touch each other. When only one bellows is used the piston and bellows can touch each other. Because the diameter of the lung bellows is smaller than the diameter of the piston the bellows will descend faster than the piston. The maximum displacement when only one bellows is used is 0.9 L. When both bellows are used in parallel the maximum total displacement of the bellows is 2.3 L. The volume of the bellows for a given position of the piston depends on the amount of water in the *LFC*.

The lung model does not fulfil the isothermal conditions as present in the lungs [80]. Isothermal means constant temperature and can be achieved by full and direct heat exchange with the surroundings; the other extreme, adiabatic, means no heat exchange. For the model a partial heat exchange exists. According to Poisson's law an exponential relationship exists between pressure and volume ($PV^{(Cp/Cv)}$ = Constant). Depending on the rate of change of pressure and volume, *(Cp/Cv)* is between 1.0 (isothermic) and 1.44 (adiabatic). Inclusion of a thermal buffer, e.g. thin copper slices to approximate isothermic condition, was not possible because of the changing volume of the bellows. For a sine-wave pattern with different frequencies we measured this value *(Cp/Cv)*. For volume changes with a sine-wave pattern of 1 Hz this value is 1.2.

Resistances

The resistance components were constructed according to Mecklenburgh [81]. They consist of a stack of layers of stainless-steel mesh. Different resistances were obtained by altering the number of layers or type of mesh. The packed layers were fitted in a Lilly pneumotachograph-head. In this way 4 resistance packages were made, namely 2.07, 1.07, 0.43, and 0.19 kPa.s.L^{-1}. The resistance components are highly linear, as shown in Figure 4.2. The resistance and pressure relationship of the compressible component has to be measured each time its characteristics, such as tension, material and length, are changed.

Electromechanical servo system

The electromechanical servo system consists of a motor (*Mavilor, model 600*), a servo-controller (*Infranor, model 90/20*) and a custom-made electronic control module. The servo-controller controls the power to the motor by a high frequency chopping of the *DC* voltage. The difference between the programmed position and the actual position of the piston is converted by the electronics to drive the piston to the programmed position. The actual position is measured by the potentiometers attached to the piston and bellows. The electronic control unit also performs a first check on the allowed position range of piston and bellows. If one of the switches is activated, further movement of the piston is blocked until the piston is directed by the computer in a reverse direction. The amplitude diagram is constant up to 0.7 Hz; the 1 dB point is at 2.25 Hz and 2 dB is at 3.35 Hz. These values are satisfactory for our applications during normal resting breathing.

Microcomputer and software

The operation of the lung model is controlled by a microcomputer. A program reads a control file from disk, in which file the measurement procedure is

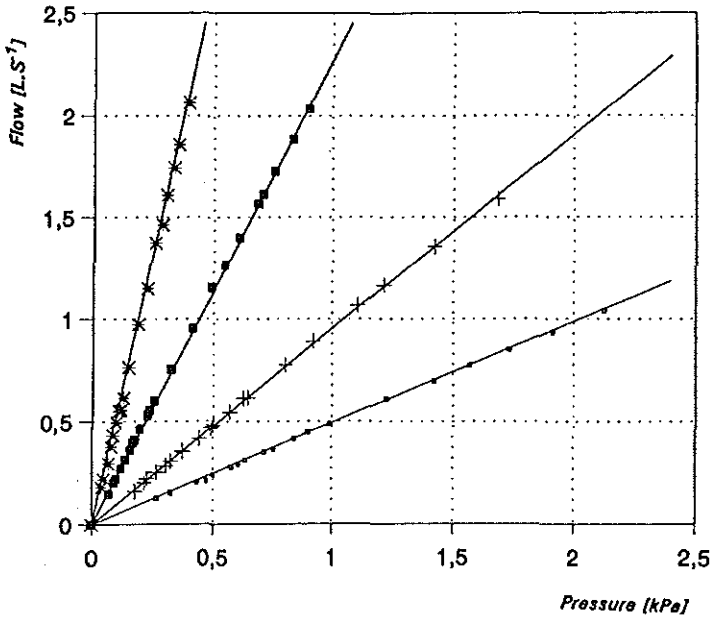

Figure 4.2:
Relationship of flow and pressure for the resistance components;
** 0.19, ■ 0.43 , + 1.07 and □ 2.07 kPa.s.L⁻¹.*

defined. The most important items to be defined are the type of breathing pattern, number of breaths to be repeated, sequence of breathing patterns and control of digital output. The program generates the analog signal which steers the piston to a defined position. To simulate breathing patterns, programmed signals as well as measured signals from patients can be used. The software also reads some digital input to detect e.g. the state of the valves of the lung function equipment. Depending on the values of these inputs the steering program waits, restarts or ends its operation. The controlling software can be imbedded in a larger program to enable the microcomputer to perform a sequence of application programs.

During operation the program calculates the next position of the piston and compares its consequences with the permitted range of positions of piston and bellows. If correct, the lung model is steered to the new position, otherwise the lung model is held in the same position and waits for the next defined position, or is stopped by the operator. At certain moments, defined in a control file, digital output can be activated during the measurements.

Calibration of the lung model

Calibration implies the definition of the relationship between the steering signal and the position of the piston, and the relationship between the signal of the displacement transducers and the position of piston and bellows. Through these relationship at each moment the distance between each bellows and piston and that between the extreme positions is known. A recalibration has to be performed if the amount of water is changed.

Transducers

The pressures at outlets P_{liq}, P_{A1} and P_{A2} are measured by pressure transducers (*Valydyne, USA*), flow is measured by a pneumotachometer (*Jaeger, Würzburg, Germany*) and volume changes are measured by a spirometer (*Lode, Holland*).

APPLICATIONS

The flexibility of the computer controlled mechanical lung model *(CCL-1)* can be illustrated by two applications.

Compliance and airway resistance

Lung compliance is the ratio between volume change (ΔV) and the simultaneous change in transpulmonary pressure (For review: Murphy et al. [82]). In routine lung function testing transpulmonary is measured as oesophageal pressure (P_{es}) minus mouth pressure. In patients the P_{es} is measured by means of a latex balloon inserted in the oesophagus. If the compliance is estimated when volume and P_{es} are continuously changing, the compliance is called dynamic. If a patient expires slowly after a deep inspiration the compliance estimate is called quasi-static.

When a patient's compliance is constant and the pressure drop in the bronchial airways is linear with flow (V'), the relation between P_{es} and V' can be described as:

$$P_{es} = P_{es,off} + R * V' + \frac{\int V' \, dt}{C_L} \qquad (4.5)$$

where:

$P_{es,off}$	*pressure offset, in kPa*
R	*flow resistance, in kPa.s.L^{-1}*
V'	*flow, in L.s^{-1}*
C_L	*constant compliance, in L.kPa^{-1}.*

If flow is almost zero during a volume change equation (4.5) gives the quasi-static compliance. During cyclic changes of the volume the dynamic compliance can be derived from this relationship.

The procedures to measure quasi-static, dynamic compliance and airway resistance can be simulated with the lung model. We used such simulations to test a software program developed for data acquisition in compliance measurements. Two examples of a P_L-V relationship during simulated tidal breathing for the situation with one lung bellows in use and without the compressible element, are given in Figure 4.3a and 4.3b. The volume changes at the outlet were measured by means of a spirometer or by integration of flow. The pressure in the water P_{meas} was measured at outlet P_{liq}. In the lung model P_{meas} represents the oesophageal pressure, P_{es}, as measured in patients.

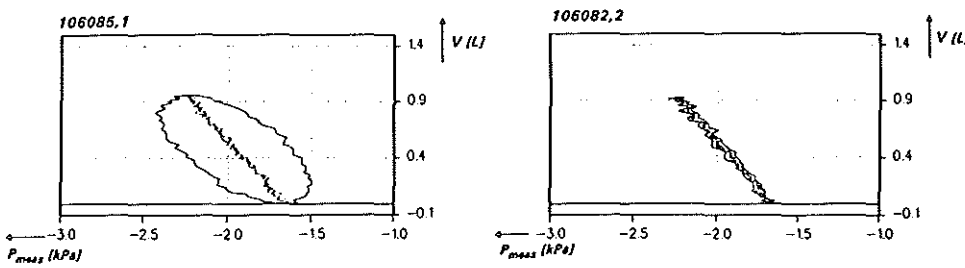

(a) (b)

Figure 4.3:
a: P_{meas} is the pressure difference between P_{liq} and ambient pressure P_{bar}, and reflects the pressure drop over the liquid, bellows, and additional resistance R_1.
b: P_{meas} is the pressure difference between P_{liq} and the pressure inside the bellows P_{A1}, which reflects the pressure over the bellows leaving the resistance element R_1 out of the loop.

Figures 4.3a and 4.3b give the measurement values for the situation with one bellows fixed in the upper position (no displacement), and the other bellows connected with resistance R_1 and without the compressible component. For the measured curves as given in Figure 4.3a the pressure difference was measured between P_{liq} and the pressure at the outlet of resistance R_1, (P_{bar}), whereas Figure 4.3b depicts the pressure that was measured between P_{liq} and P_{A1}. In first situation P_{meas} gives the pressure drop over liquid, bellows and resistance whereas in the second situation P_{meas} gives the pressure drop over the liquid and bellows without the pressure drop over the resistance component. Thus the additional resistance can be calculated from the difference between the two measurements. In both Figures the continuous line shows the relationship

between P_{meas} and volume during one cycle (inspiration and expiration). The dotted line shows the values for P_{es} when P_{meas} is corrected for the pressure drop over the resistance component. This pressure drop is calculated as the effective flow resistance ($R_{L,eff}$) according to equation (4.6). The irregularities on the curves are due to movement resistance (stick-slip) of the conducting rods.

Table 4.1:
Measurements 1-5 are for the set-up in *Figure* 4.3a and 4.3b, when the pressure P_{meas} is measured between the liquid and outlet of the lung model; measurements 6-10 are for the set-up of in Figure 4.3b where pressure P_{meas} is measured between the liquid and air inside the bellows. The second column gives the values used for the resistance elements. The stroke volume, the calculated values for C_{eff} and R_{eff} are given together with the standard deviation (*sd*). The last column $\Delta R_{eff,cor}$ is the calculated resistance value R_{eff} of each row diminished by the first element in the same row, where no additional resistance is implemented (e.g. 0.195 is 0.252 minus 0.057). The last column for measurements 1-5 give the percentage deviation between implemented resistance and $\Delta R_{eff,cor}$.

Set	Meas. Numb.	Imple-mented resistance	Stroke volume		Calculated Compliance		Calculated Resistance		Corrected Resistance	
		R_1	V	sd	C_{eff}	(sd)	R_{eff}	(sd)	$R_{eff,cor}$	(sd)
		kPa.s.L^{-1}	L		L.kPa^{-1}		kPa.s.L^{-1}		kPa.s.L^{-1}	
a	1	0.00	0.909	0.004	1.666	0.012	0.057	0.001	0.000	
	2	0.19	0.909	0.004	1.634	0.014	0.252	0.001	0.195	3%
	3	0.43	0.902	0.004	1.585	0.010	0.501	0.003	0.444	3%
	4	1.07	0.897	0.002	1.458	0.025	1.159	0.004	1.102	3%
	5	2.07	0.877	0.003	1.390	0.051	2.249	0.009	2.192	6%
b	6	0.00	0.914	0.003	1.653	0.010	0.010	0.001	0.000	
	7	0.19	0.908	0.002	1.641	0.008	0.011	0.001	0.001	
	8	0.43	0.904	0.002	1.636	0.009	0.013	0.001	0.003	
	9	1.07	0.899	0.004	1.628	0.006	0.017	0.000	0.007	
	10	2.07	0.874	0.004	1.621	0.012	0.023	0.001	0.013	

The resistance $R_{L,eff}$ is calculated by means of the calculation of the effective flow resistance according to equation (6):

$$R_{L,eff} = \frac{\oint P_{es}\, dV}{\oint V'\, dV} \qquad (4.6)$$

It was previously demonstrated [45] that the effective flow resistance is a valid measure for the resistance over the whole loop. With this resistance each measured point P_{meas} is corrected for pressure drop due to the airflow, whereafter $P_{liq,eff}$ and (from the slope of regression lines through the corrected points) C_{eff} were calculated. The values calculated with these methods are presented for the situation when pressure is measured over bellows and additional resistance (Table 4.1 a), and when pressure is measured over the bellows alone (Table 4.1b).

The actual resistance values of the inserted resistance components are given. The influence of bellows and water on these values ("null-resistance") can be calculated from Table 4.1;a when no extra resistance is added, or from Table 4.1b when the pressure is measured between *LFC* and the air in the bellows. The calculated resistances from Table 4.1a, were corrected for the null-resistance, which is the first value of each row for the calculated resistances. This results in the corrected resistance value $\Delta R_{eff,cor}$ given in Table 4.1a. These corrected resistance values have a discrepancy of approximately 1%. The value for the compliance in Table 4.1a decreases with increasing resistance whereas in Table 4.1b this values remains almost constant at approximately 1.64 $L.kPa^{-1}$.

Body plethysmography

With the lung model, body plethysmographic measurements can be simulated; for this the lung model has to be placed in the body plethysmograph. With the body plethysmograph [51], which has become a standard technique in many clinical and research laboratories, the thoracic gas volume (*TGV*) and airway resistance can be determined. The body plethysmograph is a rigid box in which a volunteer or patient is seated surrounded by air. When a volume change occurs in a patient by compression or expansion of air (ΔV_C) the volume of air in the box outside the patient (ΔV_{bx}) will change in the opposite way ($\Delta V_C = -\Delta V_{bx}$), which results in a pressure change ΔP_{bx} (Boyle-Gay Lussac). The relationship between ΔP_{bx} and ΔV_{bx} is found by calibration of ΔP_{bx} against imposed volume changes of air in the closed box. Then ΔV_C can be found by measuring ΔP_{bx} in the body

plethysmograph. Of course the volume of the air in the box, when a patient is seated in the body plethysmograph, has to be corrected for the patient's volume which is taken equal to bodyweight in kg. Calculated ΔV_C is equal to compressed alveolar volume when influences of other closed air spaces inside the patient, such as air in the abdomen, are neglected.

In general, two types of measurements are performed. Phase A: Breathing against a shutter. *TGV* can then be calculated from the relationship between the pressure changes at the mouth, which reflect the pressure changes inside the lung (no flow situation), and the volume changes of the lung. Phase B: during tidal breathing, when lung volume of the patient is known from the procedure described in phase A, the alveolar pressure changes ΔP_A can be derived from ΔP_{bx}. When there is more than one lung compartment, the measured ΔP_A is the volume weighted mean of the pressures in the different compartments. The slope of the relationship between P_A and flow at the mouth (V'_m) reflects the flow resistance of the airways.

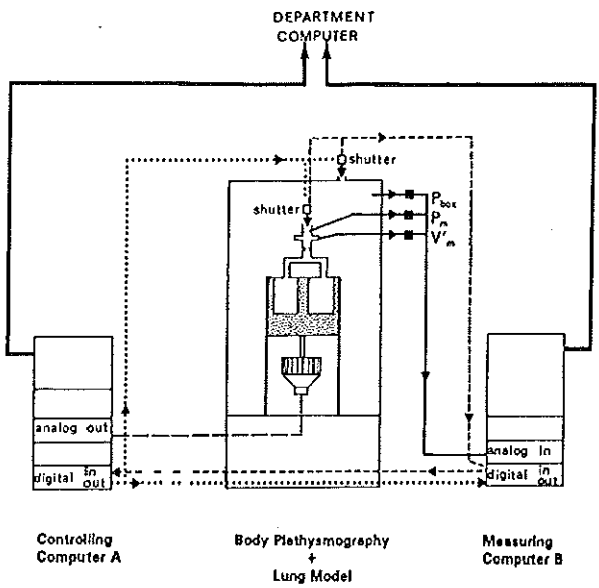

Figure 4.4:
The lung model placed inside the body plethysmograph. The model and body plethysmograph were controlled by computer A, while computer B performed the real-time measurements. P_{box} is the measured pressure in the box; P_{model} and V'_{model} are pressure and flow, respectively, at the combined outlet of both bellows.

Figure 4.4 shows the situation with the mechanical lung model placed in the body plethysmograph. When the lung model is used, control of the body plethysmograph is taken over by the computer which steers the lung model. The hand

control of the body plethysmograph *(Bodytest, Jaeger, Würzburg, Germany)* was extended with a program selection by means of external control lines. This was done in two ways:

1. by simulating the circuit interruption of the push-buttons and,
2. by direct control of the valves.

The 'controlling' microcomputer steers the model and sets the digital output for the lung function equipment to select the different phases of the measurement. The direct connections between the 'controlling' and 'measuring' computers are also indicated in Figure 4.4. These connections are optional and can be used in situations where the 'measuring' computer also has to perform signal analysis of the measurement, e.g. the 'measuring' computer holds up the 'controlling' computer until the measured signals are analyzed. In this way, together with the developed software, a number of predefined measurements can be performed.

A typical example of calculated P_A and V' is given in Figure 4.5a and 4.5b. In Figure 4.5a only an additional constant resistance of 1.07 kPa.s.L^{-1} was attached to the lung model. The calculation of the effective flow resistance was performed according to equation (6) where instead of P_{es}, P_A was used. For the measurement of Figure 4.5b a compressible component was inserted which simulates patients with expiratory flow resistance. The inspiratory resistance, $R_{eff,in}$, remained the same (1.15 - 1.06 kPa.s.L^{-1}) whereas the resistance during the expiration part, $R_{eff,ex}$ increased from 1.11 to 1.88 kPa.s.L^{-1}. $R_{eff,tot}$ was the resistance over inspiration and expiration together. The reproducibility is shown in the Figure, where at least three loops are plotted in one Figure. The irregularities, seen in Figure 4.5b, are due to the stick-slip of the rods.

DISCUSSION AND CONCLUSIONS

The computer controlled mechanical lung model *(CCL-1)* was used to test lung function equipment and to validate software. Due to its construction it can only be used as an active lung model, which means that it can not be used to simulate an artificially ventilated lung.

The examples illustrate some of the possibilities of the mechanical lung model. Furthermore, it has been used to test other lung function measurements in the pulmonary laboratory such as spirography, the closed circuit helium-dilution method, and pneumotachography; these are not discussed in this paper. All simulations had to be performed within a frequency and tidal volume range restricted by the dynamical properties of the model.

Up to now we used the piston only as a flow generator. Therefore, during occlusion of the airway the pressure inside the bellows can become very high. To

cope with this problem it is possible to measure the pressure inside the bellows and, together with the known volume of the bellows, to calculate mean alveolar pressure. The software can be altered to steer the piston for following a predefined pressure pattern to simulate body plethysmography with pressure signals as measured in patients. The software detects too high pressures due to occlusion of the airways.

The *CCL-1* fulfils most of the demands. One problem of the model is the stick-slip (also called stiction) of the rods, which causes irregularities on the signal, as shown in Figures 4.3a, 4.3b and 4.5b, due to irregular movement of the bars through the guiding bearings. As can be seen for the simulation performed without the compressible component (Figure 4.5a), the stick-slip was absent. In the situation shown in Figure 4.5a a little stick-slip will result in a higher pressure in the water which directly counteracts the effect of stick-slip on the movement of the lung bellows. In Figure 4.5b the stick-slip is more pronounced due to the parallel compliance of compressible component and lung bellows. So, a sudden pressure increase in the liquid is partially shunted to the surrounding of the compressible element. A little stiction of a rod during an expiration will therefore result in a pressure increase in the water causing a higher expiratory resistance by compression of the compressible element. This pressure increase amplifies the primary effect of the stick-slip on the movement of the lung bellows. This higher pressure will also cause an extra movement of the bellows which counteracts the stick-slip. Because there is a complex time relationship between the effects of stick-slip and resistance of the compressible component, alveolar pressure disturbances occur which can be seen on measured alveolar pressures. An improvement may be obtained if the guiding bars are positioned in the centre of the bellows. The differences between implemented and calculated resistances were 2.6 - 5.8%. The calculated compliance in Table 4.1b is in the expected range. A good quantification of the resistance and compliance values is an important aspect of the mechanical model when used with the parameter estimation techniques, as reported earlier [78]. The change of the calculated compliance with high increased resistance components must have its origin in the additional pressure components over the pipe system because the value for the compliance, measured over the bellows alone, remains almost constant.

The amount of water which has to be displaced during operation causes a phase shift between the programmed volume displacement and the actual volume displacement of the piston. At high frequencies this inertia of the system also results in a lower amplitude response. The compliance of each bellows can not

be changed yet. A change in compliance, for instance by additional springs, will be of value for extending the simulation possibilities of the model.

Although the model still has some limitations with respect to the mechanical construction and the limited flexibility in representing lung mechanics, it has proven useful for testing equipment and software.

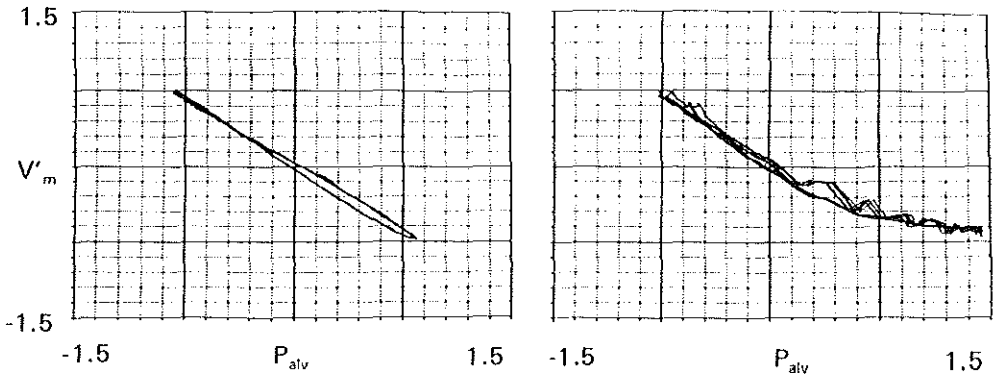

A TV:	0.23	L	**B** *TV*:	0.22	L
$R_{eff,in}$:	1.15	kPa.s.L^{-1}	$R_{eff,in}$:	1.06	kPa.s.L^{-1}
$R_{eff,ex}$:	1.11	kPa.s.L^{-1}	$R_{eff,ex}$:	1.88	kPa.s.L^{-1}
$R_{eff,tot}$:	1.13	kPa.s.L^{-1}	$R_{eff,tot}$:	1.46	kPa.s.L^{-1}

Figure 4.5:
Alveolar pressure (P_{alv}; kPa) - flow (V'_{m}; L.s^{-1}) curve.
***A**: with a resistance of 1.07 kPa.s.L^{-1}. **B**: with an additional compressible segment. TV is tidal volume, $R_{eff,total}$ is effective resistance over the whole curve, $R_{eff,in}$ is effective resistance for inspiration and $R_{eff,ex}$ is effective resistance for expiration.*

CHAPTER 5
A COMPUTER-CONTROLLED FLOW RESISTANCE

AFM Verbraak, W Holland, BN Mulder, JM Bogaard, A Versprille

INTRODUCTION

In a previous mechanical lung model [83, 84] (Chapter 4) we used resistance components [81] of fixed values, which limited the flexibility of the model. For each resistance a specific resistance component had to be implied. Furthermore, variation in flow resistance during a simulation was impossible. To improve simulation of lung and airway mechanics it is necessary to change flow resistance during inspiration and expiration.

Flow resistances which were controlled have been applied in the expiratory parts of mechanical ventilators to control expiratory pressure [85, 86]. In the Siemens Servo ventilator (*Siemens-Elema, Solna, Sweden*) the expiratory flow through a rubber tube is controlled by means of a magnet acting on a lever arm squeezing a flexible tube against a fixed arm. The force of the lever is controlled by the ventilator. This device is designed to establish an end-expiratory pressure [85]. In the César ventilator (*Taema, CFPO, France*) a tube is squeezed by means of a motor driven roller arm [86]. The position of the arm itself is independent of counter force. This device can impose several expiration patterns in patients. In both ventilators the resistance is changed by varying the lumen of a tube. These types of resistances are non-linear with flow rate and sensitive to minor changes in cross-section in case of a small baseline aperture. Therefore, a specific flow resistance under conditions of changing flow is hard to control.

To improve control of flow resistance, we developed a new type of flow resistance device to be controlled by computer under operational conditions. In this paper we describe the construction and the characteristics of this flow resistance.

METHODS

General construction

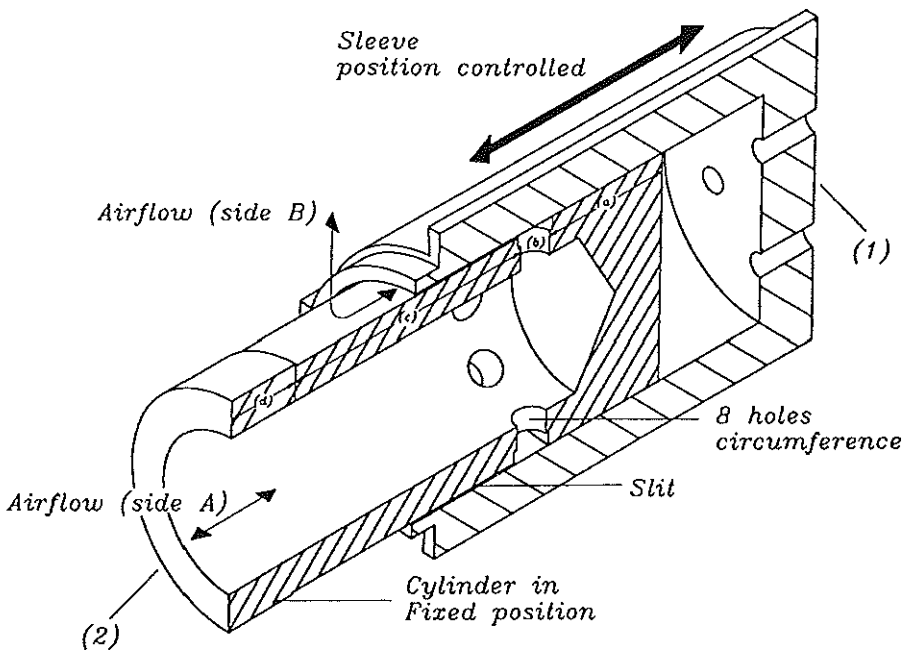

Figure 5.1:
A schematic view showing the basic components of the computer- controlled resistance. For explanation, see text.

The two basic components of the *CCR* (Figure 5.1) are a sleeve (*1*) to be moved over a cylinder (*2*), both made of dellrin (*DuPont, USA*). The internal diameter of the sleeve (D_{sle}) is equal to 33.98 mm. The end sections *a* and *d* of the hollow cylinder fit closely in the sleeve. In section *b* eight holes are equally distributed in the circumference to enable the gas to pass the cylinder. The diameter of the cylinder section *c*, situated between sections *a* and *d*, is slightly smaller than the

inner diameter of the sleeve. If the sleeve covers section *b* and a part of section *c* the gas has to pass the slit between sleeve and cylinder. The groove in the circumference of section *b* enables the gas passing the holes to redistribute in the circumference before it enters the slit. The external diameter of section *c* of the cylinder is fixed for a specific cylinder. The cylinder can be replaced by a cylinder of different dimensions in section *c*. The cylinder has a maximum length of 74 mm; the diameters of sections *a* and *d* are 33.88 mm and the lengths are 20 and 15 mm, respectively. These dimensions limit leakage of gas to a negligible amount by a high flow resistance.

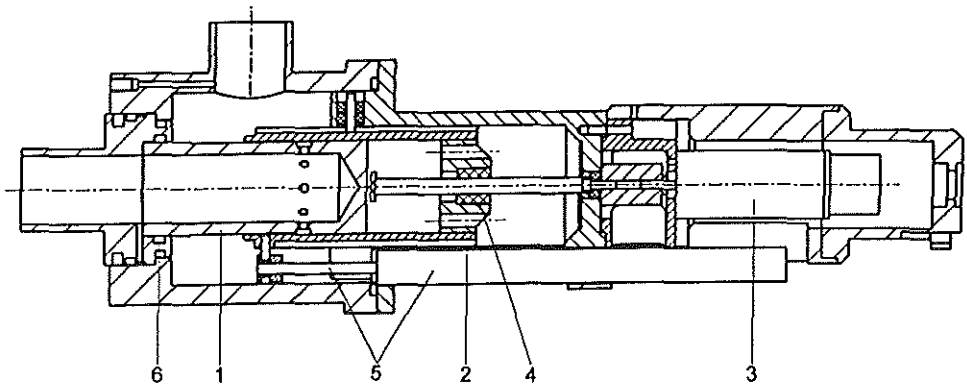

Figure 5.2:
Construction of the computer-controlled resistance device. The cylinder (1), sleeve (2), motor (3), roller screws (4), potentiometer (5), and rubber O-ring (6) are indicated.

The total construction of the *CCR* is shown in Figure 5.2. The sleeve (*1*) is moved by an electrical stepper motor (*3*). Its rotation is transformed by means of roller screws (*4*) to longitudinal displacement of the cylinder (*2*). A potentiometer (*5*) attached to the sleeve determines its actual position with respect to the cylinder and thus length of the slit. Electronic monitoring of the position of the sleeve protects movements beyond the functional range. The displacement is stopped when magnetic switches at the two extreme positions are activated. Then the *CCR* can only be reactivated by resetting the control unit. This double protection prevents damage to mechanical parts of the *CCR*. The motor and linear servo control (*Maxon re025-05534, Inter electric AG, Sachsel, Switzerland*) position the sleeve at a given set point, which is controlled by computer or set by hand.

During an expiration, flow enters the connection *side A* (see Figure 5.1), passes the cylinder, the holes and the slit and leaves the *CCR* at *side B*; during

inspiration flow is in reverse direction. The flow resistance of the *CCR* implies flow resistance of the slit and the additional resistances caused by the holes and connecting parts. The flow resistance of the slit depends on the length (l_{sli}) and the height of the slit (h_{sli}) which is the distance between sleeve and section *c* of the cylinder. The circular width of the slit depends mainly on the internal diameter of the sleeve and is fixed for the construction chosen. If the sleeve shifts over section *d* the flow resistance increases quickly until it is locked by a rubber O-ring (*6*). Then, the *CCR* is closed.

Cylinders

The resistance calculations performed in this paper were based on two cylinders (I and II) with an external diameter over whole part *c* (D_{cyl}) of 33.23 mm and 33.44 mm, respectively. Then, the height of the slit h_{sli} is equal to 0.375 mm and 0.27 mm, respectively. The eight holes in the cylinder have a diameter and length of 5 mm. The movement of the sleeve was restricted to 35 mm maximally. l_{sli} is the position of the sleeve from section *a* to section *d*, where l_{sli} = 0 at the border between sections *b* and *c* resulting in a positioning of the slit between -4 and 33 mm.

Flow resistance

The flow resistance of a given cylinder depends on the position of the sleeve:

1. in the normal range the sleeve covers section *b* and a part of section *c*,
2. if the *CCR* is fully open the sleeve does not cover any part of section *b* or *c*, and,
3. in a transitional range the sleeve partly covers section *b*.

1) Flow through the slit

For calculations of flow resistances in a pipe it is important to define whether the flow is laminar or turbulent according to the Reynolds number. The Reynolds number (*Re*) is defined as:

$$Re = \frac{\rho_{air} D_{hydr}}{\eta_{air}} \cdot \frac{10^3 \, V'}{A} \qquad (5.1)$$

where:

ρ_{air}	*specific mass of air at room temperature, 1.205, in* $Kg.m^{-3}$,
D_{hydr}	*hydraulic diameter of the pipe, in m,*
η_{air}	*dynamic viscosity of air, 18.3* 10^{-6}, *inPa.s,*
V'	*airflow, in* $L.s^{-1}$
A	*cross-sectional area of flow, in* m^2.

The hydraulic diameter is defined as:

$$d_{hydr} = 4 * \frac{A}{W_p} \qquad (5.2)$$

where:

W_p *wetted-perimeter of the surface (A) through which the air flows, in m.*

The hydraulic diameter for the slit is equal to:

$$d_{hydr,sli} = 4 * \frac{A_{sli}}{W_p} = 4 * \frac{\pi(D_{sle}^2 - D_{cyl}^2)}{2*\pi(D_{sle} + D_{cyl})} = 2*h_{sli} \qquad (5.3)$$

where:

A_{sli} *is the cross-sectional area of the slit, in m².*

According to the Reynolds number the flow is mainly laminar for $Re < 2000$, whereas for $Re > 2500$ flow is fully turbulent. Using both cylinders the Reynolds number in the slit (Re_{sli}) is about 1250 at a flow of 1 L.s^{-1} according to equation 5.1. Because flow is normally below 1.5 L.s^{-1} we assumed the flow to be laminar in the slit. The laminar flow resistance of the slit ($R_{sli\text{-}lam}$, in kPa.s.L^{-1}) is given by [87, 88]:

$$R_{sli\text{-}lam} = \frac{12*\eta}{\pi} * \frac{1}{h_{sli}^3 * D_{cyl}} * l_{sli} \qquad (5.4)$$

which results in a $R_{sli\text{-}lam}$ for cylinders I and II of $40*l_{sli}$ and $104.5*l_{sli}$ kPa.s.L^{-1}, respectively.

2) CCR fully opened

With the sleeve in position the resistance is low, because of the dimensions of the holes and connecting pipes. It is less than 0.06 kPa.s.L^{-1}.

3) Transitional zone

We have no description in mathematical terms of the changes in flow resistances in the transitional zone for l_{sli} is -4 to 0 mm. The resistance (R_{in}) at position $l_{sli} = 0$ when the transitional zone is fully covered by the sleeve can be described by the Rohrer equation [65]

$$R_{in} = c_0 + c_1 * V' \qquad (5.5)$$

where:

c_0 *is related to the laminar flow, in kPa.s.L^{-1}*

c_1 *is related to the turbulent flow, in kPa.s^2.L^{-2}*

5.3a

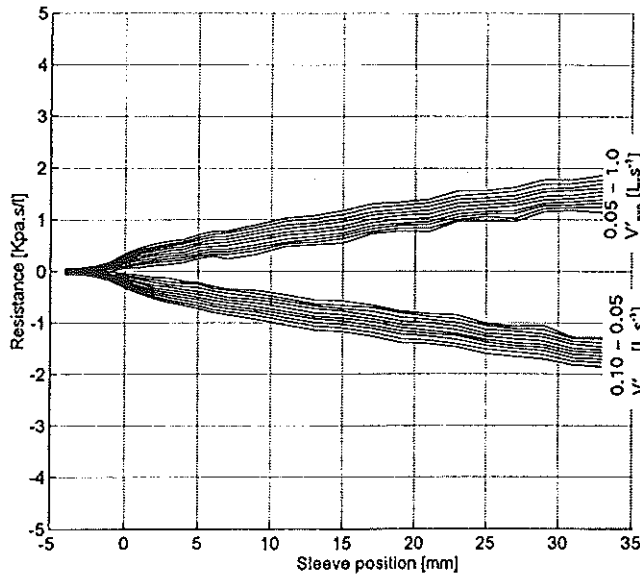

5.3b

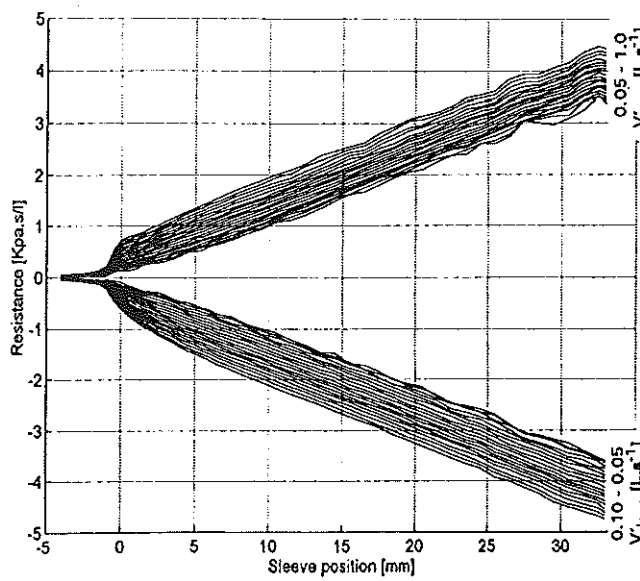

Figure 5.3:
Flow resistances of the CCR as function of sleeve position (l_{sl}) with expirator flow (V'_{exp}) and inspiratory flow (V'_{in}) as parameters. Flow is changed from 0.1 L.s^{-1} up to 1.0 L.s^{-1} to measure the inspiratory resistance and from -0.1 L.s^{-1} down to -1.0 L.s^{-1} to measure expiratory resistance.
Figure 5.3a: cylinder I, in steps of 0.1 L.s^{-1}.
Figure 5.3b: cylinder II, in steps of 0.05 L.s^{-1}.

Calibration

The *CCR* was calibrated by connecting it to the different sides of a flow generator (*59007, Mijnhardt, de Bilt, The Netherlands*), simulating inspiratory and expiratory flow. Flow was changed between 0.05 and 1.0 $L.s^{-1}$ by changing the voltage on the flow generator and was measured with a pneumotachometer (*Lilly, Jaeger, Würzburg, Germany* and *Validyne P45-transducer, Validyne, Northridge, USA*). The pressure gradient over the *CCR*, measured with a pressure transducer (*Celesco, Canoga Park, CA, USA*), was divided by flow to determine flow resistance. The sleeve was gradually increased between -4 and 33 mm and for each sleeve position the flow and pressure were stored in multiples of 0.5 $L.s^{-1}$. In Figure 5.3 A and B, for both elements the flow resistance is plotted as a function of the position of the sleeve for these different values of flow. From -4 to 0 mm the sleeve gradually overlapped the holes, leading to a non-linear increase in pressure over the *CCR*. This non-linear rise continued with a linear increase if the slit was lengthened.

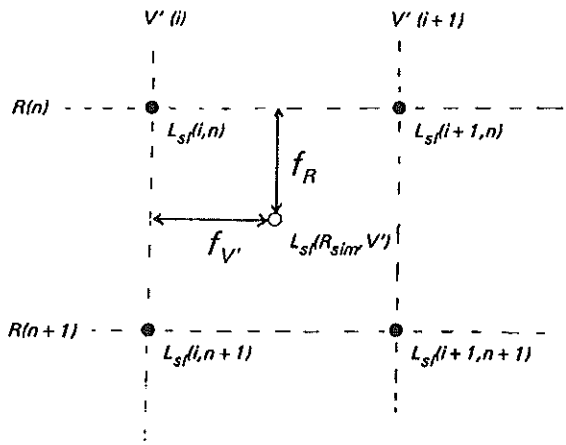

Figure 5.4:
Part of a two-dimensional matrix of measured data.
$f_{V'}$ and f_R: fractional distances.
Open circle: the resistance to be simulated (R_{sim}) at a measured flow (V').
Closed circles: the nearest points $I_{sh}(i,n)$, $I_{sh}(i+1,n)$, $I_{sh}(i,n+1)$ and $I_{sh}(i+1,n+1)$.

Sleeve control

The position of the sleeve has to be controlled accurately to establish a correct resistance. This control method was based on spline function techniques [89, 90]. The measurements of resistance as a function of position and flow were converted to a matrix with position as a function of resistance and flow. A part of a two-dimensional matrix of measured data is shown in Figure 5.4. Resistance was positioned in rows (n) and flow in columns (i). This matrix conversion was performed with *MATLAB* (*The Math Works Inc, Natick, USA*). The resistance increased from 0 to 6 kPa.s.L^{-1} in steps of 0.05 kPa.s.L^{-1} and flow was equally spaced from 0.05 to 1.0 L.s^{-1} in steps of 0.05 L.s^{-1}. Because the converted matrix was equally spaced for resistance and flow, a standard linear interpolation technique could be used. To establish a flow resistance (R_{sim}) at flow V', the nearest lower and higher rows and columns in the matrix are searched, as shown in Figure 5.4. For each pair of resistance and flow values the positions are known. Then, the fractional distance of R_{sim} from the lowest nearest resistance value (f_R) and the fractional distance of flow V' from the lowest nearest flow ($f_{V'}$) are calculated (eq. 6 and 7). The calculated position (l_{cal}, in m) is obtained from equation 5.8.

$$f_R = (R_{sim}-R(n)) \,/\, (R(n+1)-R(n)) \tag{5.6}$$

$$f_{V'} = (V'-V'(i)) \,/\, (V'(i+1)-V'(i)) \tag{5.7}$$

$$l_{cal} = [(l_{n,i} \cdot (1-f_R) + l_{n+1,i} \cdot f_R) \cdot (1-f_{V'})] + [(l_{n,i+1} \cdot (1-f_R) + l_{n+1,i+1} \cdot f_R) \cdot f_{V'}] \tag{5.8}$$

As flow is continuously changing and resistance depends on flow, this calculation is performed on-line real-time to position the sleeve such that R_{sim} is imposed. Not only flow but also the resistance R_{sim} is continuously changing during inspiration and expiration.

RESULTS

Resistance of the CCR

For the same two cylinders with different dimensions the resistance was calculated and only the measured data between l_{sli} = 5 and l_{sli} = 33 mm were considered (Figure 5.5) and fitted to equation 5.9.

$$R_{sim} = c_0 + c_1 * V' + (c_2 + c_3 * V') * l_{sli} \qquad l_{sli} \geq 0 \tag{5.9}$$

The coefficients c_0 and c_1 describe the resistance at extrapolated position l_{sli} = 0 and c_2, and c_3 describe the position-dependent resistance of the slit. For both cylinders the fitted data from the measurements as calculated in accordance with equation 5.9 are given in Table 5.1.

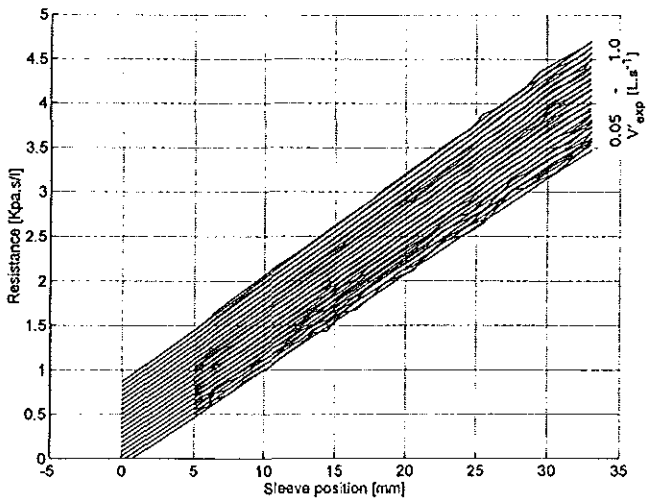

Figure 5.5:
Measured flow resistances in the slit for l_{sli} = 5 - 33 mm. The resistance lines for l_{sli} = 0 up to 33 mm, are fitted according to equation 9.

Table 5.1: Resistance in the slit.

Cylinder		c_0 kPa.s.L^{-1}	c_1 kPa.s^2.L^{-2}	c_2 kPa.s.L^{-1}.m^{-1}	c_3 kPa.s^2.L^{-2}.m^{-1}
I	Insp.	-0.0218	0.5457	37.8	1.6
	Exp.	-0.0055	0.4898	35.1	3.7
II	Insp.	-0.5709	0.8443	103.4	15.3
	Exp.	-0.5775	0.7835	103.2	8.7

The resistances of the slit per unit of length, calculated according to equations 5.4 were 41.0 and 104.5 kPa.s.L^{-1}.m^{-1} for cylinders I and II, respectively. These values can be compared with the coefficient c_2 of equation 5.9.

In Figure 5.6 the change in flow resistances versus sleeve length is shown, starting at a sleeve length of l_{sli} = 5 mm, where the measured pressure gradients for $l_{sli} \geq 5$ were diminished with the pressure gradient at position l_{sli} = 5 mm. When these data were fitted to the position-dependent components c_2 and c_3 of

equation 5.9, including a correction for the shift of l_{sli} there was a slight difference in calculated values, as given in Table 5.2.

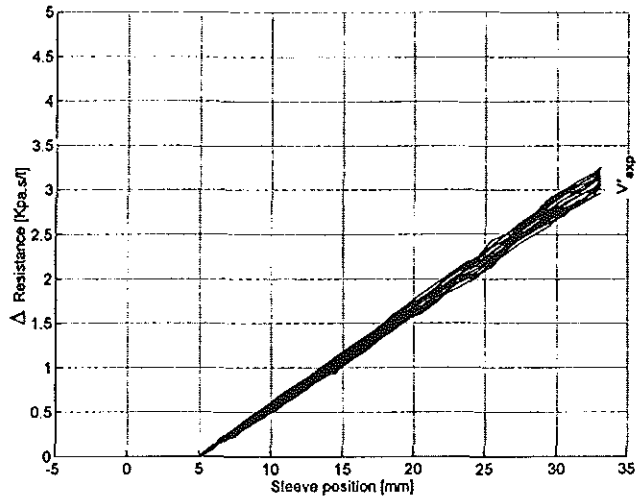

Figure 5.6:
Change in measured flow resistances (Δ resistance) between l_{sli} = 5 and to 33 mm . To calculate flow resistance the measured pressure gradients for l_{sli} ≥ 5 were diminished with the pressure gradient at l_{sli} = 5 mm. V'_{exp} from 0.05 up to 1.0 $L.s^{-1}$.

Table 5.2: Resistance change in the last part of the slit.

Cylinder	$R_{sl\text{-}lam}$ kPa.s.L^{-1}.m^{-1}		c_2 kPa.s.L^{-1}.m^{-1}	c_3 kPa.s^2.L^{-2}.m^{-1}
I	41.0	Insp.	39.1	1.2
		Exp.	35.0	5.1
II	104.5	Insp.	98.2	28.0
		Exp.	97.8	15.8

Time response

The maximum speed of the sleeve is 200 $mm.s^{-1}$. Based on the values in Table 5.1 for cylinders I and II, this will result in a maximal resistance change of 7.62 and 21.10 kPa.s.L^{-1} per second at a flow of 0.1 $L.s^{-1}$, and 9.04 and 23.24 per second at a flow of 1.0 $L.s^{-1}$. At low values of l_{sli} the maximal range in resistance per second will be larger due to the turbulence in the holes and the first part of the slit. When R_{slm} was stepwise changed between 0.5 and 1.5 kPa.s/L at a

constant flow of 0.5 $L.s^{-1}$ (Figure 5.7), the calculated resistance response was 12 $kPa.s.L^{-1}$ per second.

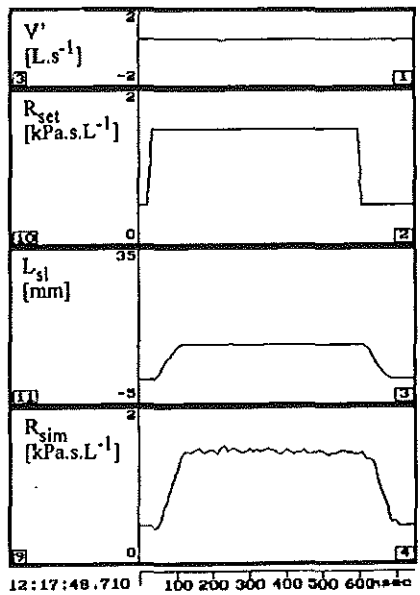

Figure 5.7:
The two upper curves show the imposed constant flow and imposed resistance (R_{sim}) which was stepwise changed from 0.5 to 1.5 and back. The calculated sleeve position and measured resistance are given in the two lower curves.

Resistance control

To test the accuracy of resistance control we connected the *CCR* to a vacuum cleaner. The resistance (R_{sim}) was initially set at 0.5 $kPa.s.L^{-1}$ and changed to 1.5 $kPa.s.L^{-1}$. For each resistance value the flow was sinusoidally changed between -1 and 1 $L.s^{-1}$ (Figure 5.8A). The position of the sleeve was calculated with the spline function algorithms. For this calculation all flows between -0.05 and 0 $L.s^{-1}$ and between 0 and 0.05 $L.s^{-1}$ were set to 0.05 and -0.05 $L.s^{-1}$, respectively. This had to be done because this was the lowest value of the matrix. Figure 5.8A shows that for flows between -0.1 and 0.1 $L.s^{-1}$ the position is constant. For R_{sim} = 0.5 $kPa.s.L^{-1}$ the position of the sleeve changed between 0 and 5 mm while for R_{sim} = 1.5 $kPa.s.L^{-1}$ it changed between 7 and 14 mm. The resistance derived from measured pressure gradient and flow is unstable for low flows due to the large influence of small flow variations on the derived resistance value. The relation between flow and pressure gradient is shown in Figure 5.8B. The two straight lines a and b for R_{sim} are and 1.5 $kPa.s.L^{-1}$,

respectively, show that the *CCR* is able to keep the resistance constant at the set value.

DISCUSSION

The mathematical description of the resistance of the slit predicts the range of the resistance with a known h_{sli} and thus predicts the diameter D_{cyl} of the cylinder which is needed to set a required resistance range. The flow resistance at the fully open position of the sleeve is the lowest value of the resistance range which can be controlled by the *CCR*. The flow dependence of the resistance was mainly caused by the transitional zone, i.e. the area where the sleeve gradually covered the side holes in the cylinder. The turbulent resistance in this transitional zone caused the sleeve to be moved over a relatively large distance to keep the flow resistance constant at different flows. During the expiration at higher flows there was a flow dependence in the first 5 mm of the slit. At larger slit lengths all resistance lines were almost in parallel, indicating only a minor effect of turbulence. The irregularities in the straight part of the resistance lines might be due to a slight variability in the imposed flows and dependent pressure gradients, which have a relative large effect on the calculated resistance at low flow values.

The interpolation method based on the matrix (Figure 5.4) controlled the *CCR* satisfactorily. The integration function in the controller reduced the difference between measured and simulated resistance, but introduced instabilities in the calculated position of the sleeve at low flow values (Figure 5.8, panel 3).

The rate of change in resistance during normal breathing and artificial ventilation was not more than 3 $kPa.s.L^{-1}$ per second according to body plethysmographic tracings [78] and 8 $kPa.s.L^{-1}$ per second in patients with airflow obstruction and flow limitation [91]. The speed of the sleeve was adequate to simulate such conditions, since the maximal speed was 12 $kPa.s.L^{-1}$ per second. For simulation of sudden collapse of airways, this resistance device will be too slow.

If the sleeve would be positioned over section *d* the resistance of the *CCR* increased quickly to infinity (not shown in the Figures). This function can be used in specific circumstances when flow has to be stopped.

An improvement of the *CCR* would be a reduction of its dependence on flow, probably due to the turbulence in the transitional zone between -5 and 0 mm. Therefore we will reshape this part of the cylinder to lower this turbulence. An extension of its applicability could be obtained by using cylinders with a changing, instead of a constant, diameter of section *c*. If during increasing slit length the diameter of the cylinder increases, the increase in flow resistance at a

given speed will be larger. On the one hand, it will improve the time response, but on the other hand it will result in a decrease in accuracy. A distribution of different diameters along the cylinder will enable a specific relation between pressure, position and flow.

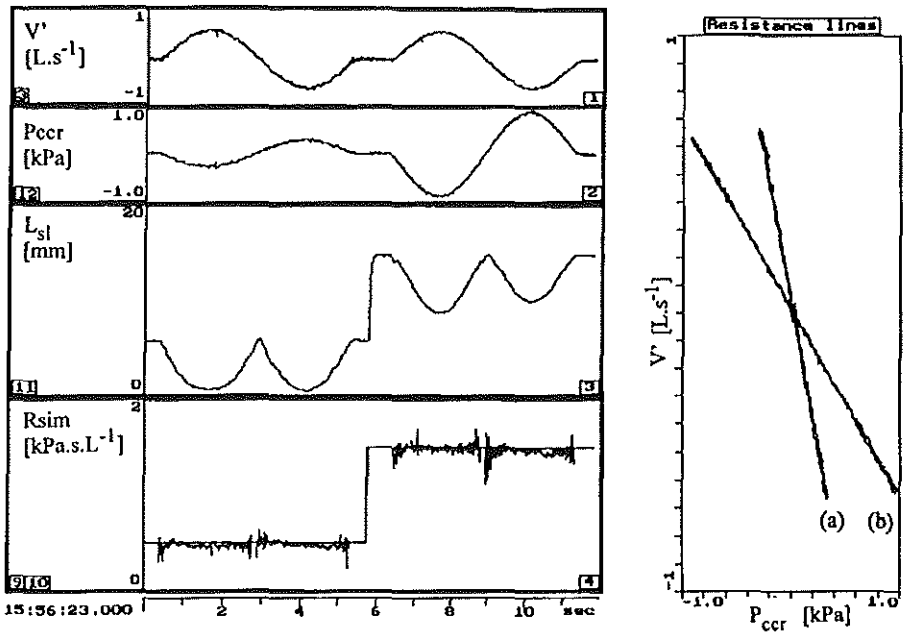

Figure 5.8:
Left: *recordings of imposed flow (V'), imposed resistance (R_{sim}), measured pressure (P_{ccr}), measured position of the sleeve ($l_{sli,m}$) and calculated resistance ($R_{ccr,m}$) against time.*
Right *plot of the pressure over the CCR (P_{ccr}) against flow.*

CONCLUSION

The *CCR* can be used in a computer-controlled lung model to simulate lung pathology. The *CCR* proved to be a flexible device to be used in situations where a constant flow resistance, or a flow resistance with a pattern which had to be a function of other variables, is needed.

CHAPTER 6
A NEW APPROACH TO MECHANICAL SIMULATION OF LUNG BEHAVIOUR

AFM Verbraak, PR Rijnbeek, JEW Beneken, JM Bogaard, A Versprille

INTRODUCTION

The complexity of the respiratory system demands simplified models to simulate its physical behaviour by either mathematical equations or mechanical components. The translation of physiological behaviour to mechanical components can be difficult, because the biological relationships often are non-linear and usually imply an interaction between different components. However, a mechanical model is needed if real measurements are to be simulated for testing lung function equipment, for evaluation of interactions between software and such equipment, and for instruction and educational purposes. Modelling in mathematical terms implies simulation of specific lung pathology by sets of defined parameters [6, 60, 92]. Mechanical simulation of the lung by means of a composition of one or more components [13, 83, 84, 93-98] is usually less flexible than mathematical simulation. Several authors [99, 100] simulated spontaneous breathing by an industrial servo-controlled volume simulator (*Dräger AG*). The pressure in the model was equal to the pressure calculated according to the resistances and compliancies incorporated in the model. In the Gainesville Anaesthesia Simulator [101, 102] computer-controlled compliance was used by means of pressure-regulated forces on a bellows.

In a previous study (Chapter 4) we developed a mechanical lung model in which lung volume patterns of patients were simulated by a computer-controlled

piston displacement [83, 84]. This mechanical lung model had several limitations, mainly inherent to the dynamic properties of the mechanical system: irregularities in the pressure and volume signals by slip-stick effects; unsatisfactory representation of airway resistance; and a limited range in lung compliance. Moreover, it could not simulate the artificially ventilated patient.

In this chapter we present a Computer-Controlled Lung Model (*CCL-2*) in which the integration of hardware and software is extended to offer new possibilities and which eliminates many disadvantages of the previous model.

METHODS

Mathematical model

In this paper the physical features of the lung, to be described in mathematical terms, are called *elements* and the mechanical parts, which simulate an element, are named *components*.

For purposes of modelling, the pulmonary system has to be simplified to elements which represent specific physical features of the lung. These elements are valid for defined conditions only. The currently used mathematical model is based on the serial model of chapter 3 (Figure 3.1), consisting of one alveolar compartment connected to ambient air by a tube representing the airways [78]. This tube consists of three parts in series, representing the small airways and the upper airways with the compressible airways in between. The lung volume (V_L) is the volume of the alveolar compartment and the volume of the airways together. In this model we omit the influence of volume changes of the compressible airways on V_L. The elastic behaviour of the alveolar compartment is described by lung compliance (C_L) and resistance of the compressible airways is a function of transmural pressure.

We extended the previous mathematical model [78] (Chapter 3) with:

1. static compliance of the thorax (C_{th}),
2. dynamic compliance of lung and thorax together,
3. a computer-controlled resistance to simulate airway resistances, and
4. effects of cardiac actions on airflow, often called cardiac oscillations.

Static compliance

In our previous mathematical model [78] (Chapter 3), lung pressure was linearly related to lung volume. In the new model we insert a mathematical description of the pressure-volume (*PV*) curve [103], which was an extension of an exponential model described by Salazar [104], according to:

$$V_L = V_{max} * (1 - e^{-k*(P_L - P_0)}) \quad (6.1)$$

where:

V_L	*lung volume, in L*
V_{max}	*maximum volume (asymptote of the exponential equation), in L*
k	*index of curvature, in kPa^{-1}*
P_L	*recoil pressure of the lung, in kPa;*
P_0	*intercept on the pressure axis at V_L is 0, in kPa*

We describe the elastic behaviour of the chest wall according to [105]:

$$V_L = C_{th} * P_{th} + 0.8 * TLC_{ref} \quad (6.2)$$

where:

C_{th}	*thorax compliance, in L.kPa^{-1}*
P_{th}	*elastic pressure due to thoracic cage compliance, in kPa*
TLC_{ref}	*predicted value of Total Lung Capacity, i.e. the volume in the lung after a maximal inspiration, in L*

The equations 6.1 and 6.2, which represent lung and thorax separately, are combined to derive the volume relationship of the total respiratory system (C_{rs}). At all lung volumes a balance in pressures is present between P_L, alveolar pressure (P_A), P_{th} and pressure exerted by the muscles (P_{mus}) according to

$$P_A - P_L = P_{pl} = -P_{th} - P_{mus} \quad (6.3)$$

The pressure-volume relationships of the lung (F_L), the thorax (F_{th}), and the lung and thorax together (F_{rs}) are shown in Figure 6.1. This type of presentation of the pressure-volume relations of lung, thorax and respiratory system was first described by Rahn et al. [106]. The lung volume, where the counteracting pressures P_L and P_{th} are equal, is the volume at normal end-expiration (zero airflow) and is called the functional residual capacity *(FRC)*. Normally the pressure-volume relationship of the thorax will have a more flattened course, close to residual volume and total lung capacity. This simplification has no consequences in explaining the fundamentals of the new approach in order to simulate lung compliancies. If better mathematical equations, which describe this flattening, become available, they can be implemented as such. For the simulation presented in Figure 6.1 we used values which represented respiratory mechanics in patients with emphysema [105, 107, 108].

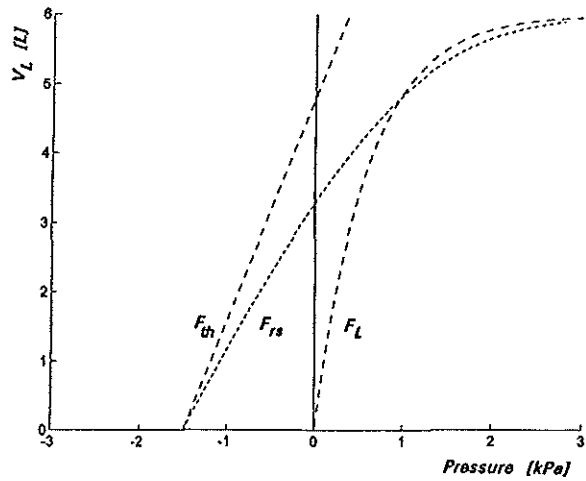

Figure 6.1:
Rahn-diagram:
Indicated are the pressure-volume diagram for chest wall (F_{th}), lung (F_l), and lung and thorax together (F_{rs}), with respectively P_{th}, P_L and P_{pl} on the X-axis and V_L on the Y-axis.
Values for this simulation:
P_0= 0.0 kPa; k = -2.0 kPa^{-1}; V_{max}= 6.0 L; TLC_{ref}= 6.0 L; C_{th} = 4.8 L/kPa.

Dynamic compliance

When pressure, volume and flow are measured at the outlet time-related effects can be observed which are due to the parallel [60], the series gas distribution model [109] and the visco-elastic model [110, 111]. The effect of parallel inhomogeneity is most pronounced in clinical routine. Similowsky [112] demonstrated that with respect to pressure, volume and flow measured at the outlet, no distinction could be made between those three causes. In mathematical terms one effect can be redefined into another. Because mechanical simulation needs the availability of one lung component and two more resistance components we simulated the time-related effects by means of the visco-elastic model.

The compliance of the lung is not purely elastic as described by equations 6.1 and 6.2. Tissue properties of lung and thorax cause that the recoil pressure is not only a function of volume, but also of lung volume history. In literature this effect was modelled by incorporating visco-elastic [110, 111, 113, 114] or plasto-elastic [115-117] elements in parallel with the components representing

static elastance. Visco-elasticity depends on the rate of change in pressure, while plasto-elastic elements are used to describe the effect of a counteracting pressure, which occurs when a certain threshold in the pressure is reached. Because visco-elasticity is most appropriate for describing the mechanical behaviour of the respiratory system we implement visco-elasticity to demonstrate the ability of simulating these kinds of lung behaviour with the mechanical model. The model with only elastic and visco-elastic elements as described by Similowsky [112] is given in Figure 6.2(top). The visco-elastic effects were implemented as a Maxwell body, in parallel with the elasticity of the lungs (E_L) and the airway resistance (R_L). The Maxwell body consists of an elastic element (E_{mxb}) in series with a viscous element (dashpot) (R_{mxb}). The elastic elements and dashpot are the mechanical representations for the elastic and dissipative (resistances) effects in the lung model. In electrical terms they can be modelled as a capacitor and resistor. A parallel or serial connection of these elements results in time-related responses. Compliance is defined as the reciprocal of elastance.

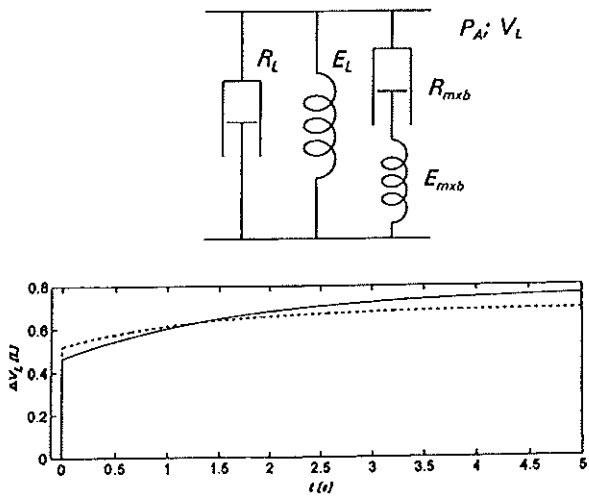

Figure 6.2:
Top: *The visco-elastic rheologic model with elastance E_L and resistance R_L for the lung and elastance E_{mxb} and resistance R_{mxb} for the Maxwell body. P_A is the alveolar pressure in the lung and V_L is lung volume.*
Bottom: *The volume change of the lung (ΔV_L) as function of time (t) after a stepwise change in P_A of 1 kPa: Normal lung, E_L = 1.44 kPa.L^{-1} and E_{mxb} = 0.49 kPa.L^{-1} (dotted line) and for the lung with COPD, E_L = 1.29 kPa.L^{-1} and E_{mxb} = 0.87 kPa.L-1 (continuous line). R_{mxb} = 1.928 kPa.s.L^{-1} in both types of lungs.*

A sudden pressure increase in the lungs extends both elastic elements, resulting in a sudden volume increase (ΔV_{init}) according to equation 6.4.

$$t = 0; \quad \Delta V_{init} = \frac{P_A}{E_L + E_{mxb}} \tag{6.4}$$

After this initial volume increase an overall relaxation of R_{mxb} follows, allowing the E_{mxb} to shorten resulting after infinite time in a total volume change (ΔV_{end}) according to eq. 6.5.

$$t = \infty ; \quad \Delta V_{end} = \frac{P_A}{E_L} \tag{6.5}$$

The change from ΔV_{init} to ΔV_{end} occurs as an exponential time course depending on the constant values of E_L, E_{mxb} and R_{mxb}. Because P_A is measured inside the *CCL-2* instead of being calculated from the pressure drop over the airways, R_L could be omitted in the calculations. The total volume change as function of time is given by equations 6.6 and 6.7.

$$t > 0 \qquad \Delta V = \Delta V_{end} - (\Delta V_{end} - \Delta V_{init}) * e^{-\frac{t}{\tau}} \tag{6.6}$$

$$\tau = \frac{E_L * E_{mxb}}{R_{mxb} * [E_L + E_{mxb}]} \tag{6.7}$$

In Figure 6.2(bottom) for a 1 kPa change in P_A at time t=0, the change in volume is indicated for a normal lung and a lung with chronic obstructive pulmonary disease (*COPD*). The values for the elastic and viscous elements for lung and thorax together are extracted from the paper of Guerin et al. [118].

Airway resistances

The resistance of the compressible element (R_c) represents the airflow resistance in those airway generations which are susceptible to the changes in transmural pressure, which is defined as intrabronchial pressure minus pleural pressure and is located at the transition between the small airways and the compressible element. As in a previous study [78] (Chapter 3), the resistance is calculated from a mathematical relationship between volume of the compressible element, transmural pressure and P_L.

The airflow resistance of small airways (R_s) is assumed to be constant; the resistance of the upper airways (R_u) has a linear (K_1) and quadratic (K_2) term which are used to describe laminar and turbulent flow [65].

The pressure over the small airways (ΔP_s) as a function of the flow (V'_L) is calculated from

$$P_s = R_s * V'_L \tag{6.8}$$

and that in the upper airways (ΔP_u) from

$$P_u = R_u * V'_L = \left[K_1 + K_2 * \left|V'_L\right|\right] * V'_L \tag{6.9}$$

Volume disturbances

Effects from outside the lung and thoracic wall can be simulated with the new model if their influence on lung volume can be described in mathematical terms. We implement cardiac oscillations in the pressure and airflow signals [118]. In many patients such oscillations occur in phenomena related to gas exchange as well as mechanical properties. In the mechanical model volume changes due to cardiac oscillations are superimposed on the volume pattern calculated from lung elasticity and visco-elasticity.

Mechanical construction

The mechanical lung is constructed in a modular way to facilitate the exchange of different components. It has a set-up similar to the theoretical model, one alveolar compartment ($V_{A,c}$) connected to ambient air by a tube system representing the airways (Figure 6.3). The modular tube system consists of exchangeable resistance components ($R_{s,c}$, $R_{c,c}$ and $R_{u,c}$), corresponding to the resistance elements of the small airways (R_s), the compressible airways (R_c) and the upper airways (R_u) of the mathematical model, respectively.

Alveolar component

The lung volume is simulated by means of a modified version of our previous piston assembly [84] (Chapter 4). In the new set-up the space between the three bellows is used as the lung compartment. Both bellows are a remainder of the previous mechanical model in which they were used as lung compartments. In the new model they are used to change the offset of $V_{L,c}$ by hand. Dynamic volume changes (1.5 L maximally) are imposed by the displacement of the piston under computer control. The electro-mechanical servo-control system of the piston consists of a motor (*Mavilor, model 600, France*), a servo-controller (*Infranor, model 90/20, France*) and a custom-made control unit. The position of the piston is sensed by a potentiometer (T_3), attached to the piston. Two optical switches (S_1 and S_2) at the two extreme positions of the piston limit the movement range of the piston. Both bellows have a conducting rod, T_1 and T_2, respectively, which are attached to their aluminum bottom plate. The pressure in

the lung compartment ($P_{A,c}$) is continuously monitored (*Pressure transducer, Validyne, USA*), in order to prevent damage.

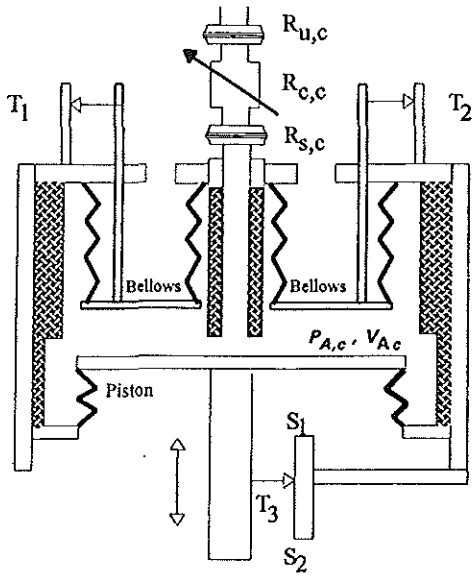

Figure 6.3:
Schematic diagram for the hydraulic model set-up.

The elastic properties of the lung are simulated by appropriate steering of the piston (Figure 6.4). When the pressure in the lung compartment changes due to inspiration or expiration, the software controlled electro-mechanical servo-system adapts the $V_{L,c}$ such that at each moment the pressure-volume relations are satisfied (equation 6.1 and 6.2). For $P_{A,c} = 0$ the volume of the model ($V_{L,c}$) is equal to *FRC* while for $P_{A,c} > 0$ the lung volume $V_{L,c}$ will increase to *FRC* + $\Delta V_{L,c}$, which is the volume at which pressure and volume are in accordance with the *PV*-curve. For pressures below zero the volume will be below *FRC*.

Compressible component
The compressible part of the airways is simulated by a component (*CCR*) of which the flow resistance is controlled by a computer. The *CCR* contains a cylinder over which a canister of unequal diameter is shifted, which results in a cylindrical slit, functioning as a flow resistance depending on a constant width and a controlled length of the slit. The length position of the canister with

respect to the cylinder is controlled by a computer. The resistance $R_{c,c}$ of this component is achieved by forcing the flow through the slit. The pressure over the slit depends on the length, height and width of the slit and on the magnitude of the flow itself. The computer controls the length of the slit such that the proper resistance value is simulated. The width and height determine the overall resistance range. Spline-function interpolation techniques [89, 90] are used to calculate the correct control signal for the *CCR* according to a specific resistance value. At each moment the $R_{c,c}$ is set to be equal to R_c. A detailed description of construction, control and dynamic behaviour of the device is described in Chapter 5. The flow is measured at one side of the *CCR*.

Small and upper resistance components

The small and upper airways are simulated by the components $R_{s,c}$ and $R_{u,c}$ corresponding to the elements R_s and R_u, respectively. They are modelled in three different ways:

1. The resistance components $R_{s,c}$ and $R_{u,c}$ are simulated separately, as in our previous mechanical model [84] (Chapter 4). For each imposed resistance a specific component had to be made, which restricted the flexibility of simulation. Four resistances were made: 2.07, 1.07, 0.43, and 0.19 kPa.s/L. We have no components to simulate the turbulent factor K_2.
2. The resistances R_s and R_u can be added to the calculated R_c and the total value (R_t) is used to control the *CCR*. Thus, *CCR* is used to simulate all resistance elements together, increasing the flexibility in simulating the resistances of lower and upper airways. Furthermore, the turbulent resistance of the upper airways can be implemented by incorporating this aspect in the equations of R_t.
3. The third method combined the two previous methods. Part of the total resistance is simulated with a constant resistance, whereas the remaining part is simulated by the *CCR*.

Computer-Control

The electro-mechanical components of the mechanical lung model are controlled by a personal computer (*Intel 80486, 66 MHz*). A software package using Turbo Pascal (*Borland International Inc., Scotts Valley, CA, USA*) is developed, allowing many functions including:

- selection of different simulation methods,
- input of parameters for the *PV*-relations for lung and thorax,
- defined moments to set a digital output port to control external equipment,
- selection of breathing patterns measured in patients or artificially generated,

- sequence and repetition number of patterns, minute volume, inspiration and expiration time, and
- many signals and variables that can be stored on disk for later analysis.

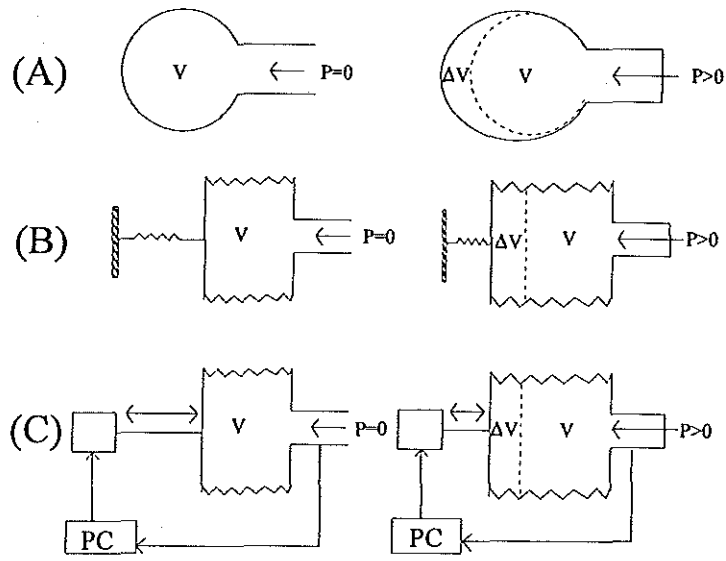

Figure 6.4:
Simulation of elastic behaviour by means of computer-controlled displacement.
A the volume for the lung with $P_A = 0$ and $P_A > 0$
B volume for a model with compliance simulated by means of a spring
C the same is given for the computer-controlled mechanical lung model. The lung volume will be equal to V_A for $P_A = 0$ while for $P_A > 0$ the lung volume will be increased to $V_A + \Delta V_A$. The PC calculated the steering signal U_L to position the piston

Alveolar component

The control of the piston during passive simulation is the most challenging part to simulate lung compliance. In order to simulate lung compliance properly at each moment the position of the piston has to be such that measured $P_{A,c}$ and controlled volume $V_{L,c}$ are in accordance with equations 6.1 and 6.2. For a constant gas amount a change of $V_{L,c}$ imposed by the piston results in a change in $P_{A,c}$ in accordance with the Law of Boyle-Guy-Lussac yielding: $P_{A,c} \cdot V_{L,c}^{(Cp/Cv)} = \text{constant}$. The factor (Cp/Cv) is taken equal to 1.2. Thus, for a constant gas amount the new position of the piston, $V_{L,c}$, can be calculated. Because flow enter or leave the alveolar compartment the condition of a constant gas amount is not valid. We approximate the relation for the change in gas

amount through measurement of airflow at the inlet/outlet of the mechanical lung model. The mathematically defined movement of the piston enables the mechanical simulation of a complex relationship between pressure and volume in lung pathology. The computer calculates the speed of piston movement from the difference between the measured and the required position.

The model can be used either to simulate active breathing or artificial ventilation. The steering of the model is called *active* if the movement of the piston is determined by the software. *Passive* steering is used for movement of the piston according to the *PV*-curve and measured P_A. We distinguished three methods to control the piston:

1. during active use of the mechanical model (CCL_A), the movement of the piston imposes the patterns, obtained from breathing patterns of patients or with special patterns defined in the software. This type of simulation is similar to that in our previous mechanical model [84] (Chapter 4).
2. during passive use of the lung model (CCL_P), the movement of the piston is based on the pressure in the lung volume component $P_{A,c}$ and the mathematically defined *PV*-curve, measured flow and the law of Boyle-Guy-Lussac. During inflation $P_{A,c}$ is imposed by the ventilator, while during expiration it depends on the elasticity and expiratory flow resistance of the lung model and the tubing of the ventilator.
3. an active use during inspiration and a passive use during expiration is also modelled. This is a simulation of normal breathing where an active inspiration is followed by an expiration in absence of muscle activity. This allows to study characteristic features during expiration without the need to impose an inflation by means of a ventilator.

Compressible component

At each moment the resistance of the compressible component $R_{c,c}$ had to be set as the resistance values of the compressible element R_c. The transmural pressure (P_{tm}) used for this calculation is derived from the pressure gradient over the small airway ($\Delta P_{s,c}$) and lung recoil pressure, $P_{L,c}$ (equation 6.1). Pressure $\Delta P_{s,c}$ is not measured but obtained from $\Delta P_{s,c} = R_s * \dot{V}_{L,c}$. As mentioned above, the $R_{c,c}$ can be combined with the resistance components for the small and upper airways, $R_{s,c}$ and $R_{u,c}$. Then the steering signal ($U_{c,c}$) for the *CCR* is calculated from $R_{c,c}$ and $\dot{V}_{L,c}$.

APPLICATIONS

The potentials of the mechanical model are illustrated by three examples.

Simulation of artificial ventilation

In a patient study on mechanical ventilation we needed to control the expiration phase to study its effect on effectiveness of ventilation. We simulated the ventilation of this patient study with our mechanical model, to develop the programs for control of the equipment which controlled the patient's expiration. We used a mechanical ventilator (*900C, Siemens-Elema, Solna, Sweden*) to ventilate the mechanical model. Special types of expiratory patterns were applied by control of the PEEP valve. The patient's values for compliance and resistance were introduced in the mechanical model. The tracheal pressure during expiration had to be controlled to follow a pattern according to the equation:

$$P_T(t) = P_T(0) - \left(P_T(0) - P_{T,end}\right) * \left(\frac{t}{t_{exp}}\right)^{N_{curve}} \qquad (6.10)$$

where:

$P_T(t)$	*tracheal pressure in the mechanical model, identical to controlled pressure at time t during the expiration*
$P_T(0)$	*tracheal pressure at the beginning of expiration*
$P_{T,end}$	*desired tracheal end-expiratory pressure*
N_{curve}	*curvature of pressure pattern*
t_{exp}	*total expiration time*

The curve was concave for $N_{curve} < 1$ and convex for $N_{curve} > 1$. In the example given in Figure 6.5, N_{curve} was chosen equal to 2. Tidal volume, frequency and minute volume were controlled by settings of the servo-ventilator. The sequence of events is given in Figure 6.5a. During part 1 there is mechanical ventilation with spontaneous expiration. The expiratory flow pattern depends on the *PV* characteristics of lung and thorax and the expiratory flow resistance. During inflation the expiration valve of the ventilator was closed. During expiration, when the expiration valve was open, a normal exponential decrease in flow and pressure through connecting tubes and ventilator resulted.

In part 2 inspiration volume and time were the same as in part 1, but during expiration the time course of P_T was determined by computer control of the PEEP valve. The slope of this course was controlled according to equation 6.10. During the first breaths less air could leave the lung during expiration, causing an increase in lung volume and alveolar (and tracheal) pressure to a level that balanced expiratory to inspiratory volume. The increase in volume and pressure depended on the compliance of the respiratory system. The new equilibrium was characterized by an increase in end-expiratory volume, end-expiratory pressure

and peak tracheal pressure. The sudden opening of valve at end-expiration causes disturbances to $V'_{L,c}$ and $P_{tr,c}$. Figure 6.5B shows the compliance curve for the same period as in Figure 6.5A. During phase 2 a shift occurred to higher volumes and pressures. The non-linear shape of this curve and small disturbances during the opening and closing of the valves can be seen.

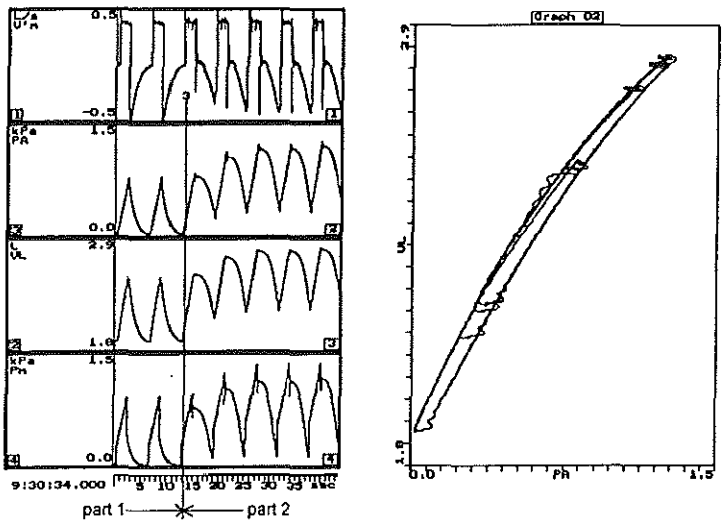

Figure 6.5:
Simulation of artificial ventilation. During part 1 the PEEP valve in the ventilator is not active while during part 2 (the expiration) the PEEP valve is controlled such that a preprogrammed pattern of P_{tr} is imposed. On the left signals $V_{L,c}$, $V'_{L,c}$, $P_{A,c}$ and P_{tr} are plotted against time. On the right $P_{A,c}$ versus $V_{L,c}$ is shown.

Simulation of patterns

In this example the values for volume and airflow resistance of the mechanical lung model, $V_{L,c}$ and $R_{t,c}$ respectively, were calculated with the mathematical equations described before [92] (Chapter 3) in the following way: the parameters were set for an emphysematic patient. A sinusoidal pressure signal was used in the mathematical serial lung model as we did previously (Chapter 3). Based on this pressure signal the mathematical serial lung model calculated V_L and the resistances R_s, R_c and R_u which were combined to give the total resistance R_t. These calculated signals were stored on disk. Then the signals V_L and R_t were used to calculate the signals $V_{L,c}$ and $R_{t,c}$ to control the piston and *CCR*, respectively. The flow-pressure relationship calculated with the mathematical

equations is shown in the upper part of Figure 6.6. In the lower part the flow and pressure measured in the mechanical lung model is plotted.
In future, the mathematical equations for serial lung model can be implemented in the software of the mechanical model itself.

6.6a

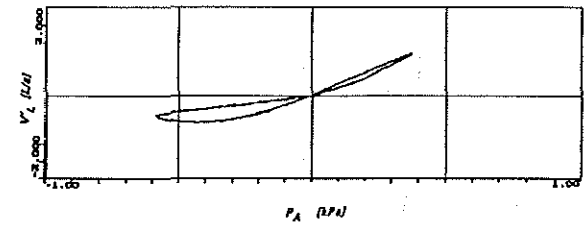

6.6b

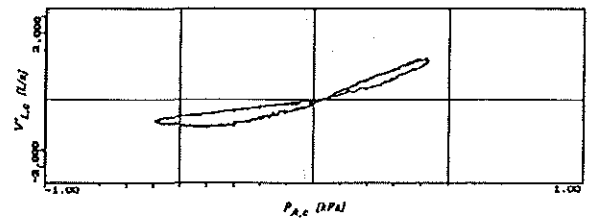

Figure 6.6:
Simulation of a calculated P_A- V'_L curve (a) and the $P_{A,c}$- $V'_{L,c}$ (b) curve measured from the mechanical model.

Visco-elasticity and cardiac influences
Figure 6.7 is an example of the simulation of artificial ventilation when both the visco-elastic properties and the effect of cardiac contractions are activated. The time constant is equal to 2 seconds and the ratio between ΔV_{init} and ΔV_{end} was set to 0.7. In this simulation we also modelled cardiac oscillation. Because we could not find an appropriate reference in literature, it was simulated as a sine wave volume variation with a beat duration of 0.5 s in each 1-second period and an amplitude of 50 ml. For the passive inflation a mechanical ventilator (*900C, Siemens-Elema, Solna, Sweden*) was used. After the second expiration the pause was prolonged by activating an expiratory-hold procedure in the 900C.

DISCUSSION AND CONCLUSIONS

In literature on mechanical lung models, the behaviour was generally entirely defined by their structure [8, 94-96, 119]. In some models components which

simulated airway resistance or compliance could be changed [13, 92, 97]. The simulation of non-linear compliancies were hardly possible with such fixed components, because non-linear springs with appropriate length-pressure relations were needed.

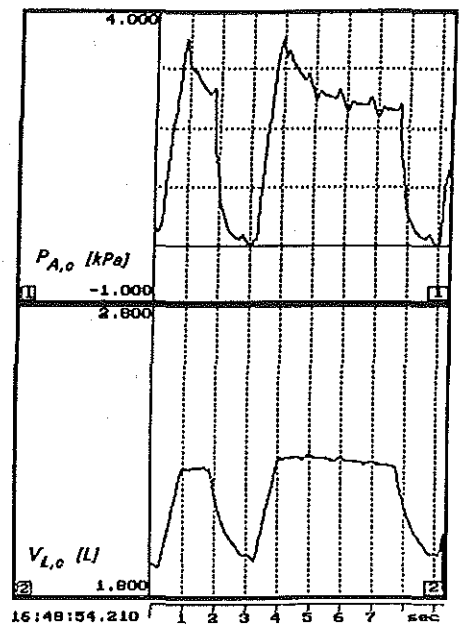

Figure 6.7:
Visco-elasticity and cardiac effects. Signals $P_{A,c}$ and $V_{L,c}$ are plotted against time. During the second breath the inspiratory pause period is prolonged by means of the inspiratory hold button on the ventilator. No manual interaction with the CCL-2 program is performed.

With the new model many limitations of earlier models are eliminated. The intense integration of computer program and mechanical components enable a large flexibility in simulation of variables and their physiologic and pathologic relationships. Thus, properties of the mechanical components in the model can be changed via the mathematical relations in the software in order to change the parameter settings without changing the construction of the mechanical model, even from one breath to another. In this way compliance of the lung and resistance of the compressible component can be changed. Time-dependent mechanisms can now be implemented, e.g. viscosity and cardiac effects. These aspects of mechanical modelling are not described in literature so far. With the

new approach it will be possible to incorporate muscle activity during simulation of artificial ventilation.

We showed the applicability of the new model in three examples. The model is suitable to simulate artificial ventilation. Although we only demonstrated the effect of additional expiratory resistances resulting in an increase of end-expiratory volume and end-expiratory pressure, many other parameters of ventilatory pattern could be tested. In the second example, the model satisfactorily simulated a complex breathing pattern as seen in patients, with proper resistances during inspiration and expiration. In the last example, we demonstrated the implementation of time-related phenomena such as cardiac oscillations. Such implementation in a mechanical model is useful to test the sensitivity of computer programs for this type of disturbance. Furthermore, for purposes of instruction to students or lung function technicians the model should be as realistic as possible.

There are some constraints with respect to inertia and static volumes. The inertia caused a small delay between the imposed position of the piston and the actual position leading to an opening (hysteresis) of the *PV*-curves (Figure 6.b). This delay had no disadvantages for the simulations, because in patients similar types of hysteresis occur. These effects will probably be reduced by improvement of the electro-mechanical servo-system and the software. In the new model, pleural pressure is not present as a physical variable but is calculated during the simulation and presented as an electrical signal through *DA*-conversion.

The importance of reliable mechanical models of the lung and thorax system will gradually increase. Especially during development and calibration of new instruments (hardware or software) an extensive testing is necessary before clinical use. The new model allows to perform these tests on simulated conditions of a broad spectrum of pulmonary pathology.

CHAPTER 7

FINAL CONSIDERATIONS

DATA PROCESSING

At the present time, most lung function measurements at the lung function laboratory are processed on-line. Throughout the years the basic set-up of the programs has not been changed. Commercial equipment including automatic data processing is more and more available now for several types of measurements. We have connected such equipment (*Jaeger, Würzburg, Germany*) to the laboratory network. The implementation of that equipment into the network is needed to integrate the results of the measurements and other administrative procedures.

Throughout the years the data processing facilities and developed software were used for many research projects at the department of Pulmonary Diseases, which resulted in several papers [45, 47, 76, 103, 120-128] and theses [129-134].

Implementation of measurements, for which devices are not commercially available, and development of new techniques will be needed to offer new information about the lung pathology of a patient. Furthermore, the development of lung function techniques for care of intensive care patients is of increasing interest.

Up to now, the medical information of a patient is primarily stored on a paper-based patient record. At the moment the paper-based records contain much more

information than the information stored in the *HIS*. Much information is generated in a way that can not yet be stored in the *HIS*. However, the recent network and software capabilities enable increasing possibilities for integration of information present in the *HIS* database, as well as information from other locations. At the department of Pulmonary Diseases this is done for the images of bronchoscopic measurements and numerical and graphical presentation of lung function results.

Modelling

The application to the complex serial model, as described in Chapter 3, for the analysis of body plethysmographic variables measured at patients is not yet possible because the signals measured are too sensitive to disturbances. Moreover, the lung pathology of a patient is far more complex than modelled by the serial model. Further research is needed to improve the analysis of body plethysmographic variables. The parameter estimation techniques, used for that study, were adapted to analyze compliance and provocation measurements [103, 134-138].

A mechanical model to simulate active breathing is described in Chapter 4 . This model was inflexible to change compliance and flow resistance and could not be used to simulate artificially ventilated patients. Therefore, a further development was needed, as is described in Chapter 5 and 6. This new mechanical modelling technique implies the computer controlled flow resistance of Chapter 5 and the mechanical model of Chapter 4. It was demonstrated that the new approach functions much better. Because the mechanical model described in Chapter 4 was not designed for the approach as described in Chapter 6 a new piston assembly was designed (Figure 7.1). This technical development was performed in cooperation with technicians from the CID and *Eltromat (Zevenbergen, The Netherlands)*. The development of new software is in progress.

The most pronounced differences with respect to the previous mechanical model (Chapter 4 and 6) are the following:

1. the maximal volume change is increased from 1.2 L to almost 5 L, to be able to simulate a change in FRC level, e.g. an increase of lung volume due to increased expiratory resistance in artificially ventilated patients.
2. two rolling-seal membranes are used instead of the concertina bellows to get a stiff construction necessary for the simulation of the compliance.
3. the use of a ball-screw spline *(NS1616A, THK-CO., Tokyo, Japan)* incorporated in the hollow axis of a servo-motor *(HW300, Kern, Friedrichshaven, Germany)*, enables a compact construction for driving the piston.

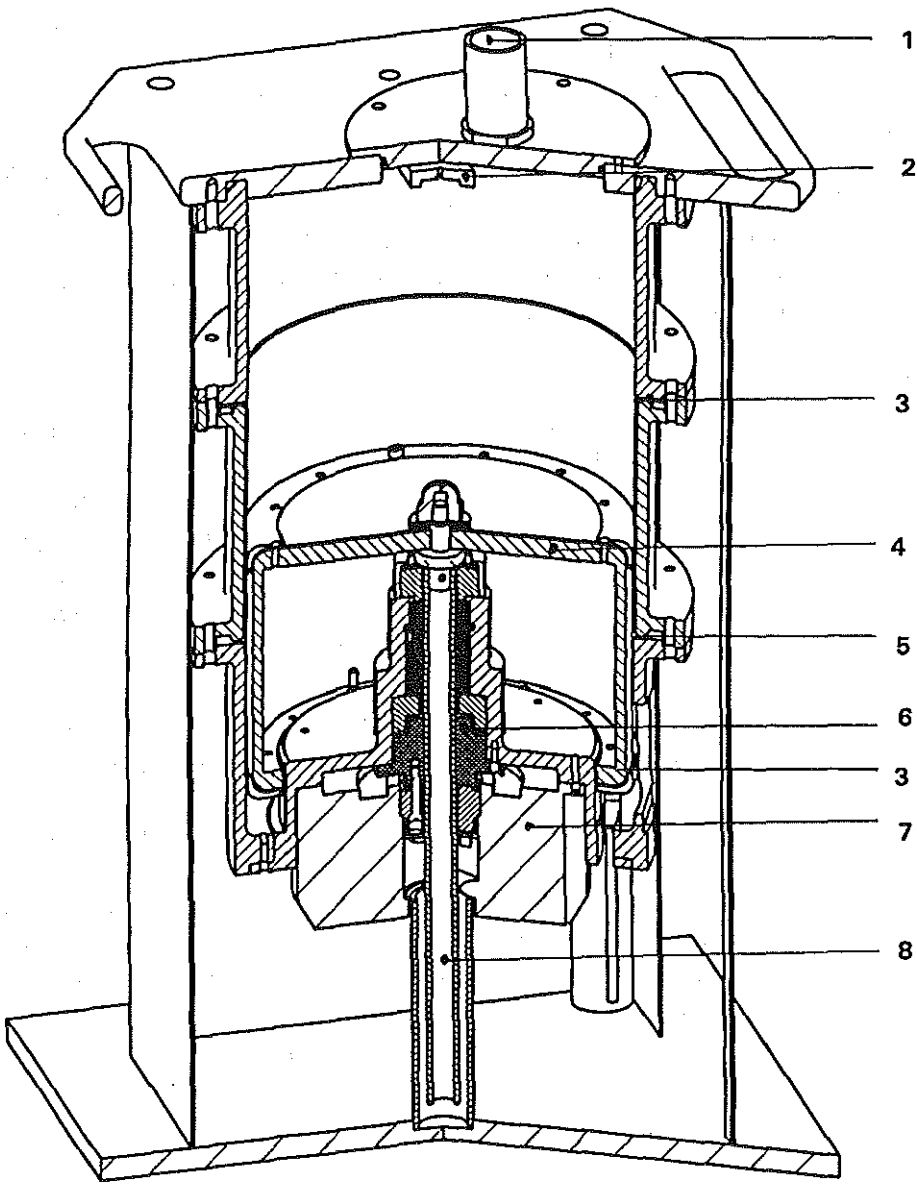

Figure 7.1:
A schematic view of the new mechanical lung model. 1) outlet and connection to computer-controlled resistance, 2) End-stop, 3) rolling seal (two times), 4) piston, 5) vacuum connection for proper functioning of both rolling seal membranes, 6) ball-screw, 7) hollow-axis motor, and 8) axis.

4. the displacement of the piston is sensed by means of an encoder and has an accuracy of about $5*10^{-3}$ L.
5. maximum displacement is designed to be at least 10 $L.s^{-1}$ and the acceleration to more than 200 $L.s^{-2}$.
6. the electronic components are renewed and in general based on commercially available equipment; power supply (*PSS-12/400R, Elmo, Petah-tikva, Israel*) and amplifier (*NBA2.5/400RE, Elmo, Petah-tikva, Israel*), encoder (*59, Elcis, Collegno, Italy*), motion controller (*DMC-1020, Galil Motion Control Inc., Sunnyvale, California*) and pressure transducer (*LCVR-100, Celesco, USA*).

Application of the mechanical model

The different techniques described in this thesis will be used in a study which is devoted to the development of techniques to establish a maximal expiratory flow in artificially ventilated patients with severe *COPD*. This will be done by changing the resistance of the outlet during the expiration. This will require complex techniques to identify the optimal pattern for controlling the expiratory resistance. The effect of maximal expiratory flow on other variables will be studied. To apply these techniques to patients the following steps have to be taken:

1. A mathematical model has to be defined, which describes the maximal expiratory flow (*IVPF*) behaviour of an artificially ventilated COPD patient.
2. Numerical simulations with this mathematical model will be performed to study the effect of a change in expiratory resistance on several lung function variables, e.g. lung volume and alveolar pressure.
3. Implementation of this mathematical model in the software of the mechanical lung model to simulate a *COPD* patient, which can be used to perform physical measurements and test it in connection to a ventilator (*Servo 900C and Servo 300, Siemens-Elema, Solna, Sweden*).
4. *IVPF* curves measured at the mechanical model will be compared with the mathematical curves defined in the mechanical model.
5. Then, optimal control algorithms to control the expiratory resistance might be found.
6. When the total set-up, mechanical lung model, ventilator and expiration control, is successfully tested it will be used for a pilot study with patients.

The approach illustrates one of the potentials of the automatic data processing and mathematical and mechanical techniques, as presented in this thesis, for future patient care.

CONCLUSIONS

The achievements presented in this thesis can be divided in three main results.

1. Through the on-line processing of lung function measurements and the integration in the hospital information system, at the moment the patient leaves the laboratory the results of lung function measurements can be at the disposal of the physician at many *PC* based systems throughout the university hospital Rotterdam.
2. the construction of the computer controlled resistance enabled a accurate and fast control of flow resistances.
3. the computer controlled piston displacement based on the pressure measured inside the simulator and a preset mathematical enabled the simulation of a elasticity as found in normals and patients.

These three steps mean a step forward in mechanical (lung) modelling.

Through integration of mathematical models into the mechanical models it is possible to combine the flexibility of a mathematical model and the capability of a mechanical model to perform simulations in a physical environment. The techniques developed will be used for the development of programs to control the expiration of artificial ventilated patients.

SUMMARY

In 1976, automatic data processing was started on the lung function laboratory to improve the data processing of lung function measurements. This thesis describes some examples of the impact that automatic data processing had on direct patient care and the research which is carried out at the lung function laboratory since that time.

In Chapter 1 the technological development in the lung function laboratory and intensive care department of the University Hospital Dijkzigt Rotterdam in which computers were an essential condition are described. First, an overview is given of the first years of the automatic data processing in the laboratory, including the change in computer technology in sense of performance. Second, the significance of modelling is mentioned, whereafter mathematical and mechanical modelling is introduced. In the last part the outline of the thesis is presented.

In Chapter 2 the development of a Lung Function Information System (*LFIS*) for the data analysis of pulmonary function tests at different locations is described. This system is connected to the Hospital Information System (*HIS*) for the retrieval of patient data and the storage of lung function variables of patients to generate follow-up reports and to support financial and administrative management.

The application programs were developed in such a way that a high flexibility with respect to the patient-computer-technician interaction. The sampled data are stored on a disk to correct eventually earlier decisions, perform recalculations and Ranales the data for research purposes. When the measurements performed on a patient are authorized, the sampled data are deleted, except when they are needed for further research.

A distributed computer system was chosen to combine the benefits of a centralized system with those of several stand-alone systems. The main tasks of the central unit are to store collected data and computer programs, generate a final lung function report on laser printer and provide a connection to the *HIS*. In the satellite computers, which are located close to the lung function equipment, the signals and raw data are processed. Furthermore, the satellite computers were in use for program development and several research projects, and for the off-line data processing of the lung function measurements from two other hospitals by means of a modem connection.

The *LFIS* improved the quantity and quality of data acquisition. It resulted in an increased capacity of about 50% concerning spirometry and facilitated time-consuming complex analysis. It also avoided miscalculations and mistakes in reports previously experienced with hand calculations and enabled new possibilities for research.

In an Appendix to this chapter the recent developments of *LFIS* are addressed. The introduction of personal computers resulted in a reduction of cost, simplifications of operation and large increases in available commercial programs, e.g text processing and statistics. The large influence of the electronic communication network on the automatic data processing in the university hospital and the pulmonary function laboratory in particular is indicated.

In Chapter 3 a serial lung model with a compressible segment to simulate different types of lung and airway disorders such as asthma, emphysema, fibrosis and upper airway obstruction during normal breathing is described. A parameter estimation technique was applied and its reliability and uniqueness were tested by means of sine wave input signals. The characteristics of the alveolar pressure-flow patterns simulated with the model agree to a great extent with those found in the literature. In the case of absence of noise the parameter estimation routine produced unique solutions for the different simulated pathologic classes. The sensitivity of the different parameters depended on the values belonging to each class of pathology. Some more simplified models are presented and their advantages over the complex model in special types of pathology are demonstrated. Noise added to the simulated flow appeared to have no influence on the estimated parameters, in contradiction to the effects with

noise added to the pressure signal. In that case effective flow resistance was accurately estimated. Where parameters had no influence, as for instance upper airway resistance in emphysema or small airway resistance in upper airway obstruction, the measurement accuracy was less. In all other cases, a satisfactory accuracy could be obtained.

In Chapter 4 the development of a computer-controlled mechanical lung model for testing lung function equipment, validation of computer programs and simulation of impaired pulmonary mechanics is presented. The construction, function and some applications are described.

The physical model is constructed from two bellows and a pipe system representing alveolar lung compartments of both lungs and airways, respectively. The bellows are surrounded by water simulating pleural and interstitial space. Volume changes of the bellows were accomplished via the fluid by a piston. The piston is driven by a servo-controlled electrical motor whose input is generated by a microcomputer. A wide range of breathing patterns can be simulated. The pipe system representing the trachea, connects both bellows to the ambient air and is provided with exchangeable parts with known resistance. A compressible component (*CC*) can be inserted into the pipe system. The fluid-filled space around the *CC* is connected with the water compartment around the bellows; The *CC* is made from a stretched Penrose drain. The outlet of the pipe system can be interrupted on command of an external microcomputer system.
An automatic sequence of measurements can be programmed and is executed without the interaction of a technician.

In Chapter 5 a computer-controlled flow resistance, to be used in a computer-controlled lung model, is presented. Flow is forced through a slit between a cylinder and a sleeve outside the cylinder. The position of the sleeve with respect to that of the cylinder is controlled by a computer. However, the total flow resistance is not only a function of the length of the slit, but also depends on inlet/outlet resistance and flow rate. The dependence on flow rate is primarily due to the shape of the inlet of the slit. The resistance of the slit itself is almost independent of flow rate. We calculated the resistance for flow values from -0.05 to 1.0 $L.s^{-1}$ in both directions during a calibration phase at different positions of the sleeve. To simulate a required resistance pattern, the position to steer is calculated by means of a spline-function interpolation from the relation between flow resistance and position of the sleeve. The internal diameter of the sleeve is fixed and by exchanging the cylinder with one of a different external diameter the slit height can be changed to tune the resistance range for a specific simulation.

In Chapter 6 a mechanical lung model as an extension of a previous mechanical model (Chapter 4) to simulate normal breathing and artificial ventilation in patients is described. The extended integration of hardware and software offers many new possibilities and advantages with respect to the former model. The properties of the components, which simulate the elastance and airway resistance of the lung, are defined in the software rather than by mechanical properties of the components themselves. Therefore, a more flexible simulation of non-linear behaviour and cross-over effects of lung properties is obtained. Furthermore, the range of lung compliance is extended to simulate patients with emphysema, and the dependency of airway resistance on lung recoil pressure and transmural pressure of the airways can be simulated. The new approach enables to incorporate time-related mechanics as, for instance, the influence of lung viscosity or cardiac oscillation. The different relations defined in the software could be changed from breath to breath.

The possibilities of the new model are demonstrated by means of three examples: 1) computer-controlled expiration in the artificially ventilated lung, 2) simulation of normal breathing, and 3) simulation of visco-elastance and cardiac influences during artificial ventilation. The mechanical model provides a reproducible and flexible environment for testing new software and equipment in the lung function laboratory and intensive care, and can be used for instruction and training.

In Chapter 7 some final considerations are made. Increasingly, commercial equipment incorporates data processing we had to develop ourselves in the past. New developments are necessary to improve the information about lung pathology of a patient and the treatment of artificially ventilated patients. The electronic patient record will become of increased importance through advanced network capabilities.

The integration of mathematical and mechanical models will be of great importance for future research. An improved mechanical model which is under construction now will be used to develop and test new measurements, techniques and algorithms for controlling the expiration of artificially ventilated patients.

The use of these models is essential for the development of the control algorithms and extensive testing before a safe application for patients can be considered.

REFERENCES

1. Board J. Grand challenges in biomedical computing. Crit Rev Biomed Eng 1992; **20**:1-24.
2. Hennessy JL, Patterson D. Computer Architecture: A quantitative approach. Morgan Kaufman, San Mateo, CA, 1990
3. Hutcheson GD, Hutcheson JD. Technology and Economics in the Semiconductor Industry. Scientific American 1996;(January):40-46.
4. Sandblad B, Meinzer HP, ed. Modelling and Simulation of Complex Control Structures in Cell Biology. 1993 ed. Stuttgart: Schattauer Verlag, 1993: 422-429. (Bemmel JHv, McCray AT, ed. Yearbook of Medical Informatics
5. Moller DPF, ed. State of the Art and Future Aspects of Modeling and Simulation in Physiology and Biomedical Engineering. New York: Springer Verlag, 1991:1-34. (van Wijk van Brievingh M, ed. Biomedical Modelling and Simulation on a PC
6. Uhl RR, Lewis FJ. Digital computer calculation of human pulmonary mechanics using a least squares fit technique. Comp Biomed Res 1974; 7: 489-495.
7. Bouhuys A, Virgulto JA. Calibration of flow-volume curves. Lung 1978; **155**: 123-130.
8. Boutellier U, Gomez U, Mader G. A piston pump for respiratory simulation. J Appl Physiol 1981;**50(3)**:663-664.
9. Meyer M. A versatile hydraulically operated respiratory servo system for ventilation and lung function testing. J. Appl. Physiol. 1983; 55: 1023-1030.
10. Pedersen OF, Naeraa N, Lyager S, Hilberg C, Larsen L. A device for evaluation of flow recording equipment. Bull Eur Physiopath Resp 1983; 19: 515-520.

11. Hartmannsgruber M, Good M, Carovano R, Lampotang S, Gravenstein JS. [Anesthesia simulators and training devices]. [German] Anasthesiesimulatoren und Trainingsgerate. Anaesthesist 1993; **42(7)**: 462-469.
12. Chopra V, Engbers FH, Geerts MJ, Filet WR, Bovill JG, Spierdijk J. The Leiden anaesthesia simulator. Br J Anaesth 1994; **73(3)**: 287-292.
13. Myojo T. Breathing pattern simulation using slit/cam valve. Am Ind Hyg Assoc J 1989; **50(5)**: 240-244.
14. Jansen JRC. The thermodilution technique during artificial ventilation. Thesis, Erasmus University Rotterdam, 1988.
15. Shonfeld EM, Kerekes J, Rademecher CA, et al. Methodology for computer measurement of pulmonary function curves. Dis. Chest 1964; **46**: 427-435.
16. Ayers WR, Ward SA, Weihrer ALV, Abraham S, Caceres CA. Description of a computer program for analysis of the forced expiratory spirogram. I. Instrumentation and programming. Comp. Biochem. Res 1969;**2**: 207-220.
17. Ayers WR, Ward SA, Weihrer ALV, Rosner SW, Caceres CA. Description of a computer program for analysis of the forced expiratory spirogram. II. Validation. Comp. Biochem. Res 1969;**2**:220-229.
18. Rosner SW, Palmer A, Caceres CA. A Computer program for computation and interpretation of pulmonary function data. Comp. Biomed. Res. 1971;**4**:141-156.
19. Derret CJ, Brown C. A System for processing by digital computer spirograms acquired in field surveys. Thorax 1975;**30**:674-677.
20. Cardus D, Newton L. Development of a computer technique for the on-line processing of respiratory variables. Comput. Biol. Med. 1970;**1**:125-133.
21. Crockett A, Smith RL. Use of on-line computer facilities in a respiratory function laboratory. Med. J. Aust. 1975;**2**:486-489.
22. Ostrander LE. A data communication system for interactive linking of remote computer and laboratory. Med. Instrum. 1975;**9**:147-149.
23. Naimark A, Cherniack RM, D. Comprehensive respiratory information system for clinical investigation of respiratory disease. Am. Rev. Resp. Dis. 1971;**103**: 229-239.
24. Chiang ST. Application of desk-top computer in clinical spirometry, an automatic calculation and diagnosis program. Am. Rev. Resp. Dis. 1972;**106**:614-617.
25. Protti DJ, Craven N, Naimark A, Cherniack RM. Computer assistance in the clinical investigation of pulmonary function studies. Meth. Inform. Med. 1973;**12**:102-108.
26. Vogel J, Moller E, Harzendorf E. EDV-gerechte respiratorische funktions diagnostik. Zeitsch. für Erkrankungen der Atmungsorgane 1973;**137**:409-424.
27. Pack AL, McCusker R, Moran F. A computer system for processing data from routine pulmonary function tests. Thorax 1977;**32**:333-341.
28. Sahakian J. A pocket computer program for normal values of selected lung function tests in children and young adults. Comput. Biol. Med. 1981;**11**:231-235.

29. Tanser AR. The use of a micro-computer system in a lung function testing laboratory. Br. J. Dis. Chest. 1982;76:130-135.
30. Dickman ML, Schmidt CD, Gardner RM, Marshall HW, Day WC, Warner HR. On-line computerized spirometry in 738 normal adults. Am. Rev. Resp. Dis. 1969;100:780-791.
31. Bunn AE. A Comprehensive on-line computerised lung function screening test. Respiration 1979;37:42-51.
32. Primiano Jr FP, Bacevice Jr AE, Lough MD, Doershuk CF. Computer analysis of slow vital capacity spirograms. Comput. Biol. Med. 1982;12:107-117.
33. Sykes TW, Haynes RL, McFadden Jr ER. On-line determinations of lung volumes by plethysmography and digital computer. Am. Rev. Resp. Dis. 1977;115: 581-586.
34. Lorino H, Laurent D, Harf A, Brault Y, Lorino AM, Atlan G. On-line calculation of lung volumes by digital computer from a plethysmographic meaasurement of ventilatory flow. Med. Biol. Eng. Comp. 1980;18:291-298.
35. Matthys H, Zaiss A, Fischer J, Kienzle P. On-line programm für die Ganzkörperplethysmographie. Atemw. Lungenkrankh. 1982;8:268-273.
36. Colebatch HJH, Nail BS, NG C. Computerized measurement of pulmonary conductance and elastic recoil. J. Appl. Physiol. 1978;44:611-619.
37. Beaver WL, Wasserman K, Whipp BJ. On-line computer analysis and breath-by--breath graphical display of exercise function tests. J. Appl. Physiol. 1973;34: 128-133.
38. Miyamoto Y, Sakakibara K, Takahashi M, et al. On-line computer for assessing respiratory and metabolic function during exercise. Med. Biol. Eng. Comp. 1981;19:340-348.
39. El-Dhaher AHG, Ahmad AJ, Hassan TS, Kaouri HA, Mustafa KY. An integrated microprocessor-based system enhanced with graphics for the evaluation of slope ratios and other flow-volume curve parameters. Comp. Prog. Biomed. 1983;17:129-136.
40. El-Dhaher AHG, Ahmad AJ, Hassan TS, Mustafa KY. Microprocessor-based system for on-line analysis of respiratory responses to exercise. Comp. Prog. Biomed. 1985;19:179-187.
41. Lord PW, Brooks AGF. A comparison of manual and automated methods of measuring airways resistance and thoracic gas volume. Thorax 1977;32:60-62.
42. Caceres CA, Ayers WR. Systems to support clinical decisions: automated medical signal analysis. Med. Instrum. 1978;12:226-229.
43. Fisher PD, Krause GS. Satellite processors lighten the burden in computer-run systems. Electronics 1976;11:105-110.
44. Smidt W. On-line Datenverarbeitung in der Lungenfunktions diagnostik. Biomed. Tech. 1976;21:138-140.
45. Holland WPJ, Verbraak AFM, Bogaard JM, Boender W. Effective airway resistance: a reliable variable from bodyplethysmography. Clin. Phys. Physiol. Meas. 1986;7(4):319-331.

46. Verbraak AFM, Bogaard JM, Hoorn E, Versprille A. Modelling lung mechanics for the interpretration of bodyplethysmographic tracings; the serial lung model. North Holland Publishing Corp., 1983:165-174. (VanSteenkiste GC, Young PC, ed. Modelling and data analysis in biotechnology and medical engineering
47. Kars AH, Goorden G, Stijnen T, Verbraak AFM, Bogaard JM. Determinants of the expired CO_2-volume curve in normals and emphysema patients. Eur. Resp J 1989;2:317s.
48. Friedman RB, Gustafson DH. Computers in clinical medicine; a critical revieuw. Comp. Biomed. Res. 1977;10:199-204.
49. Blankenstein Mv. The audio-pictorial endoscopy reporting system (AUPERS). Illustr. Case Reports in Gastr. 1997;4:73-78.
50. Moorman PW. Towards formal medical reporting. Thesis, Erasmus University Rotterdam, 1995.
51. Du Bois AB, Botelho SY, Comroe JH. A new method for measuring airway resistance in man using a body plethysmograph; values in normal subjects and in patients with respiratory disease. J. Clin. Invest. 1956;35:327-335.
52. Matthys H. Ganzkörperplethysmography. Pneumologie 1971;146:216-231.
53. Reinert M, Heise D, Trendelenburg F. Zum Auswertemodus phasenverschobener Resistancekurven. Pneumologie 1975;152:147-156.
54. Ulmer WT, Reif E. Die obstructiven Erkrankungen der Atemwege. Dtsch. Med. Wschr. 1965;90:1803-1809.
55. Guyatt AR, Alpers JH, Hill I, Bramley AC. Variability of plethysmographic measurements of airway resistance in man. J. Appl. Physiol. 1967;22:383-389.
56. Smidt U, Finkenzeller P, Rennings C. On-line Computereinsatz in der Ganzkörperplethysmographie zur Berechnung der mittleren Resistance. Pneumologie 1975;151:223-231.
57. Bekey GA, Beneken JEW. Identification of biological systems: a survey. Automatica 1978;14:41-47.
58. Banerjee M, Evans JN, Jaeger MJ. Uneven ventilation in smokers. Respiration. Physiol. 1976;27:277-291.
59. Cettl L, Dvorak J, Felkel H, Feuereisl R. Results of simulation of nonhomogeneous ventilatory mechanics for a patient-computer arrangement. Int. J. Biol-Med. Comput. 1979;10:67-74.
60. Otis AB, McKerrow CB, Bartlett RA, et al. Mechanical factors in distribution of pulmonary ventilation. J Appl Physiol 1956;8:427-443.
61. Pride NB, Permutt S, Riley RL, Bromberger-Barnea B. Determinants of maximal expiratory flow from the lungs. J. Appl. Physiol. 1967;23(5):646-662.
62. Feinberg BN, Chester EH, Schoeffler JD. Parameter estimation: a diagnostic aid for lung diseases. Instrumen. Technol. 1970;:40-46.
63. Feinberg BN, Chester EH. A dynamic model of pulmonary mechanics to simulate a panting maneuver. Bull. Physiopath. Resp. 1972;8:305-322.
64. Golden JF, Clark Jr. JW, Stevens PM. Mathematical modeling of pulmonary airway dynamics. IEEE Trans BME 1973;20:397-404.

65. Rohrer F. Der Strömungswiderstand in der menschlichen Atemwegen und der Einfluss der unregelmässigen Verzweigung des Bronchialsystems auf der Atmungsverlauf in verschiedenen Lungenbezirken. Pflügers Arch Ges Physiol 1915;162:225-259.
66. Mead J, Turner JM, Macklem PT, Little JB. Significance of the relationship between lung recoil and maximum expiratory flow. J. Appl. Physiol. 1967; 22:95-108.
67. Hyatt RE. Expiratory flow limitation. J. Appl. Physiol. 1983;55:1-8.
68. Lambert RK, Wilson TA, Hyatt RE, Rodarte JR. A computational model for expiratory flow. J. Appl. Physiol. 1982;52(1):44-56.
69. Martin HB, Proctor DF. Pressure-volume measurements on dog bronchi. J. Appl. Physiol. 1958;13:337-343.
70. Martin CJ, Young AC, Ishilawa K. Regional lung mechanics in pulmonary disease. J. Clin. Invest. 1965;44:906-913.
71. Macklem PT, Mead J. Factors determining maximum expiratory flow in dogs. J. Appl. Physiol. 1968;25:159-169.
72. Murtagh PS, Proctor DF, Permutt S, Kelly BL, Evering S. Bronchial mechanics in excised dog lobes. J. Appl. Physiol. 1971;31(3):403-408.
73. Marquardt DW. An algorithm for least-squares estimation of nonlinear parameters. SIAM J. 1963;11:431-441.
74. Pride NB. The assessment of airflow obstruction (role of measurements of airway resistance and of tests of forced expirations). Br. J. Dis. Chest. 1971;65: 135-169.
75. Cotes JE. Lung function. Assessment and application in medicine. Blackwell Scientific Publications, 1975
76. Bogaard JM, Pauw KH, Versprille A, Stam H, Verbraak AFM, Maas AJJ. Maximal expiratory and inspiratory flow-volume curves in bilateral vocal-cord paralysis. ORL 1987;49:35-41.
77. Matthys H, Fischer J, Ulrichs HC, Rühle KH. Functional patterns of different lung diseases for computer-assisted diagnostic procedures. Progres Respir. Res. 1979;11:188-201.
78. Verbraak AFM, Bogaard JMB, Beneken JEW, Hoorn E, Versprille A. Serial lung model for simulation and parameter estimation in body plethysmography. Med & Biol Eng & Comput 1991;29:309-317.
79. Jansen JRC, Hoorn E, Goudoever J, Versprille A. A computerized respiratory system including test functions of lung and circulation. J. Appl. Physiol. 1989;67(4):1687-1691.
80. Bargeton D, Barrès G. Time characteristics and frequency response of body plethysmography. Prog. Resp. Res. 1969;4:2-23.
81. Mecklenburgh JS. Construction of linear resistance units for a model lung. Med & Biol Eng & Comput 1988;26:552-554.
82. Murphy BG, Engel LA. Models of the pressure-volume relationship of the human lung. Respir. Physiol. 1978;32:183-194.

83. Verbraak AFM, Bogaard JM, den Ouden AH, Jansen JRC, Versprille A. A computer-controlled mechanical lung model. In: Faust U, Beneken JEW, ed. Second European Conference on Engineering and Medicine. Stuttgart, Germany: Elsevier, 1993: 156-157.
84. Verbraak AFM, Beneken JEW, Bogaard JM, Versprille A. A computer controlled mechanical lung model for application in pulmonary function studies. Med & Biol Eng & Comput 1995;33:776-783.
85. Ingelstedt S, Johnson B, Nordstrom L, Olsson SG. On automatic ventilation. Acta Anaesthesiol Scand 1972;47s:9-27.
86. Boiteau R, Lherm T, Tenaillon A, Masson P. Influence of the expiration control on respiratory mechanics. Am Rev Respir Dis 1993;147:A889.
87. Curie IG. Fundamental mechanics of fluids. (2nd ed. ed.) Mc-Graw-Hill Inc., 1993
88. Happel J. Low Reynolds hydrodynamics. Prentice-Hall, Englewood Cliffs, 1965
89. de Boor C. A practical guide to splines. Springer Verlag, 1978
90. Press WH. Numerical Recipes in Turbo Pascal. Cambridge University, 1989
91. Hage R, Aerts JGJV, Verbraak AFM, van den Berg B, Bogaard JM. Detection of flow limitation during tidal breathing by interruption technique. Eur Respir J 1995;8:1910-1914.
92. Verbraak AFM, Hoorn E, de Vries JJ, Bogaard JMB, Versprille A. A lung function information system. J Biomed Eng 1991;13:27-34.
93. Braun U, Zundel J, Freiboth K, et al. Evaluation of methods for indirect calorimetry with a ventilated lung model. Intensive Care Med. 1989;1989(15): 196-202.
94. Chinet AE. Chest-lung statics: a realistic analog for student laboratory. Am. J. Physiol. 1989;256:S9-S10.
95. Damia G, Cigada M, Solca M, Pelizzola A. A new active lung model. Intensive Care Med. 1988;14:60-63.
96. Dekker J, Steketee J. A lung model for use in medical education. Eur. J. Phys. 1984;5:139-146.
97. Lyle DJR, Nunn JF, Hawes DWC, Dickins J, Tate M, Baker JA. A Model Lung with the capacity for simulated spontaneous breathing. Br. J. Anestth. 1984;56:646-649.
98. Williams EM, Gale LB, Oakley PA, Sainsbury MC, Hahn CE. Development of a concentric water-displacement model lung. J Biomed Eng 1993;15(5):420-4.
99. Samodelov LF, Falke KJ. Total inspiratory work with modern demand valve devices compared to continuous flow CPAP. Intensive Care Med 1988;14: 632-639.
100. Fabry B, Guttmann J, Eberhard L, Wolff G. Automatic compensation of tracheal tube resistance in spontaneously breathing patients. Technology and Health Care 1994;1:281-291.
101. Good ML, Lampotang S, Ritchie G, et al. Hybrid lung model for use in anesthesia research and education. Anesthesiology 1989;71(3A):A982.

102. Sajan IS, Meurs WLv, Lampotang S, Good ML, Principe JC. Computer controlled mechanical lung model for an anesthesia simulator. Int J Clin Montoring & Comp 1993;**10(3)**:194-195.
103. Bogaard JM, Jonker W, Verbraak AFM, Versprille A. A simplified procedure for exponential fitting of pressure-volume curves of normal and diseased lungs. Respiration 1986;**49**:181-186.
104. Salazar E, Knowles JH. An analysis of pressure-volume chacteristics of the lungs. J Appl Physiol 1964;**19**:97-104.
105. Mead J, Agostoni E. Dynamics of Breathing. Handbook of Physiology 1964;**1(Section 3)**:411-427.
106. Rahn H, Otis AB, Chadwick LE, Fenn WO. The pressure-volume diagram of the thorax and lung. Am. J. Physiol 1946;**146(6)**:161-178.
107. Kimball WR, Leith DE, Robins AG. Dynamic Hyperinflation and ventilator dependence in chronic obstructive pulmonary disease. Am Rev Respir Dis 1982;**126**:991-995.
108. Raneiri VM, Giuliana R, Cinnella G, et al. Physiologic effects of positive end-expiratory pressure in patients with chronic obstructive pulmonary disease during acute ventilatory failure and controlled mechanical ventilation. Am Rev Respir Dis 1993;**147**:5-13.
109. Mead J. Contribution of compliance of airways to frequency dependent behaviour of lungs. J Appl Physiol 1969;**26**:670-673.
110. Hoppin FG, Hildebrandt J, ed. Mechanical properties of the lung. New York: Dekker, 1977:83-162. (West JB, ed. Lung Biology in Health and Disease, Bioengineering aspects of the lung.; 3).
111. Brusasco V, Pellegrino R. Hysteresis of airways and lung parenchyma. Resp. Medicine 1995;**89**:317-332.
112. Similowsky T, Bates JHT. Two-compartment modelling of respiratory system mechanics at low frequencies: gas redistribution or tissue rheology? Eur.Respir. J 1991;**4**:353-358.
113. Sharp JT, Johnson FN, Goldberg NB, van Lith P. Hysteresis and stress adaptation in the human respiratory system. J Appl Physiol 1989;**23**:487-497.
114. Bates JHT, Brown KA, Kochi T. Respiratory mechanics in the normal dog determined by expiratory flow interruption. J Appl Physiol 1989;**67**:2276-2285.
115. Hildebrandt J. Pressure-volume data of cat lung interpreted by a plasto-elastic, linear visco-elastic model. J Appl Physiol 1970;**28**:365-372.
116. Fredberg JJ, Stamenovic D. On the imperfect elasticity of lung tissue. J Appl Physiol 1989;**67**:2408-2419.
117. Stamenovic D, Glass GM, Barnas GM, Fredberg JJ. A model of imperfect elasticity of the human chest wall. The Physiologist 1988;**31**:A220.
118. Guerin C, Coussa ML, Eissa NT, et al. Lung and chest wall mechanics in mechanically ventilated COPD patients. J Appl Physiol 1993;**74(4)**:1570-1580.
119. Loughlin PJ, Bowes WA, Westenskow DR. An oil-based model of inhalation anesthetic uptake and elimination. Anesthesiology 1989;**17**:278-282.

120. Jansen JRC, Bogaard JM, Spritzer R, Verbraak AFM, Versprille A. Automatic analysis of circulatory shunts during artificial ventilation. Plenum Press, 1980:219-221. (Prakash O, ed. Computers in critical care and pulmonary medicine; vol 2).
121. Verbraak A, Bogaard J, Jansen R, Versprille A. Automatic data processing in the clinical lung function laboratory. Plenum Press, 1980:85-87. (Prakash O, ed. Computers in critical care and pulmonary medicine; vol 2).
122. Bogaard JM, Pauw KH, Versprille A. Flow limitation in upper airway obstruction (theoretical analysis). ORL 1987;49:42-47.
123. Bogaard JM, Slingerland R, Verbraak AFM. Dose-effect relationship of terbutaline using a multi-dose powder inhalation system ('Turbuhaler') and salbutamol administered by powder inhalation ('Rotahaler') in asthmatics. Pharmatherapeutica 1989;5(6):400.
124. Bogaard JM, Verbraak AFM, Jonker W. Failure of bodyplethysmography. Airways 1989;8(2):69-72.
125. Smit JM, Bogaard JM, Goorden G, Verbraak AFM, Dalinghaus P. A quasi steady state ramp method for the estimation of the ventilatory response to CO2. Respiration 1992;59(1):9-15.
126. Kars A, Goorden G, Stijnen T, Bogaard J, Verbraak A, Hilvering C. Does phase 2 of the expiratory PCO2 versus volume curve have diagnostic value in emphysema patients? Eur Respir J. 1995;8:86-92.
127. Aerts JGJV, van den Berg B, Bogaard JM. Controlled expiration in mechanically-ventilated patients with chronic obstructive pulmonary disease (COPD). Eur Respir J 1997;10:550-556.
128. Kars AH, Bogaard JM, Stijnen T, de Vries JJ, Verbraak AFM, Hilvering C. Dead space and slope indices from the expiratory carbon tension-volume curve. Eur Respir J 1997;10:1829-1836.
129. Bogaard JM. Interpretatie van indicator-verdunningscurven met behulp van een random walk model. Thesis, Erasmus University Rotterdam, 1980.
130. Pauw KH. Endolaryngeale superolateralisatie bij tweezijdige stemband verlamming. Thesis, 1981.
131. Kars AH. Clinical application of capnography in chronic obstructive pulmonary disease. Thesis, Erasmus University Rotterdam, 1995.
132. Stam H. CO diffusing capacity in the human lung dependend on alveolar volume. Thesis, Erasmus University Rotterdam, 1995.
133. Aerts JGJV. Controlled expiration in patients with chronic obstructive pulmonary disease on ventilatory support. [ISBN 90-9010047-4]Thesis, Erasmus University Rotterdam, 1996.
134. Overbeek SH. Inhaled corticosteroids in astma; effects on inflamation and lung function. [ISBN 90-9010133]Thesis, Erasmus University Rotterdam, 1997.
135. Aerts JGJV, Bogaard JM, Overbeek SE, Verbraak AFM, Thio P. Extrapolation of methacholine log-dose response curves with a cumulative gaussian distribution function. Eur Respir J 1994;7:895-900.

136. Overbeek SE, Bogaard JM, Aerts JGJV, Verbraak AFM, Hoogsteden HC. Interrelationship of indices from methacholine log-dose (MLDR) curves in allergic asthmatics. 1995;
137. Moller GM. Bronchial mucosal inflamation in asthma, modulation by glucocorticoids. Thesis, Erasmus University Rotterdam, The Netherlands, 1996.
138. Verhoeven GT, Verbraak AFM, Rijnbeek PR, Hoogsteden HC, Bogaard JM. Lung elasticity and CO-diffusion in COPD patients with bronchial hyperresponsiveness. 1996;

SAMENVATTING

De computer heeft in de laatste decennia grote invloed gehad op de directe patiëntenzorg en onderzoek. Enerzijds heeft dit betrekking op de kwantitatieve en kwalitatieve verbetering van bestaande werkzaamheden en anderzijds op het ontstaan van nieuwe toepassingen die zonder gebruik van de computer niet mogelijk zouden zijn.

Hoofdstuk 1 beschrijft de invloed van de technologische ontwikkelingen van de computer op het longfunctielaboratorium vanaf ongeveer 1977 tot op heden. Dit wordt nader uitgewerkt voor de geautomatiseerde verwerking van longfunctiemetingen die bij patiënten worden verricht en de ontwikkeling van mathematische en fysische modellen.

Verwerking longfunctiemetingen.

In de eerste jaren was op het longfunctie laboratorium de computer slechts zeer beperkt beschikbaar. Aan het einde van de dag werden meetgegevens via een invoersysteem op de medische faculteit electronisch overgebracht naar een computer systeem van IBM in Zoetermeer. Deze gegevens werden 's nachts verwerkt waarna de volgende ochtend de verwerkte gegevens konden worden opgehaald.

Via een reeks van tussenstappen is inmiddels een longfunctie informatie systeem (*LFIS*) ontwikkeld waarmee de meetgegevens nog tijdens de uitvoering van de onderzoeken worden verwerkt. De longfunctieassistent krijgt nog tijdens

de meting de resultaten beschikbaar, die dan gelijktijdig vergeleken zijn met de bij de betreffende patiënt behorende referentiewaarden. Door de opslag van resultaten van de longfunctiemetingen zijn de gegevens over een langere periode te vervolgen. Het *LFIS* wordt beschreven in hoofdstuk 2.

Toepassing van modellen..

Van medisch-biologische systemen kunnen modellen worden afgeleid die de werkelijkheid op een andere wijze beschrijven. Deze modellen geven meestal de werkelijkheid in beperkte mate weer en zijn dan ook alleen maar toepasbaar voor een specifieke vraagstelling. In dit proefschrift wordt een toepassing van een wiskundig en een fysisch model van het mechanisch gedrag (relaties tussen drukken, volumes en luchtstroomsterkten) van de long beschreven.

Wiskundige modellen vertalen werkingsmechanismen in algebraïsche vergelijkingen die met behulp van computerprogramma's worden vastgelegd. Aan de hand van deze wiskundige modellen krijgt men meer inzicht in het gedrag van de long en komt informatie beschikbaar die niet op een andere wijze kan worden verkregen. In hoofdstuk 3 staat een beschrijving van de toepassing van een wiskundig longmodel.

Fysische modellen, in de Angelsaksische literatuur ook vaak mechanische modellen genoemd, zijn een vereenvoudiging van een werkelijkheid in fysische componenten. In fysische modellen worden meetbare fysische grootheden gemeten en weergegeven in getallen met eenheden. Bij een fysisch longmodel zal bijvoorbeeld tijdens de simulatie van de uitademing daadwerkelijk de gasstroom aanwezig zijn. Het zal duidelijk zijn dat met een fysisch model andere toepassingsmogelijkheden ontstaan dan bij wiskundige longmodellen. Deze modellen zullen met name worden gebruikt voor het simuleren van patiënten in een echte meetsituatie, waarbij de patiënt is gekoppeld aan bestaande meet en/of beademingsapparatuur. Deze "kunst-patiënt' vertoont dan steeds een gelijk gedrag en is op ieder moment beschikbaar. Hierdoor kunnen programma's worden ontwikkeld en getest, waarbij op ieder moment een gewenst type "kunst-patiënt" is te simuleren. Hoofdstuk 4 beschrijft een longsimulator (*CCL-1*) waarin de computer wordt gebruikt voor het genereren van ademhalingspatronen. De hoofdstukken 5 en 6 beschrijven een vervolg ontwikkeling op basis van de *CCL-1*, waarbij een meer verregaande integratie van computer-software en fysische-componenten is gerealiseerd. De toepasbaarheid hiervan is getest met behulp van een aangepaste versie van de *CCL-1*. De grote flexibiliteit en nieuwe mogelijkheden die door deze verregaande integratie ontstonden, hebben geleid tot het ontwerp van een tweede generatie longsimulator (*CCL-2*). In het laatste hoofdstuk staat een korte beschrijving van het ontwerp van de *CCL-2* en het belang van dit fysische model voor toepassing bij onderzoek bij beademde patiënten.

Hoofdstuk 2 beschrijft de ontwikkeling van het *LFIS*. Dit systeem verwerkt de longfunctiemetingen die op verschillende locaties in het ziekenhuis bij patiënten worden uitgevoerd. Het *LFIS* is verbonden met het Ziekenhuis Informatie Systeem (*ZIS*) voor de uitwisseling van patiëntgegevens ten behoeve van de longfunctiemetingen en voor financiële en administratieve doeleinden.

De toegepaste programma's zijn zodanig ontwikkeld dat een hoge mate van flexibiliteit mogelijk is bij de interactie tussen patiënt-computer-longfunctie-assistent. De verkregen gegevens worden opgeslagen om later eventueel eerdere beslissingen te kunnen corrigeren of om nieuwe methoden in het kader van wetenschappelijk onderzoek te testen. Op deze manier krijgt men meer en betere informatie bij het routine patiënten onderzoek. Berekende longfunctiegegevens worden ook opgeslagen om het verloop van het ziekteproces in de tijd te kunnen volgen (trendonderzoek).

In 1980 is gekozen voor een ster-netwerk van computers waarbij de verschillende meetcomputers één op één waren verbonden met een centraal computersysteem op de afdeling (zie figuur 2.1, blz. 18). Hierdoor werden de voordelen van het tot dan toe gebruikelijke centrale computersysteem gecombineerd met de voordelen van de computersystemen die zijn verbonden met slechts één meetopstelling. In het ster-netwerk zijn de belangrijkste taken van het centrale systeem: de centrale opslag van bij verschillende meetopstellingen verzamelde gegevens en de opslag van computerprogramma's, de aanmaak van een longfunctierapport, waarbij de resultaten van verschillende meetopstellingen worden samengevoegd tot een overzichtelijk rapport, en de informatie uitwisseling met het *ZIS*. De taken van de satellietcomputer, die dicht bij de longfunctieapparatuur staat, zijn: de verwerking van de signalen tijdens de meting, de rapportage en verdere administratieve afhandeling van de meting, het ontwikkelen van programmatuur, en tot enkele jaren geleden het gebruik voor de off-line gegevensverwerking van de longfunctiemetingen van twee andere ziekenhuizen in de regio door middel van een modemverbinding.

Het *LFIS* verbeterde de kwantiteit en kwaliteit van de gegevensverwerking. Het resulteerde in: een toegenomen capaciteit van ongeveer 50 % voor de spirometrie, een vereenvoudiging van tijdrovende, complexe analyses, een vermijding van eventuele misrekeningen en fouten in rapporten die bij handmatige verwerking groter is, en nieuwe mogelijkheden voor wetenschappelijk onderzoek.

In de appendix van hoofdstuk 2 worden de recente uitbreidingen en ontwikkelingen van het *LFIS* genoemd. De introductie van de "personal computer" heeft geresulteerd in een reductie van de kosten, vereenvoudigingen van de bewerking en een grotere toename van commerciële programma's, zoals ten behoeve van tekstverwerking en statistiek. De grote invloed van het elektronische

communicatienetwerk op de automatische gegevensverwerking in het Academisch Ziekenhuis en het longfunctielaboratorium in het bijzonder, is hierin aangegeven. Momenteel zijn de resultaten, verkregen op één van de longfunctielaboratoria, zeer snel via *PC*-systemen voor de aanvragende arts via het *ZIS* beschikbaar in het Academisch Ziekenhuis Rotterdam, bestaande uit het Sophia Kinderziekenhuis, Dijkzigt Ziekenhuis en de Daniel den Hoed Kliniek.

In hoofdstuk 3 wordt een wiskundig longmodel met een samendrukbaar segment beschreven voor het nabootsen van verschillende typen long- en luchtwegafwijkingen, zoals astma, emfyseem, fybrosis en bovenste luchtwegobstructie gedurende de normale ademhaling. De longen worden gesimuleerd door een compartiment dat het volumegedrag van de long beschrijft met daarin in serie verschillende luchtwegsegmenten die de kleine, de samendrukbare en grote luchtwegen simuleren (figuur 3.1, blz. 40). Met dit wiskundig model werden door verandering van parameters, meetsignalen (de alveolaire druk en de luchtstroomsterkte) behorend bij specifieke ziektebeelden gemaakt. De kenmerken van deze signalen kwamen overeen met eerder in de literatuur beschreven metingen bij patiënten.

Deze signalen werden daarna gebruikt om na te gaan of door toepassing van parameterschattingstechnieken de ziektebeelden konden worden herkend. Bij afwezigheid van kunstmatig aangebrachte verstoringen op het signaal (ruis), produceerden de parameterschattingsroutines eenduidige oplossingen voor de verschillende gesimuleerde ziektebeelden. De gevoeligheid van de verschillende parameters hing af van de waarden die behoren bij ieder ziektebeeld. In tegenstelling tot het toevoegen van verstoringen (ruis) op het druksignaal, hadden toegevoegde verstoringen aan de gesimuleerde luchtstroomsterkte geen invloed op de geschatte parameters. Hierbij kon de effectieve luchtwegweerstand goed worden geschat. Waar parameters weinig invloed hadden, zoals bijvoorbeeld op de weerstand van de bovenste luchtwegen bij emfyseem of op de perifere luchtwegweerstand bij een grote luchtwegobstructie in de hogere luchtwegen, was de berekening minder nauwkeurig. In alle andere gevallen kon een bevredigende nauwkeurigheid worden verkregen.

Dit hoofdstuk beschrijft verder meer vereenvoudigde longmodellen. Indien de invloed van de samendrukbare luchtwegen klein is, geven deze vereenvoudigde modellen een meer betrouwbare schatting dan het complexe model.

Hoofdstuk 4 geeft een beschrijving van de ontwikkeling van een computer-gecontroleerd, fysisch longmodel (*CCL-1*). Dit fysische longmodel was geconstrueerd uit twee balgen en een buissysteem (figuur 4.1, blz. 61). Deze onderdelen

stelden respectievelijk de alveolaire longcompartimenten van beide longen en de luchtwegen voor.

De balgen waren met water omgeven om de ruimte tussen long en borstkas te simuleren. Volume veranderingen van de balgen werden via het water tot stand gebracht door een zuiger, die werd aangedreven door een computer-gestuurde elektrische motor. Hiermee kon een breed scala van ademhalingspatronen worden gesimuleerd.

Het buissysteem, dat de luchtwegen representeerde, verbond beide balgen met de omringende lucht en was voorzien van uitwisselbare gedeelten met bekende weerstanden. Een samendrukbaar element, dat de samendrukbare luchtwegen simuleerde, kon in het buissysteem worden ingebracht. De met vloeistof gevulde ruimte rond het samendrukbare element was met het watercompartiment rond de balgen verbonden. Voor het samendrukbare element werd gebruik gemaakt van een rekbare latex buis. De uitgang van het buissysteem sloot af op commando van een extern microcomputersysteem..

Een automatische volgorde van metingen kon worden geprogrammeerd en zonder tussenkomst van de onderzoeker uitgevoerd. Dit fysisch longmodel is gebruikt voor het testen van longfunctieapparatuur en computerprogramma's (figuur 4.4, blz. 70).

In hoofdstuk 5 wordt een computer-gestuurde weerstand (*CCR*) voor luchtstroomsterkte beschreven (figuur 5.2, blz 76). Deze wordt onder meer gebruikt in de tweede generatie van het computer-gestuurde fysisch longmodel (hoofdstuk 6). De luchtstroomsterkte wordt door een nauwe cilindrische gleuf (spleet) tussen een binnen- en buitencilinder geleid. De computer bepaalt de positie van de buitencilinder ten opzichte van de binnencilinder. De totale luchtstroomsterkteweerstand hangt niet alleen af van de lengte van de spleet, maar ook af van de grootte van de luchtstroomsterkte. De afhankelijkheid van de luchtstroomsterkte komt in de eerste plaats door de vorm van de in- en uitgang van de spleet. De weerstand van de spleet is nagenoeg onafhankelijk van de luchtstroomsterkte. Gedurende een ijkingsfase wordt de weerstand bij luchtstroomsterkten van -0.05 tot 1.0 liter per seconde in beide richtingen bepaald. Om op ieder moment een gewenste weerstand te simuleren wordt continue de gewenste positie van de buitenste cilinder berekend met behulp van de ijkgegevens en de op dat moment aanwezige luchtstroomsterkte.

De inwendige diameter van de buitencilinder ligt vast. Door de buitendiameter van de binnencilinder te veranderen, verandert de spleetdikte en daardoor het gebied waarbinnen de weerstand kan worden ingesteld. Hierdoor is een

afstemming mogelijk van het weerstandsbereik van de *CCR* op een gewenst bereik.

Hoofdstuk 6 geeft een beschrijving van een nieuwe methode van aansturing van het fysisch longmodel (figuur 6.4, blz. 97). Er is een verdere integratie van computer en mechanische componenten gerealiseerd. In de *CCL-1* werden alle fysische eigenschappen uitsluitend door de onderdelen bepaald, waardoor dit longmodel weinig flexibel was. In de nieuwe opzet worden de eigenschappen van de computergestuurde mechanische onderdelen meer bepaald door de software dan door de fysische eigenschappen van de onderdelen zelf. Met het nieuwe longmodel kan een betere simulatie van het gedrag van long en luchtwegen worden verkregen.

Een belangrijke innovatie is de wijze van simulatie van de longcompliantie. De stand van de piston en dus het long volume, is nu bepaald door de gemeten druk in het longcompartiment en de in de computer vastgelegde relatie tussen deze druk en het longvolume. Met behulp van de *CCR* die is opgenomen in de *CCL-2* kan de tijdens de ademhaling variërende luchtweg-weerstand worden gesimuleerd. Door dit alles is het mogelijk om:

- niet alleen de normale ademhaling te simuleren zoals bij de *CCL-1*, maar ook de kunstmatig beademde patiënt,
- niet alleen de astma en fibrotische patiënt, maar ook de emfyseem patiënt te simuleren,
- tijd-gerelateerde mechanismen te verenigen, zoals bijvoorbeeld de invloed van de viscositeit van de long of de volumefluctuaties, te zien als druk en luchtstroomsterkte veranderingen, ten gevolge van hartactiviteit,
- de in de software gedefinieerde relaties zijn van ademhaling op ademhaling aan te passen,
- de luchtweg weerstand kan afhankelijk zijn van meerdere variabelen die in het fysische model worden gemeten en daardoor beter worden afgestemd op de fysiologische werkelijkheid, en
- er kan een normale inademing en passieve uitademing worden gesimuleerd.

De nieuwe methode van aansturen is getest met hulp van het in hoofdstuk 4 beschreven *CCL-1* met daarin opgenomen enkele aanpassingen. De mogelijkheden van de nieuwe methode worden gedemonstreerd door middel van drie voorbeelden:

1. Beademde patiënten werden gesimuleerd waarbij ook werd aangetoond dat het patroon van de uitademing door middel van een computer kon worden opgelegd.
2. De met het wiskundig longmodel gesimuleerde relatie tussen alveolaire druk en luchtstroomsterkte aan de mond is met het fysisch longmodel gesimuleerd.

3. De mogelijkheid van de toevoeging van tijdsafhankelijke aspecten in de simulatie zijn gedemonstreerd door middel van de simulatie van de viscoelasticiteit van de long, en het aanbrengen van drukvariaties ten gevolge van de invloed van het hart op de long.

In het hoofdstuk 7 is ingegaan op enkele te verwachten ontwikkelingen met betrekking tot de geautomatiseerde gegevensverwerking en het ontwerp en toepassing van de *CCL-2*.

De toepassing van de computer neemt voortdurend in omvang toe. In het verleden moest alle programmatuur voor de analyse van longfunctiemetingen zelf worden ontwikkeld. Momenteel komen steeds meer geautomatiseerde commerciële apparaten beschikbaar die worden opgenomen in het gegevensverwerkende netwerk op de afdeling. De opname en het vastleggen van steeds meer gegevens met behulp van computers zal leiden tot een elektronisch medisch dossier dat de (papieren) patiëntenstatus kan vervangen. Hierdoor zijn gegevens op meerdere locaties met behulp van een computer gemakkelijker bereikbaar. Door de beschikbaarheid van snelle en goedkope computer-systemen zal de ontwikkeling en invoering van nieuwe methodieken voor het meten en behandeling van patiënten mogelijk maken.

De integratie van wiskundige en fysische longmodellen is van groot belang voor toekomstig onderzoek. De in hoofdstuk 6 beschreven technieken worden thans verwerkt bij de constructie van een nieuw fysisch longmodel (*CCL-2*). De *CCL-2* (figuur 7.1, blz. 106) verschaft een reproduktieve en flexibele omgeving om nieuwe software en apparatuur voor het longfunctielaboratorium en de beademingsafdeling te testen. De toepassing als simulator voor training van arts en student zal mogelijk bij kunnen dragen voor een betere patiëntenzorg.

Concluderend kunnen de resultaten die zijn gepresenteerd in dit proefschrift, in twee hoofdgebieden worden onderscheiden.

- Door de momentane verwerking van de longfunctiemetingen en de integratie van de resultaten in het ziekenhuis-informatie-systeem zijn de onderzoeksresultaten onmiddellijk voor de arts beschikbaar via het elektronisch netwerk van het ziekenhuis, kort nadat de patiënt het laboratorium heeft verlaten.
- Voorts is een belangrijke stap gezet in de fysische modellering van het gedrag van de normale en zieke long. Door de integratie van wiskundige modellen via computeraansturing van onderdelen in het fysische longmodel kan de flexibiliteit van wiskundige longmodellen worden gecombineerd met de mogelijkheden van fysische modellen. Hierdoor kunnen patiënten zo getrouw mogelijk worden nagebootst teneinde hiermee meetproceduren en behandelingsmethoden te testen en te trainen.

DANKWOORD

Graag wil ik iedereen bedanken die behulpzaam is geweest bij het tot stand komen van de in dit proefschrift beschreven onderzoek. Zonder compleet te kunnen zijn noem ik een aantal die echt onmisbaar waren.

Prof. dr. ir. J.E.W. Beneken, beste Jan, jij hebt mijn belangstelling voor de medische techniek op de Technische Universiteit Eindhoven gevoed. Na de aanstelling bij de longfunctie afdeling van het Academisch Ziekenhuis Rotterdam is het contact gebleven, onder andere door de begeleiding bij dit proefschrift.
Prof. dr.A. Versprille, beste Ad, jouw interesse voor de technische toepassingen in de gezondheidszorg en de wetenschappelijke belangstelling hebben veel mogelijk gemaakt van wat in dit proefschrift is neergelegd. De discussies over de artikelen hebben niet alleen geleid tot een hoger wetenschappelijk niveau, maar zeker ook tot een beter taalkundige zuiverheid.
Prof. dr. J.M. Bogaard, beste Jan, je deskundigheid, je dagelijkse enthousiasme en goede humeur hebben zich niet alleen beperkt tot dit proefschrift. Niet in dit proefschrift beschreven projecten ter ondersteuning van klinisch onderzoek, hebben geleid tot meerdere gezamenlijke publikaties.

Een speciaal woord gaat uit naar alle medewerkers van de longfunctie, waarvan dr. Henk Stam, Judith Haazebroek, Ineke den Burger en Caroline Vons het hele automatiseringsproces hebben mee gemaakt. Jullie kritische instelling was een voorwaarde voor een optimale automatisering. De collegialiteit waardeer ik zeer, zeker op momenten dat nieuwe toepassingen nog niet optimaal functioneren.
Dr. J.R.C. Jansen, beste Jos, jij hebt de eerste stappen gezet voor de automatisering op het longfunctie laboratorium. In de jaren erna heb je van nabij mee kunnen maken hoe dit alles een hoge vlucht heeft genomen.

Drs. G.J. van Boven, beste Gert-Jan, al enkele jaren heb ik zeer prettig met je samen gewerkt. Als hoofd van de *CDAI* heb je de leiding over een gemotiveerde groep mensen.

Ing. E. Hoorn, beste Ed, jij bent steeds betrokken geweest bij de automatisering. Van de keuze om jou als natuurkundige voor de automatisering te selecteren heb ik nooit spijt gehad. Van je professionele en enthousiaste instelling heeft niet alleen de longfunctie profijt gehad, maar ook vele anderen die momenteel via de *CDA!* een beroep op je doen.
Ing. J.J. de Vries, beste Julius, de laatste jaren ben jij het zeer intensief bij de automatisering en op veel programmatuur heb jij een belangrijke stempel gezet. Samen met L. de Baat, wordt nu veel werk verzet met betrekking tot de beschikbaarstelling van longfunctie gegevens en bronchoscopie beelden via het netwerk van het ziekenhuis aan de artsen.
Ing. J. Zwijgers, beste Joor, de programmatuur voor de longfunktie en beademing die jij eertijds hebt geschreven is nog steeds intensief op de longfunktie en beademing in gebruik.
Bijna alle andere medewerkers zijn meer of minder regelmatig betrokken bij werkzaamheden ten behoeve van de afdeling Longziekten. Ik denk hierbij ondermeer aan ir. P.G.B. Driever, C.J. Jongkind, P.vd Ster, drs. B. V. Ooijen A.J. Sandee, drs. R.S. Smidt en A. Verhoeven.

Vele medewerkers van de *CID* zijn betrokken geweest bij de ontwikkeling van de automatisering en het ontwerp en de bouw van de mechanische modellen. Ir. W.P. Holland en ing. B.N. Mulder, beste Wim en Bernhard, jullie inbreng komt tot uiting in de gezamenlijke publicaties.
Ondanks het feit dat ik er beslist enkelen tekort doe, wil ik W.J. v. Alphen, C.P. Bakker, W. Boender, C. Pakvis en A. Vlasveld bedanken voor de betrokkenheid bij de mechanische en electronische werkzaamheden.

B. Nijssen, technische dienst en A. Slingerland, inkoop en de medewerkers bedank ik voor hun voortdurende inzet. Met C. Weergang en M.M. Jerphanion, noem ik de financieel economische dienst, die vele uren hebben besteed aan de afstemming van de declaratie systemen.

De bijdragen van de stagiaires en afstudeerders van de Technische Hogeschool Rijswijk en de Technische Universiteiten Delft en Eindhoven zijn steeds zeer welkom geweest. Zij vormden een radertje in het grote geheel. Hierbij wil ik speciaal ir. P. Pieterman, ir. R.I.L. Pijl, C. Buurman en I. de Graaf van de Technische Hogeschool Rijswijk en dr.ir. M. Verhaegen en dr.ir. R.P. van Wijk van Brievingh van de Technische Universiteit Delft vermelden.

Ir. P.R. Rijnbeek, beste Peter, als stagiaire van de TH-Rijswijk, collega tijdens de universitaire vervolg studie en als afstudeerder van de TU-Delft heb jij een grote bijdrage geleverd aan dit proefschrift. Peter, ik hoop dat we elkaar blijven inspireren, en via je huidige plaats op de afdeling Medische Informatica van de Erasmus Universiteit kunnen samenwerken.

Prof. dr. J.C. de Jongste en I. Beckers, beste Johan en Simone, de samenwerking heeft geleid tot een gezamenlijk gebruik van de geautomatiseerde gegevensverwerking op de afdelingen Kinderpulmonologie en Longziekten van het AZR.

Prof. dr. C. Hilvering en Prof. dr. H. Hoogsteden, beste Chris en Henk, jullie zien beiden het belang, dat de medische technologie heeft voor de patiënt met long problemen.
Chris, jij hebt mijn belangstelling in jouw vak verdiept terwijl ik je voor mijn vakgebied heb kunnen interesseren. Dit laatste blijkt uit het intensieve gebruik van je computer thuis.
Henk, ik hoop dat we nog vele jaren intensief en prettig zullen samenwerken aan de ontwikkeling en invoering van technologische ontwikkelingen ten behoeve van de klinische patiënten zorg op de kliniek, de longfunctie en de beademing.

Tenslotte wil ik het thuisfront noemen. Lieve Anneke, Wouter en Saskia, jullie hebben steeds vertrouwen gegeven en getracht een evenwicht te zoeken in belangrijke zaken en interesses van ieder. Wouter en Saskia, ik hoop dat jullie in de fysische oceanografie en de psychologie ook met veel plezier zullen werken. Lieve Anneke, na de eerste 25 jaar samen van studie en tenslotte de promotie zullen we hopelijk de gezamenlijke hobby van zeezeilen nog lang kunnen beoefenen. Bedankt en we gaan samen op de ingeslagen koers door.

CURRICULUM VITAE

Ton Verbraak, born 31 March 1946 at Tilburg, passed through the Modern School (*HBS-b*), St. Paulus, at Tilburg from 1958 to 1964. He studied electro technical engineering at the College of Advanced Technology St. Virgilius at Breda and received the certificate in 1968. Thereafter, he studied at the Technical University of Eindhoven (*TUE*) at the faculty of electrical engineering. March 1976 he graduated at the department of Medical Electrical Engineering headed by Prof. Dr. ir. J.E.W. Beneken on the study of "Identification and control of a physiological process". At the *TUE* he was involved as student member in the commission of Biomedical and health technics (*BMGT*). He was active in the foundation of the Science shop for Health Care.

Since March 1976 he is working at the Academic Hospital of Rotterdam (*AZR*), until October 1994 as staff-member of the lung function laboratory of the department of Pulmonary diseases. Two years he was member of the department of Automatic Data processing (*CDAI*), whereafter he became again staff-member of the department of Pulmonary Diseases and the Respiratory Intensive Care Unit of the University of Rotterdam.
He is registrated as a Clinical Physicist.

He is member of the European Society of Engineering and Medicine (*ESEM*), the society of medical and biomedical information processing (*VMBI*) and the society of Biophysics (*VvB*). At the moment he is chairman of the section of Biomedical technics, and member of the sections Pulmonary function and Physics of breathing (*ALRIC*). For the *VvB* he delegates to the International Federation of Medical and Biological Engineering (*IFMBE*). He was referee for the Journal of Medical & Engineering & Computing and the transactions on Biomedical Engineering of the *IEEE*. Finally, he is external examiner at the College of Advanced Technology at Rijswijk.